FINITE DIFFERENCE METHODS FOR SINGULARLY PERTURBED PROBLEMS ON NON-RECTANGULAR DOMAINS

Raymond K. Dunne, B.Sc.

School of Mathematical Sciences

Dublin City University

Supervisor: Prof. Eugene O'Riordan

A Thesis submitted for the Degree of Doctor of Philosophy

July 2005

Declaration

I hereby certify that this material, which I now submit for assessment on the programme of study leading to the award of Doctor of Philosophy is entirely my own work and has not been taken from the work of others save and to the extent that such work has been cited and acknowledged within the text of my work.

Signed: Raymond Dunne ID No.: 95034285

Date: 25-01-06

Acknowledgements

It is a great pleasure to thank my supervisor, Prof. Eugene O'Riordan. I have benefited greatly from his knowledge, encouragement and advice throughout the completion of my Ph.D. His unique combination of enthusiasm and insight is an inspiration and a profound influence.

I wish to thank Prof. Grigorii Shishkin for much technical advice and comments on my work.

I would like to thank the staff and post-graduates of the School of Mathematical Sciences for their help and friendship and countless great nights! Thanks to all of my friends for their love and support, particularly in the hard times.

I am indebted to Helena Ahern for her wisdom and guidance that have helped me greatly in the last couple of years.

I would like to express my thanks to my siblings, Louis, Marie and Elizabeth for their love and support. I would also like to thank my Dad for always believing in me and for his endless help in every possible way. I want to thank my Mam for her boundless love and for all that she gave me throughout her life. Your memory will never diminish in my heart.

Finally, I wish to thank Louise for her love and devotion, and for her support throughout the writing of the thesis. You are my heart and soul.

Contents

Abstract

Singularly perturbed problems arise in many branches of science and are characterised mathematically by the presence of a small parameter multiplying one or more of the highest derivatives in a differential equation. This thesis concerns singularly perturbed problems posed on non-rectangular domains. The methodology used is to perform a co-ordinate transformation to pose the problem on a rectangular domain and to then study the transformed problem.

We first consider a class of parabolic problems. We classify the problems in the transformed problem class according to the nature and location of the layers present in their solution. This classification then enables us to design numerical methods specific to each class of problems. Known theoretical results are stated for the convergence of some of the methods. We then examine in detail one particular method. Under certain assumptions it is shown that the numerical solutions generated by the method converge uniformly with respect to the singularly perturbed parameter. Detailed numerical results are then presented which verify the theoretical results.

The next class of problems considered is a class of elliptic problems. In this case the transformed differential equation contains a new term and the situation is thus more complex. For this reason we consider only the case when regular layers are present. An appropriate numerical method is constructed and under various assumptions it is proved that the numerical solutions converge uniformly, in the perturbed case, i.e., when the singularly perturbed parameter is small. This is the central result of the thesis. Extensive numerical computations are presented which verify the theoretical result.

List of Tables

List of Figures

"I can't help it, gas escapes from my fundament on the least pretext, it's hard not to mention it now and then, however great my distaste. One day I counted them. Three hundred and fifteen farts in nineteen hours, or an average of over sixteen farts an hour. After all it's not excessive. Four farts every fifteen minutes. It's nothing. Not even one fart every four minutes. It's unbelievable. Damn it, I hardly fart at all, I should never have mentioned it. Extraordinary how mathematics help you to know yourself."

Molloy, Samuel Beckett.

Notation and conventions

We gather together some notation and conventions that are used throughout the thesis. Let Z^N be any mesh function. The partial finite difference operators D_x^+, D_x^- and δ_x^2 are defined as

$$D_x^+ Z_{i,j}^N = \frac{Z_{i+1,j}^N - Z_{i,j}^N}{x_{i+1} - x_i},$$
$$D_x^- Z_{i,j}^N = \frac{Z_{i,j}^N - Z_{i-1,j}^N}{x_i - x_{i-1}},$$
$$\delta_x^2 Z_{i,j}^N = \frac{2(D_x^+ Z_{i,j}^N - D_x^- Z_{i,j}^N)}{x_{i+1} - x_{i-1}},$$

with analogous definitions for the corresponding difference operators with respect to t and y.

We represent solutions of continuous problems by lower case letters, for example u, and solutions of discrete problems by upper case letters, for example U^N. We use hats for functions and operators on the original domain of definition of a problem, for example $\hat{a}$. We use tildes to indicate stretched variables and corresponding functions, for example $\tilde{x}$.

We denote by $C^{\nu,k}(\Omega)$ the space of Hölder continuous functions where k is an integer and $\nu \in (0,1]$, with corresponding norms $\|\cdot\|_\nu$ and semi-norms $|\cdot|_k$. The norm, $\|\cdot\|$, is the maximum norm. Sometimes the above norms are subscripted to indicate the appropriate domain.

The generic constant C, sometimes subscripted, is independent of ε and N.

Chapter 1

Introduction

1.1 The aim of the thesis

In this thesis we will examine the application of numerical methods to the approximation of solutions of singularly perturbed partial differential equations posed on non-rectangular domains. In particular we will investigate the use of finite difference numerical methods based on special piecewise-uniform meshes sometimes referred to as Shishkin meshes. The purpose of this introduction is to give an overview of the types of problems we are concerned with, to provide a brief summary of the numerical techniques that have been employed in the area and to put the main results and findings of the thesis into this context.

1.2 Numerical methods for singularly perturbed problems

Singularly perturbed problems arise in a diverse array of physical phenomena from the modelling of fluid flow and heat transfer [37] to option pricing in financial mathematics [5]. Such problems are described by differential equations and are characterised mathematically by the presence of a small parameter called the singular perturbation parameter, in the coefficient of the highest order derivative in the equation. The solutions to these problems may exhibit what are termed layer phenomena, that is there

exist regions in the domain of definition of these problems in which their solutions change rapidly. Such regions are called boundary layers or interior layers depending on their location.

One particularly important class of singularly perturbed problems are convection-diffusion problems, so-called as they model physical phenomena where both convection and diffusion processes are present. In this context our problem becomes singularly perturbed when the convection processes dominate the diffusion processes. This usually gives rise to boundary layers of various types. This class of problems is the main focus of this thesis.

Perhaps the simplest example of a convection-diffusion problem is the following linear problem in one-dimension on the interval $\Omega = (0, 1)$.

Problem Class 1.2.1.

$$\varepsilon u_\varepsilon'' + a(x)u_\varepsilon' = f(x) \quad \text{in } \Omega, \tag{1.2.1a}$$

$$u_\varepsilon(0) = u_0, \quad u_\varepsilon(1) = u_1, \tag{1.2.1b}$$

$$\text{where} \quad a(x) \geq \alpha > 0, \quad x \in \overline{\Omega}. \tag{1.2.1c}$$

It is well known that the solution to this problem contains a boundary layer of width $\mathcal{O}(\varepsilon)$ in a neighbourhood of $x = 0$. Despite its simplicity it will prove convenient for highlighting the drawbacks in some well known numerical methods.

Of course singularly perturbed problems that arise in practice are much more complicated and the majority involve partial differential equations, which are in general hard to solve analytically. Therefore it should come as no surprise that there is a vast literature devoted to numerical methods designed to generate approximations to their solutions. These methods can be broadly divided into two different categories: finite element & finite volume methods, and finite difference methods.

In this thesis we will not investigate finite element and finite volume methods and confine ourselves to some brief remarks on their relevance to the problems that we are studying. A description of these methods may be found in many books. For a detailed account of their application to singularly perturbed problems and a survey of some theoretical results we refer the reader to the books [40], [37] and [34].

Finite difference numerical methods applied to the approximation of solutions to

differential equations have a long history (see [41]). Their application to singularly perturbed problems however, is much more recent, though already an extensive literature has been developed. Early methods that were devised were classical in approach and were based upon uniform meshes and so-called fitted difference operators. The first such method was described by Allen and Southwell [8] and analysed by Il'in [20]. Similar methods were described by Hemker [19] and El-Mistikawy and Werle [14], the former derived via a finite element framework. The shortcomings of these methods when applied to Problem Class 1.2.1 are expounded in [15, §2.5]. We remark that the primary difficulty lies in the fact that when a uniform mesh is employed there will be no mesh points present in the boundary layer region when the singular perturbation parameter is small. In this case one says that the methods do not *resolve* the layers present.

It should be noted that it is possible to construct a finite element method based on a uniform mesh (see O'Riordan [38]) that resolves the boundary layers in Problem Class 1.2.1 if a complicated form of interpolation is used (based on the exponential basis functions introduced by Hemker in [19]). However, the extension of this method to problems in more than one dimension is difficult.

In [4] Bakhvalov proposed a numerical method that was based on a special non-uniform mesh and a standard finite difference operator. Thus in contrast to the above approaches it was the mesh that was tailored to the boundary layer rather than the operator. He was able to show that this method resolved the layers present in solutions to (1.2.1). However, the complicated construction of the Bakhvalov mesh and the difficulty of the theoretical analysis has meant that extension of the method to problems in more than one dimension has been limited (see [24] and [44]). For further discussion of this mesh and other non-uniform meshes we refer to [15, §3.1] and [40, §2.4.2].

The preceding discussion highlights the fact that the consideration of Problem Class 1.2.1 is most useful for identifying disadvantages in a numerical method. This is because of the simple fact that numerical methods that are appropriate for this simple problem may not be suitable for more general problems in more than one dimension. This is a key point. The application and analysis of numerical methods for partial differential equations (PDEs) is considerably more difficult than for ordinary

differential equations. There are numerous technical difficulties that are simply not present in one dimension. We shall take up these issues in §1.5.

In this thesis we study singularly perturbed problems which are much more complicated than (1.2.1) yet which are still simpler than what one encounters in practice. Hence even for these problems we must bear in mind that the methods we develop should be capable of extension to more general situations.

1.3 Robust layer-resolving methods

The authors in [15] require the following key properties from a numerical method designed to be applied to singularly perturbed problems with layer phenomena:

1. Globally defined: defined at each point of the domain of the exact solution.

2. Pointwise-accurate: the error between the computed solution and the actual solution should be measured in the global maximum norm.

3. Parameter-uniform: the numerical solutions converge ε-uniformly to the exact solution and can be computed using an ε-uniform amount of computational effort.

4. Monotone: the discrete operator used in the numerical method should be a monotone operator.

A comprehensive discussion of these properties may be found in [15]. It is worth noting that it can be difficult to establish theoretical results in the global maximum norm for the finite element method applied to convection-diffusion problems, particularly in more than one dimension. It is also hard to guarantee the monotonicity of such schemes.

These requirements were formalised in the following definition of a robust layer-resolving numerical method [15, §1.4].

Definition 1.3.1. Let (P_ε) be a class of singularly perturbed problems parameterised by a singular perturbation parameter ε, such that $0 < \varepsilon \leq 1$. Assume that each problem in (P_ε) has a unique solution u_ε, and that each u_ε is approximated by a sequence

of numerical solutions $\{(U_\varepsilon^N, \overline{\Omega}^N)\}_{N=1}^{\infty}$ obtained using a monotone numerical method (P_ε^N), where U_ε^N is defined on the mesh $\overline{\Omega}^N$ and N is a discretisation parameter. Let $\overline{U}_\varepsilon^N$ denote the piecewise linear interpolant over $\overline{\Omega}$ of the discrete solution. Then (P_ε^N) is said to be a robust layer-resolving method if the numerical solutions are computable with an ε-uniform amount of computational work and converge ε-uniformly, in the sense that there exists a positive integer N_0, and positive numbers C and p where N_0, C and p are independent of N and ε, such that for all $N \geq N_0$ we have

$$\sup_{0<\varepsilon\leq 1} \left\| \overline{U}_\varepsilon^N - u_\varepsilon \right\|_{\overline{\Omega}} \leq CN^{-p}. \tag{1.3.1}$$

1.4 Finite difference methods based on piecewise-uniform fitted meshes

As should be clear from the preceding discussion finite difference numerical methods based on uniform meshes are in general inadequate for the resolution of boundary layers in the solutions of singularly perturbed problems. Indeed, it is essential to use a non-uniform mesh. One particularly simple type of non-uniform mesh was introduced by Shishkin [45]. It essentially comprises two uniform meshes of differing widths joined at an appropriately chosen transition point. For the one-dimensional convection-diffusion problem (1.2.1) the transition point is defined as

$$\sigma = \min\left\{\frac{1}{2}, \frac{\varepsilon}{\alpha}\ln N\right\}.$$

When the mesh is chosen in this way it is referred to as a piecewise-uniform fitted mesh. In the literature it is sometimes also referred to as a Shishkin mesh. We shall use the former terminology. A finite difference method based on this mesh and a simple upwind finite difference operator is robust and layer-resolving in the sense defined in the previous section when applied to Problem Class 1.2.1 (see [15, Chapter 3]) with the following error bound: for all $N \geq 4$ we have

$$\sup_{0<\varepsilon\leq 1} \left\| \overline{U}_\varepsilon^N - u_\varepsilon \right\|_{\overline{\Omega}} \leq CN^{-1}\ln N. \tag{1.4.1}$$

The great virtue of the mesh is its simplicity and this fact makes it readily applicable to more complicated problems. Indeed, even before it became widely known in the Western literature Shishkin went on to apply his mesh to very general classes of singularly perturbed problems in many dimensions. He presented a wide collection of results in the seminal work [47]. Currently only available in Russian, this book includes a huge amount of material in a highly condensed style with few proofs and little in the way of explanatory detail. All of these facts have meant that it was a relatively long time before Shishkin's ideas and methods became widely known. It wasn't until the mid-90's, when he began a collaboration with a group of Irish mathematicians, that the analysis of his methods was expounded in a more constructive fashion. This endeavour culminated in the monographs [35] and [15]. All of this is far removed from the situation today where research on piecewise-uniform fitted meshes is one of the dominant areas in the field.

It should be noted that to implement the mesh one must know the nature and location of the layers present in the solution of the problem being considered *a priori*. This is the case for the problems we study in this thesis but for more complicated problems it may be hard to establish this information. One technique that may prove fruitful in this regard is adaptive mesh refinement based on *a posteriori* error indicators. A summary of some of the current theory for these methods may be found in [27]. We will not consider such methods in this thesis.

1.5 Singularly perturbed partial differential equations

Practical problems involving singular perturbations involve PDEs. For example the full Navier-Stokes equations are a system of non-linear PDEs. Hence if we are to have any chance of developing adequate numerical methods for problems such as these it is essential that we contemplate problems that involve PDEs. In this regard consider the following two-dimensional convection-diffusion problem on the square domain $\Omega = (0,1) \times (0,1)$.

Problem Class 1.5.1.

$$\varepsilon \Delta u_\varepsilon + \mathbf{a}(x,y) \cdot \nabla u_\varepsilon = f(x,y) \quad in \ \ \Omega, \tag{1.5.1a}$$

$$u_\varepsilon = g(x,y) \quad on \ \ \partial\Omega. \tag{1.5.1b}$$

Depending on the particular form of the coefficient of the convection term in the equation, $\mathbf{a}$, different types of layers can appear in the solutions of problems from this class. Under suitable assumptions on the data of the problem the nature and location of these layers can be determined using the techniques of matched asymptotic expansions (see the books [21] and [13] among others). For example, if we have

$$\mathbf{a}(x,y) > (\alpha_1, \alpha_2) > (0,0), \quad \forall (x,y) \in \overline{\Omega}, \tag{1.5.2}$$

then the solutions of problems from this class possess regular layers in a neighbourhood of the sides $x = 0$ and $y = 0$ and a corner layer near the corner $(0,0)$; while if

$$\mathbf{a}(x,y) = (a_1(x,y), 0), \quad \text{with} \quad a_1(x,y) > \alpha_1 > 0, \quad \forall (x,y) \in \overline{\Omega}, \tag{1.5.3}$$

then the solutions will exhibit parabolic layers in a neighbourhood of the sides $y = 0$ and $y = 1$, a regular layer in a neighbourhood of $x = 0$ and corner layers near $(0,0)$ and $(0,1)$.

It is clear that the solutions of singularly perturbed partial differential equations can exhibit much more complex layer phenomena than can one-dimensional problems. In particular parabolic layers and corner layers cannot occur in the solution of ordinary differential equations. Further evidence that numerical methods with a fitted operator on a uniform mesh are inadequate for singularly perturbed problems is provided by considering a problem where parabolic boundary layers are present.

In [46] Shishkin showed that for a class of parabolic problems containing parabolic boundary layers there is no fitted operator method on a uniform mesh that is ε-uniform. A clearer demonstration in a simpler case can be found in Miller *et al* [35] and a similar result for a class of elliptic problems with parabolic boundary layers is given in Shihskin [43]. As parabolic layers only arise in solutions to partial differential equations this limitation of fitted operator methods can only be seen

when contemplating problems in more than one dimension. In contrast a numerical method consisting of a standard finite difference operator on an appropriately defined piecewise-uniform fitted mesh is robust and layer-resolving for a class of problems with parabolic boundary layers (see for example Miller *et al* [36]).

Another difficulty that arises when we consider problems in more than one dimension is the question of the existence and regularity of a classical solution. Roughly speaking, for problems posed on smooth domains the regularity of the solution is determined by the regularity of the data of the problem. A general theory for elliptic equations can be found in [26]. However, for problems such as (1.5.1) posed on a domain with a piecewise-smooth boundary, we need to impose additional conditions, known as compatibility conditions, in order for a similar statement to hold.

In [18] Han and Kellogg give sufficient conditions for the solution to (1.5.1) to be in $C^{3,\nu}(\overline{\Omega})$ under the assumption (1.5.2). These conditions are local conditions in the sense that they involve the boundary data and the coefficients of the differential equations evaluated at each of the corners of the square. Conditions that ensure more regularity are not in general local and there does not seem to be explicit formulae for them except in the case of constant coefficients.

If the appropriate compatibility conditions are not satisfied then the solution of a differential equation will in general possess corner singularities in a neighbourhood of the corners of the domain. In other words the solution will be regular in a classical sense up to a finite number of singular functions. The theory of corner singularities is presented in the books by Grisvard [16, 17] and Dauge [6] amongst others.

The situation is even more complex when the domain is non-rectangular. In this case it seems that no explicit formulae for the compatibility conditions exist to guarantee that the solution is even in $C^{3,\nu}(\overline{\Omega})$. In this thesis we will not study corner singularities that may be present in the solutions of problems such as (1.5.1). Thus to derive the main result in Chapter 4 we need to make an assumption that no such singularities exist in the solutions of problems from the class we are studying. As regards the convergence result that we prove, we can say that our numerical method is appropriate for resolving the boundary layers present in the regular (in a classical sense) part of the solution. Note that for the class of parabolic problems that we study in Chapter 3 it turns out that the compatibility conditions can be stated explicitly

and no equivalent assumption is needed.

The issue of compatibility conditions is of theoretical importance as the analysis of numerical methods for problems such as (1.5.1) usually requires a higher level of regularity of the solution than may be expected from practical problems. This is discussed in more detail in the next section.

1.6 Theoretical results for numerical methods based on piecewise-uniform fitted meshes

In this section we present a brief survey of the theoretical results that have been obtained for numerical methods based on piecewise-uniform fitted meshes for singularly perturbed problems involving PDEs. As already stated these methods have proved capable of application to quite general singular perturbation problems involving diverse kinds of layers. We intend to provide a sketch of the development of this theory for the Problem Class 1.5.1 under condition (1.5.2), i.e. when only regular and corner layers are present in the solution. We also provide a discussion of the analytical tools that have been employed. This will better enable us to put the results of this thesis into the proper context. For a more general discussion of layer-adapted meshes applied to singularly perturbed problems see the review articles [39] and [27].

It was first shown by Shishkin in [47], under certain strong assumptions on the regularity of the data of the problem and on the compatibility conditions, that a numerical method based on a piecewise-uniform fitted mesh and an upwind finite difference operator was ε-uniform when applied to a more general problem than that given in (1.5.1). The error estimate is of the form

$$\sup_{0<\varepsilon\leq 1} \left\| \overline{U}_{\varepsilon}^{N} - u_{\varepsilon} \right\|_{\overline{\Omega}} \leq CN^{-1}(\ln N)^2, \tag{1.6.1}$$

where the constants N_0 and C are independent of ε and N.

It should be noted however, that under much weaker assumptions the following bound was also proven [47, Chapter 3]

$$\sup_{0<\varepsilon\leq 1} \left\| \overline{U}_{\varepsilon}^{N} - u_{\varepsilon} \right\|_{\overline{\Omega}} \leq C(N^{-1}(\ln N)^2)^p, \tag{1.6.2}$$

where $p = 1/4$ or $1/8$ depending on the precise assumptions made.

The proof of estimates of the kind (1.6.1) generally requires precise bounds on the derivatives of the solution of the problem being studied. An asymptotic expansion of the solution while revealing about the layer structure of singularly perturbed problems, is inadequate for obtaining these bounds. Therefore a different approach must be taken. Shishkin introduced the following decomposition of the solution into a regular component and a layer component (sometimes referred to as a Shishkin splitting in the literature). Let

$$u = v + w, \tag{1.6.3a}$$

$$\text{where} \quad L_\varepsilon v = f, \quad L_\varepsilon w = 0, \tag{1.6.3b}$$

where L_ε is the differential operator in question. The key feature of this construction is that the component w, representing the boundary layer behaviour of the solution, is in the null space of the differential operator, L_ε. Shishkin employed this kind of decomposition in analysing methods for quite general problems (again see [47]). An analogous decomposition of the numerical solution can also be constructed and used to analyse the error in the numerical scheme.

Since these results appeared the complexity of the presentation and the implicitness of the assumptions in [47] have prompted efforts by various authors to provide a more constructive proof and to make the compatibility assumptions more precise. An initial effort was made by Miller *et al* in [35], where the maximum principle and barrier function technique first introduced by Kellogg and Tsan [22], is used along with the decomposition (1.6.3) to prove the estimate (1.6.1) in a simpler case. Flaws in this proof due to the compatibility assumptions were pointed out in Dobrowolski and Roos [9] where a splitting based on an asymptotic expansion was constructed to obtain the bounds on the derivatives. Linß and Stynes [30] employed a similar splitting and used it in [29] to analyse a hybrid difference scheme on a piecewise-uniform fitted mesh where the error bound derived was $\mathcal{O}(N^{-1})$. They also improved the error bound for the upwind scheme to $\mathcal{O}(N^{-1} \ln N)$. In [23] Kopteva provides an expansion of the error for the upwind scheme which requires less compatibility conditions than the other approaches but which is only valid in the perturbed case (i.e. when $\varepsilon \leq CN^{-1}$). She uses it to obtain error estimates for the Richardson extrapolation

technique and for the approximation of derivatives of the solution.

In the theoretical analysis in this thesis we shall use decompositions of the form (1.6.3) in conjunction with the maximum principle and barrier function technique. For this approach to work the finite difference operator must be monotone. If this is not the case then a different technique must be employed. One such technique is due to Andreev and Savin [3]. It involves bounding the discrete Green's function associated with the finite difference operator. It was used in Andreev and Kopteva [2] to prove an $\mathcal{O}((N^{-1}\ln N)^2)$ error estimate for the central difference scheme on a piecewise-uniform fitted mesh for the one-dimensional problem (1.2.1). A recent extension of the technique to the problem (1.5.1) can be found in [1], where it was used to obtain *a priori* estimates for the Green's function of a monotone difference scheme on an arbitrary mesh.

It should be noted that a lot of the technical considerations in the above papers related to the compatibility conditions can be circumvented if one uses the technique of extending the domain when one is defining the regular part of the decomposition. For an example of this see §4.4. Following on from the discussion in the previous section we remark that none of the work cited above considers problems where corner singularities are in general present in the solutions of the problem except for [47]. Also, in [49] Shishkin proves that for problem (1.5.1) with low regularity on the data of the problem and no compatibility, a numerical method based on a piecewise-uniform fitted mesh is ε-uniform with the error estimate

$$\sup_{0<\varepsilon\leq 1} \left\| \overline{U}_{\varepsilon}^{N} - u_{\varepsilon} \right\|_{\overline{\Omega}} \leq \mu(N), \tag{1.6.4}$$

where μ is independent of ε and $\mu(N) \to 0$ as $N \to \infty$.

1.7 Singularly perturbed problems on non-rectangular domains

It should be clear from the previous section that there exists a lot of results for methods involving piecewise-uniform fitted meshes even if we restrict ourselves to considering the model problem (1.5.1). However, all of the results quoted in the

previous section are only valid on a rectangular domain. It should be noted however that in [47] Shishkin gives appropriate constructions for convex polygonal domains but the results are not widely known. For non-convex domains see [48].

It is worth noting that it is somewhat more convenient to deal with more general domains when using finite element methods, as the geometry of the problem is naturally incorporated into the discretisation. However, as already stated the derivation of error estimates in the maximum norm, particularly for convection-diffusion problems is difficult. The main purpose of this thesis is to study the application of finite difference numerical methods for singularly perturbed problems on non-rectangular domains, and to derive error estimates of the kind presented in §1.6.

The procedure for this study is now outlined. Given a class of problems on a non-rectangular domain we make a change of variables to transform the class to an equivalent one on the usual rectangular domain. This simplification of the geometry produces a more complicated differential equation as the information about the geometry is incorporated into the coefficients of the equation. However, it is a convenient approach as it allows us to study problems defined on different types of domains in the one setting. It also more convenient from a practical point of view to design and implement a numerical method on a rectangular domain. As we are interested in employing meshes which are fitted to boundary layers, discretising on a possibly complicated domain could prove troublesome in general.

In Chapter 2 we begin our study of singularly perturbed problems posed on non-rectangular domains by considering a class of parabolic problems. Using a suitable co-ordinate transformation the problem is posed on a rectangular domain. The nature and location of some of the boundary layers that can occur are identified and subclasses of problems are defined that have the same behaviour. In the special case of a domain with straight line boundary and an equation with constant coefficients it is shown that it is possible to classify every possible problem into one of these subclasses. Numerical methods consisting of an upwind finite difference operator and an appropriate piecewise-uniform fitted mesh are constructed for each subclass. Numerical results are presented that show computationally that the methods described are ε-uniform for particular problems from each subclass. Finally, more complicated domains are considered and numerical results are presented for a sample problem.

In Chapter 3 theoretical results are presented for a numerical method applied to a class of parabolic problems with a boundary turning point. This class of problems is a slight generalisation of one identified in Chapter 2 whose solutions possess a parabolic boundary layer in a neighbourhood of $x = 0$. A numerical method based on a piecewise-uniform fitted mesh is constructed and it is shown that the numerical solutions generated by the method converge ε-uniformly to the solution of the continuous problem. Numerical results are presented that validate the theoretical result proven. Finally, a similar but related problem is examined. Some analysis is given that motivates the construction of an appropriate numerical method. Numerical results are provided that show computationally that the numerical solutions converge.

In Chapter 4 we move on to consider a class of elliptic problems on a non-rectangular domain. We restrict our attention to the case when only regular layers are present in the solutions of problems from this class. We assume that there exists a sufficiently regular co-ordinate transformation from the domain to the unit square. The transformed problem class is then studied. In contrast to the parabolic case we note the presence of a new term in the differential equation which contains the mixed derivative of the solution. This fact makes the construction and analysis of an appropriate numerical method much more difficult. Particular attention is paid to the establishment of a discrete comparison principle. In the perturbed case, i.e. when $\varepsilon \leq CN^{-1}$, it is shown that the numerical solutions generated by our method converge uniformly with respect to the singular perturbation parameter. This is the central result of the thesis.

In Chapter 5 we present extensive numerical results demonstrating the application of the method developed in Chapter 4. Firstly, in the case of a domain whose boundary is a parallelogram, we verify computationally the theoretical result proved in the previous chapter. Some of the computational issues related to the presence of the mixed derivative of the solution in the differential equation are then examined. We conclude the thesis with some numerical results where our method is applied to a problem posed on a domain whose boundary is more complicated. It is again demonstrated that the numerical solutions generated converge uniformly with respect to the singular perturbation parameter. We feel that this example offers an indication of the wider applicability of the method developed.

Chapter 2

Numerical methods for a class of singularly perturbed parabolic problems

2.1 Introduction

In this chapter we begin our study of singularly perturbed problems on non-rectangular domains by considering a parabolic problem posed on a domain with a piecewise-smooth boundary. Using a change of variables the problem is transformed to one on a rectangular domain. We are interested in the nature and location of the boundary layers that can occur in solutions to problems from this class. As the form of the differential equation is complicated in the general case we consider the special case when the boundary of the domain is made up of straight lines. It is then possible to identify all possible types of boundary layer behaviour.

This information enables us to construct numerical methods based on upwind finite difference operators and appropriate piecewise-uniform fitted meshes which resolve the layers present. It is shown computationally that each of these methods is ε-uniform when applied to particular problems. We also consider more general domains.

This chapter is organised as follows. In §2.2 we introduce a class of problems posed on a non-rectangular domain and perform a transformation of the independent

variables to obtain an equivalent class of problems posed on a rectangular domain. In §2.3 we consider a particularly simple kind of geometry, namely when the boundary of the original domain is given by straight lines. Each problem from the corresponding transformed problem class is then classified into a particular subclass according to the behaviour of the convective term in the differential equation. In §2.4 we identify the nature and location of the boundary layers that are present in the solutions of problems from each of the subclasses. In §2.5 we construct numerical methods that will resolve the layers present in each of the subclasses identified and in §2.6 we present detailed numerical results. Finally, in §2.7 we consider problems posed on more complicated domains and present some numerical results for a sample problem. Some of the material in this chapter has appeared in [10] and [11].

The computations in this chapter and the following one were performed using C++.

2.2 Statement of problem

We consider the following class of singularly perturbed parabolic problems

Problem Class 2.2.1.

$$\hat{L}_\varepsilon \hat{u}(\xi,t) \equiv (\varepsilon \hat{u}_{\xi\xi} + \hat{a}\hat{u}_\xi - \hat{b}\hat{u}_t - \hat{d}\hat{u})(\xi,t) = \hat{f}(\xi,t) \quad \text{in } \hat{\Omega}, \tag{2.2.1a}$$

$$\hat{u}(\xi,t) = \hat{g}(\xi,t) \quad \text{on } \Gamma = \overline{\hat{\Omega}} \setminus \hat{\Omega}, \tag{2.2.1b}$$

$$\hat{a}(\xi,t) \geq \hat{\alpha}, \qquad \hat{b}(\xi,t) \geq \hat{\beta} > 0, \qquad \hat{d}(\xi,t) \geq \hat{\delta} \geq 0, \qquad \forall (\xi,t) \in \overline{\hat{\Omega}}, \tag{2.2.1c}$$

where $\hat{\Omega} = (\phi_1(t), \phi_2(t)) \times (0,T]$ *is a non-rectangular domain bounded by the curves* $\xi = \phi_1(t)$, $\xi = \phi_2(t)$ *such that*

$$\phi_1(0) = 0, \quad \phi_2(0) = 1, \quad \phi_1(t) < \phi_2(t), \quad \forall t \in [0,T], \tag{2.2.2}$$

and $0 < \varepsilon \leq 1$ *is the perturbation parameter.*

We also assume that the data $\hat{a}, \hat{b}, \hat{d}, \hat{f}$, $\hat{g}$ and ϕ_1, ϕ_2 are sufficiently regular, and that f and g satisfy sufficient compatibility conditions at the corners of the domain.

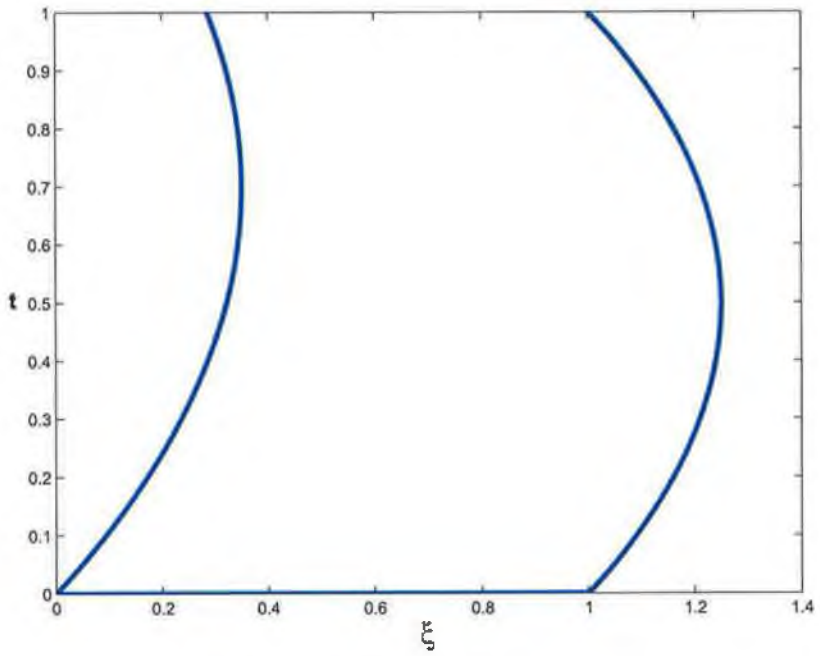

Figure 2.1: A non-rectangular domain $\hat{\Omega}$.

The problem is now transformed to one on a rectangular domain. This is achieved by introducing the new co-ordinate system (x, t) and the change of variables

$$x = x(\xi, t) \equiv \frac{\xi - \phi_1(t)}{\phi_2(t) - \phi_1(t)}, \tag{2.2.3}$$

Note that this transformation exists by virtue of (2.2.2). The transformed class of problems, P_ε, is then

Problem Class 2.2.2.

$$L_\varepsilon u(x,t) \equiv (\varepsilon u_{xx} + a u_x - b u_t - d u)(x,t) = f(x,t) \quad in \ \ \Omega, \tag{2.2.4a}$$

$$u(x,t) = g(x,t) \quad on \ \ \Gamma, \tag{2.2.4b}$$

where

$$\Omega = (0,1) \times (0,T], \quad \Gamma = \overline{\Omega} \setminus \Omega, \quad u(x,t) = \hat{u}(\xi,t),$$
$$a(x,t) = (\hat{a}(\xi,t) + \hat{b}(\xi,t)(x(\phi_2'(t) - \phi_1'(t)) + \phi_1'(t)))(\phi_2(t) - \phi_1(t)),$$
$$b(x,t) = \hat{b}(\xi,t)(\phi_2(t) - \phi_1(t))^2, \quad d(x,t) = \hat{d}(\xi,t)(\phi_2(t) - \phi_1(t))^2,$$
$$f(x,t) = \hat{f}(\xi,t)(\phi_2(t) - \phi_1(t))^2, \quad g(x,t) = \hat{g}(\xi,t),$$
$$\xi = \xi(x,t) \equiv x(\phi_2(t) - \phi_1(t)) + \phi_1(t).$$

Notice that irrespective of the functions ϕ_1 and ϕ_2,

$$b(x,t) > 0, \quad d(x,t) \geq 0, \quad \forall (x,t) \in \overline{\Omega},$$

similar to $\hat{b}$ and $\hat{d}$. However, in general, the behaviour of a may be such that it becomes zero or changes sign at certain points of the domain. When ε is small boundary layers of various types are in general present in solutions of problems from Problem Class 2.2.2, and it is precisely the behaviour of a that determines the nature and locations of these layers. Thus the choice of numerical method will depend critically on a which in turn depends on the relationship between the geometry of the original domain and the original coefficient functions.

Ideally we would like to identify all the possible types of layer behaviour that could appear in the solution to problems from the transformed class. If we could do this then it would be possible to decompose P_ε into distinct subclasses. Each subclass would consist of problems whose solution had similar behaviour (i.e. possessed the same type of layer in the same region of $\overline{\Omega}$). The reason for this is that we strive to design numerical methods that will be applicable to all problems with the same behaviour. Thus the classification of a particular problem into a subclass amounts to deciding what the appropriate numerical method to apply to the problem is.

The difficulty with this approach is that we must be able to determine, for all possible choices of a, the layer behaviour of the solution *a priori*. This is a difficult task in general so we will confine ourselves to some specific situations where this information can be determined. It will be shown in the next section that if the original domain is bounded by straight lines and the coefficient functions are constant then

a complete classification of every problem in the transformed problem class can be achieved. This enables us to explore in a relatively simple setting the diverse kinds of boundary layer behaviour that problems posed on the same geometry can exhibit.

2.3 Special case-straight line boundary

We will assume that the original domain has a boundary given by straight lines. That is we will assume that $\hat{\Omega} = \hat{\Omega}_L$ is a domain bounded by the lines

$$\phi_1(t) = -m_1 t, \quad \phi_2(t) = 1 - m_2 t, \quad \forall t \in [0, T],$$

where m_1 and m_2 are constants. For simplicity it is also assumed that the original coefficient functions are constant.

$$\hat{a}(\xi, t) = \hat{\alpha}, \quad \hat{b}(\xi, t) = \hat{\beta}, \quad \forall (\xi, t) \in \overline{\hat{\Omega}}.$$

The resulting transformed problem class, $P_\varepsilon^1 \subset P_\varepsilon$, is

Problem Class 2.3.1.

$$\begin{aligned} L_\varepsilon u(x,t) \equiv (\varepsilon u_{xx} + a u_x - b u_t - d u)(x,t) = f(x,t) \quad & \text{in } \Omega, \\ u(x,t) = g(x,t) \quad & \text{on } \Gamma, \end{aligned}$$

where

$$\begin{aligned} a(x,t) = h(t)(\hat{\alpha} - \hat{\beta}(x(m_2 - m_1) + m_1)), \quad b(x,t) = \hat{\beta}(h(t))^2, \\ d(x,t) = \hat{d}(\xi,t)(h(t))^2, \quad f(x,t) = \hat{f}(\xi,t)(h(t))^2, \quad g(x,t) = \hat{g}(\xi,t), \\ \xi = \xi(x,t) \equiv x h(t) - m_1 t, \quad h(t) = (1 - (m_2 - m_1)t). \end{aligned}$$

Note that $h(t) > 0$, which follows from condition (2.2.2).

The form of this problem class is sufficiently simple to allow us to identify all of the possible types of behaviour of a (i.e. different sign patterns) and the layer structure of the corresponding solutions. This will enable us to classify any problem from P_ε^1 into a subclass of P_ε. In this case we can identify nine such subclasses. These are

defined as follows:

$$P_\varepsilon^+ = \left\{ P_\varepsilon \,|\quad a(x,t) > 0, \quad \forall\, (x,t) \in \overline{\Omega} \right\},$$

$$P_\varepsilon^0 = \left\{ P_\varepsilon \,|\quad a(x,t) = 0, \quad \forall\, (x,t) \in \overline{\Omega} \right\},$$

$$P_\varepsilon^- = \left\{ P_\varepsilon \,|\quad a(x,t) < 0, \quad \forall\, (x,t) \in \overline{\Omega} \right\},$$

$$P_\varepsilon^{0+} = \left\{ P_\varepsilon \;\middle|\; a(x,t) \begin{cases} = 0 & x = 0, \quad \forall t \in [0,T] \\ > 0 & 0 < x \le 1, \quad \forall t \in [0,T] \end{cases} \right\},$$

$$P_\varepsilon^{0-} = \left\{ P_\varepsilon \;\middle|\; a(x,t) \begin{cases} = 0 & x = 0, \quad \forall t \in [0,T] \\ < 0 & 0 < x \le 1, \quad \forall t \in [0,T] \end{cases} \right\},$$

$$P_\varepsilon^{-0} = \left\{ P_\varepsilon \;\middle|\; a(x,t) \begin{cases} < 0 & 0 \le x < 1, \quad \forall t \in [0,T] \\ = 0 & x = 1, \quad \forall t \in [0,T] \end{cases} \right\},$$

$$P_\varepsilon^{+0} = \left\{ P_\varepsilon \;\middle|\; a(x,t) \begin{cases} > 0 & 0 \le x < 1, \quad \forall t \in [0,T] \\ = 0 & x = 1, \quad \forall t \in [0,T] \end{cases} \right\},$$

$$P_\varepsilon^{-+} = \left\{ P_\varepsilon \;\middle|\; a(x,t) \begin{cases} < 0 & x < \zeta, \quad \forall t \in [0,T] \\ = 0 & x = \zeta, \quad \forall t \in [0,T] \\ > 0 & x > \zeta, \quad \forall t \in [0,T] \end{cases} \right\},$$

$$P_\varepsilon^{+-} = \left\{ P_\varepsilon \;\middle|\; a(x,t) \begin{cases} > 0 & x < \zeta, \quad \forall t \in [0,T] \\ = 0 & x = \zeta, \quad \forall t \in [0,T] \\ < 0 & x > \zeta, \quad \forall t \in [0,T] \end{cases} \right\},$$

where $\zeta \in (0,1)$.

Of course these nine subclasses are properly contained in $\hat{P}_\varepsilon$. That is

$$P_\varepsilon^+ \cup P_\varepsilon^0 \cup P_\varepsilon^- \cup P_\varepsilon^{0+} \cup P_\varepsilon^{0-} \cup P_\varepsilon^{-0} \cup P_\varepsilon^{+0} \cup P_\varepsilon^{-+} \cup P_\varepsilon^{+-} \subsetneqq P_\varepsilon.$$

Actually we need only be concerned with six of these subclasses as three pairs of them, *viz.* $(P_\varepsilon^+, P_\varepsilon^-)$, $(P_\varepsilon^{0+}, P_\varepsilon^{-0})$ and $(P_\varepsilon^{0-}, P_\varepsilon^{+0})$, are equivalent under the transformation $\tilde{x} = 1 - x$.

Now we may state simple relationships between the slopes of the lines defining

the boundary, m_1 and m_2, and the coefficients, $\hat{\alpha}$ and $\hat{\beta}$, which determine if a given problem in P_ε^1 will be an element of a certain subclass of P_ε. These are shown in Table 2.1. The form of the transformed function, a, is also given to show that it has the required behaviour. The constants γ, γ_1 and γ_2 are all strictly positive. The value of ζ is the same for the two applicable cases:

$$\zeta = \frac{\hat{\alpha} - \hat{\beta} m_1}{\hat{\beta}(m_2 - m_1)}$$

and we clearly have $\zeta \in (0, 1)$.

2.4 Location and nature of boundary layers

In the final column of Table 2.1 we have indicated the location of the kinds of boundary layers that can occur in the solutions of particular problems from P_ε^1. In this section we show how this information can be determined. To do this we will consider the original problem class 2.2.1 corresponding to P_ε^1 where the boundary is given by straight lines and show how the relationship between the geometry of the domain and the coefficients in the differential equation give rise to boundary layers in the solutions to problems from this class.

The reduced problem corresponding to (2.2.1a) is obtained by formally setting $\varepsilon = 0$. This gives us the first order hyperbolic partial differential equation

$$(\hat{a} v_\xi - \hat{b} v_t - \hat{d} v)(\xi, t) = \hat{f}(\xi, t) \quad \text{in } \hat{\Omega}. \tag{2.4.1}$$

As we have assumed that $\hat{a}$ and $\hat{b}$ are constant this becomes the simpler

$$(\hat{\alpha} v_\xi - \hat{\beta} v_t - \hat{d} v)(\xi, t) = \hat{f}(\xi, t) \quad \text{in } \hat{\Omega}.$$

It is clear that we cannot impose all of the boundary conditions (2.2.1b) on v as this reduced problem is only of first order. To figure out on which part of $\hat{\Gamma}$ we can specify conditions we consider the characteristic curves of the reduced problem. It can be

Case	Condition	Subclass	$a(x,t)$	Behaviour
$m_1 > m_2$	$\hat{\alpha} = \hat{\beta} m_1$	P_ε^{0+}	$h(t)\gamma x$	P.L. near $x = 0$
	$\hat{\alpha} = \hat{\beta} m_2$	P_ε^{-0}	$-h(t)\gamma(1-x)$	P.L. near $x = 1$
	$\hat{\beta} m_2 < \hat{\alpha} < \hat{\beta} m_1$	P_ε^{-+}	$h(t)\gamma(x-\zeta)$	Smooth
	$\hat{\alpha} > \hat{\beta} m_1$	P_ε^{+}	$h(t)(\gamma_1 + \gamma_2 x)$	R.L. near $x = 0$
	$\hat{\alpha} < \hat{\beta} m_2$	P_ε^{-}	$-h(t)(\gamma_1 - \gamma_2 x), \quad \gamma_1 > \gamma_2$	R.L. near $x = 1$
$m_2 > m_1$	$\hat{\alpha} = \hat{\beta} m_1$	P_ε^{0-}	$-h(t)\gamma x$	P.L. near $x = 0$, R.L. near $x = 1$
	$\hat{\alpha} = \hat{\beta} m_2$	P_ε^{+0}	$h(t)\gamma(1-x)$	R.L. near $x = 0$, P.L. near $x = 1$
	$\hat{\beta} m_1 < \hat{\alpha} < \hat{\beta} m_2$	P_ε^{+-}	$h(t)\gamma(\zeta - x)$	R.L. near $x = 0$, R.L. near $x = 1$
	$\hat{\alpha} < \hat{\beta} m_1$	P_ε^{-}	$-h(t)(\gamma_1 + \gamma_2 x)$	R.L. near $x = 1$
	$\hat{\alpha} > \hat{\beta} m_2$	P_ε^{+}	$h(t)(\gamma_1 - \gamma_2 x), \quad \gamma_1 > \gamma_2$	R.L. near $x = 0$
$m_1 = m_2$	$\hat{\alpha} = \hat{\beta} m_1$	P_ε^{0}	0	P.L. near $x = 0$, P.L. near $x = 1$
	$\hat{\alpha} > \hat{\beta} m_1$	P_ε^{+}	γ	R.L. near $x = 0$
	$\hat{\alpha} < \hat{\beta} m_1$	P_ε^{-}	$-\gamma$	R.L. near $x = 1$

Table 2.1: Classification of problems from P_ε^1, R.L.=Regular Layer, P.L.=Parabolic Layer.

easily shown that these are the straight lines given by

$$\xi = -\frac{\hat{\alpha}}{\hat{\beta}}t + c.$$

where c is an arbitrary constant. Along each characteristic the reduced equation becomes the first order ordinary differential equation

$$v_s - \hat{d}v = \hat{f}$$

which means that if v is specified at any point on a characteristic then its value at all other points on the characteristic is fully determined.

As $\hat{\beta}$ is strictly positive it follows that the characteristics are oriented positively in time. So the value of v on each of the characteristics is determined by the boundary value at the point on the boundary where they begin. The set of all such points is called the inflow boundary. Similarly the set of all points on the boundary that are endpoints of characteristics is called the outflow boundary, and a region of the boundary that is itself a characteristic of the reduced problem is called the characteristic part of the boundary. We denote these regions by $\hat{\Gamma}_I$, $\hat{\Gamma}_O$ and $\hat{\Gamma}_C$ respectively. We have $\hat{\Gamma} = \hat{\Gamma}_I \cup \hat{\Gamma}_O \cup \hat{\Gamma}_C$. Clearly, the relationships between the slopes of the characteristics and the slopes of the boundary walls determine what parts of the boundary belong to which set (Figures 2.2 and 2.3).

It can be shown that for points on $\hat{\Gamma}$ that are not part of the inflow boundary the solution of the reduced problem will not in general be equal to that of the full problem and thus we will have a boundary layer in a neighbourhood of these points. There are many different types of boundary layers but we will be concerned with just two distinct types, *viz.* regular boundary layers and parabolic boundary layers. It can be shown using the techniques of matched asymptotic expansions (see [21] and [13]) that the solution of the original problem will have a regular layer in a neighbourhood of $\hat{\Gamma}_O$ and a parabolic layer in a neighbourhood of $\hat{\Gamma}_C$. The width of the regular layers in all cases is $\mathcal{O}(\varepsilon)$ while the parabolic layers have width $\mathcal{O}(\sqrt{\varepsilon})$.

In terms of the transformed problem class the existence of a regular layer near $\xi = \phi_1$ for example, corresponds to a regular layer near $x = 0$ as $\xi = \phi_1$ is mapped to $x = 0$ by the transformation (2.2.3), with similar statements for the other types of

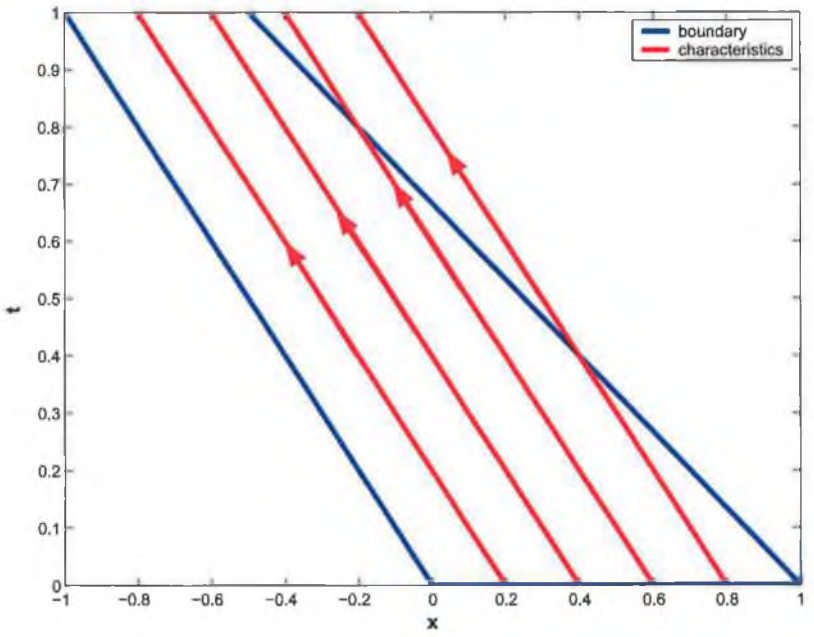

Figure 2.2: Characteristic curves of the reduced problem (2.4.1) in the case $P_\varepsilon^{0,-}$.

behaviour.

We will not be concerned with problems from subclass P_ε^{-+} as there are in general no boundary layers present in their solutions and standard numerical methods suffice for generating adequate approximations. It is well known that this is not the case for problems from the other subclasses where boundary layers are present.

In Chapter 3 we will develop a numerical method that is adequate for resolving the layers that are present in problems from a more general class than $P_\varepsilon^1 \cap P_\varepsilon^{0+}$. We will consider problems where we have

$$a(x,t) = a_0(x,t)x^p, \quad p \geq 1, \quad a_0(x,t) > 0,$$

which corresponds to the form of a in problems from $P_\varepsilon^1 \cap P_\varepsilon^{0+}$ when $p = 1$ (see Table 2.1). Therefore, in this chapter we will not concern ourselves any further with problems from $P_\varepsilon^1 \cap P_\varepsilon^{0+}$.

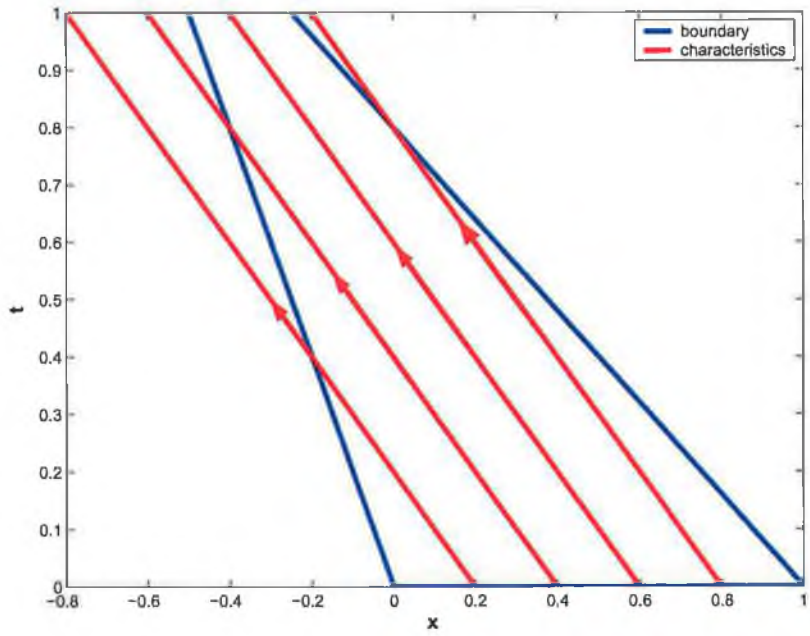

Figure 2.3: Characteristic curves of the reduced problem (2.4.1) in the case $P_\varepsilon^{+,-}$.

In the next section we will construct appropriate numerical methods to resolve the layers that are present in all problems from P_ε^1 except those in the two subclasses mentioned above. That is we are concerned with generating numerical solutions to problems from the intersections between problem class P_ε^1 and the four subclasses of the general problem class P_ε:

$$P_\varepsilon^1 \cap P_\varepsilon^+, P_\varepsilon^1 \cap P_\varepsilon^0, P_\varepsilon^1 \cap P_\varepsilon^{0-}, P_\varepsilon^1 \cap P_\varepsilon^{+-}. \tag{2.4.2}$$

Note that while we now deal exclusively with problems from the transformed class, the numerical methods we design will provide us with adequate numerical solutions to problems from the original class as well, because the two classes are equivalent under the transformation (2.2.3). We implement the numerical methods on the transformed domain as it is more convenient computationally to deal with a rectangular geometry.

2.5 Numerical methods

We now construct numerical methods that will generate approximations to solutions of problems from each of the four classes in (2.4.2). These consist of an upwind finite difference operator, and an appropriate piecewise-uniform fitted mesh. The difference operator L_ε^N, on a mesh Ω^N, is defined for any mesh function Z^N, as

$$L_\varepsilon^N Z^N(x_i,t_j) \equiv (\varepsilon\delta_x^2 Z^N + aD_x^S Z^N - bD_t^- Z^N - dZ^N)(x_i,t_j), \quad \forall (x_i,t_j)\in\Omega^N,$$

where

$$D_x^S Z^N(x_i,t_j) = \begin{cases} D_x^+ Z^N(x_i,t_j), & a(x_i,t_j) > 0 \\ 0, & a(x_i,t_j) = 0 \\ D_x^- Z^N(x_i,t_j), & a(x_i,t_j) < 0 \end{cases}.$$

Note that the definition of D_x^S assures us that L_ε^N satisfies a discrete comparison principle and is thus a monotone difference operator.

We use N_x mesh intervals in the x co-ordinate direction and N_t mesh intervals in the t co-ordinate direction. Define the mesh, $\overline{\Omega}_u^{N_t}$, that discretises $[0,T]$ with N_t uniform mesh elements, as

$$\overline{\Omega}_u^{N_t} = \{t_j \mid t_j = j/N_t, \quad 0\le j\le N_t\},$$

and the piecewise-uniform meshes, $\overline{\Omega}_\sigma^{N_x}$ and $\overline{\Omega}_{\tau_1,\tau_2}^{N_x}$, that discretise $\overline{\Omega}=[0,1]$ with N_x mesh elements, as

$$\overline{\Omega}_\sigma^{N_x} = \left\{ x_i \middle| x_i = \begin{cases} 2i\sigma/N_x & 0\le i\le N_x/2 \\ \sigma + 2(i-N_x/2)(1-\sigma)/N_x & N_x/2 < i \le N_x \end{cases} \right\},$$

$$\overline{\Omega}_{\tau_1,\tau_2}^{N_x} = \left\{ x_i \middle| x_i = \begin{cases} 4i\tau_1/N_x & 0\le i\le N_x/4 \\ \tau_1 + 2(i-N_x/4)(\tau_2-\tau_1)/N_x & N_x/4 < i \le 3N_x/4 \\ \tau_1 + 4(i-3N_x/4)(1-\tau_2)/N_x & 3N_x/4 < i \le N_x \end{cases} \right\}.$$

It can be seen that $\overline{\Omega}_\sigma^{N_x}$ consists of two uniform meshes, with $N_x/2$ mesh elements, joined together at the transition point σ and that $\overline{\Omega}_{\tau_1,\tau_2}^{N_x}$ consists of three uniform meshes, with $N_x/4$, $N_x/2$ and $N_x/4$ mesh elements, respectively, joined at the two

transition points τ_1 and τ_2. Clearly we must take N_x to be a multiple of 2 when using the first mesh and a multiple of 4 when using the second mesh. We intend to apply the first mesh to problems that possess a boundary layer near $x = 0$ and the second mesh to problems that have boundary layers near both $x = 0$ and $x = 1$. The transition points will be chosen appropriately according to the particular problem class.

We define the resulting piecewise uniform fitted meshes to be the tensor products

$$\overline{\Omega}_{\sigma}^{N} = \overline{\Omega}_{\sigma}^{N_x} \times \overline{\Omega}_{u}^{N_t}, \tag{2.5.1}$$

$$\overline{\Omega}_{\tau_1,\tau_2}^{N} = \overline{\Omega}_{\tau_1,\tau_2}^{N_x} \times \overline{\Omega}_{u}^{N_t}. \tag{2.5.2}$$

Setting $\Gamma_{\sigma}^{N} = \overline{\Omega}_{\sigma}^{N} \cap \Gamma$ and $\Gamma_{\tau_1,\tau_2}^{N} = \overline{\Omega}_{\tau_1,\tau_2}^{N} \cap \Gamma$ gives us the following fitted mesh finite difference methods

Method 2.5.1.

$$\begin{aligned} L_{\varepsilon}^{N} U^{N}(x_i,t_j) &= f(x_i,t_j) \quad \text{in } \Omega_{\tau_1,\tau_2}^{N_x}, \\ U^{N}(x_i,t_j) &= g(x_i,t_j) \quad \text{on } \Gamma_{\sigma}^{N}. \end{aligned}$$

Method 2.5.2.

$$\begin{aligned} L_{\varepsilon}^{N} U^{N}(x_i,t_j) &= f(x_i,t_j) \quad \text{in } \Omega_{\tau_1,\tau_2}^{N}, \\ U^{N}(x_i,t_j) &= g(x_i,t_j) \quad \text{on } \Gamma_{\tau_1,\tau_2}^{N}. \end{aligned}$$

Finally we specify for each of the four problem classes in (2.4.2) the appropriate numerical method and the correct choice for the transition point(s) in each case. These are stated in Table 2.2. Note that α is the lower/upper bound on a.

We now state known theoretical results concerning the first two methods given in Table 2.2.

Theorem 2.5.1. *For problems from class P_{ε}^{+}, which are sufficiently compatible at the corners, the numerical approximations generated by Method 2.5.1 with σ defined*

Problem Class	Method	Transition Point(s)
$P_\varepsilon^1 \cap P_\varepsilon^+$	2.5.1	$\sigma = \min\left\{\frac{1}{2}, \frac{\varepsilon}{\alpha}\ln N_x\right\}$
$P_\varepsilon^1 \cap P_\varepsilon^0$	2.5.2	$\tau_1 = \min\left\{\frac{1}{4}, 2\sqrt{\varepsilon}\ln N_x\right\},\ \tau_2 = 1-\tau_1$
$P_\varepsilon^1 \cap P_\varepsilon^{0-}$	2.5.2	$\tau_1 = \min\left\{\frac{1}{4}, \sqrt{\varepsilon}\ln N_x\right\},\ \tau_2 = 1-\min\left\{\frac{1}{4}, \frac{\varepsilon}{\alpha}\ln N_x\right\}$
$P_\varepsilon^1 \cap P_\varepsilon^{+-}$	2.5.2	$\tau_1 = \min\left\{\frac{1}{4}, \frac{\varepsilon}{\alpha}\ln N_x\right\},\ \tau_2 = 1-\tau_1$

Table 2.2: Appropriate numerical methods and transition points for each of the classes (2.4.2).

as in Table 2.2 are ε-uniform and satisfy the following error estimate

$$\sup_{0<\varepsilon\leq 1}\left\|\overline{U}^N - u\right\|_{\overline{\Omega}} \leq CN_x^{-1}(\ln N_x)^2 + CN_t^{-1},$$

where C is a constant independent of N_x, N_t and ε.

Proof. See, for example, Shishkin [47]. □

Theorem 2.5.2. *For problems from class P_ε^0, which are sufficiently compatible at the corners, the numerical approximations generated by Method 2.5.2 with τ_1 and τ_2 defined as in Table 2.2 are ε-uniform and satisfy the following error estimate*

$$\sup_{0<\varepsilon\leq 1}\left\|\overline{U}^N - u\right\|_{\overline{\Omega}} \leq C(N_x^{-1}\ln N_x)^2 + CN_t^{-1},$$

where C is a constant independent of N_x, N_t and ε.

Proof. See, for example, Miller *et al.* [36]. □

2.6 Numerical results

In this section we present comprehensive numerical results that demonstrate the numerical methods introduced in §2.5 applied to each of the problem classes given in

Example	m_1	m_2	Subclass
1	0.5	0.25	$\hat{P}_\varepsilon^1 \cap \hat{P}_\varepsilon^+$
2	1.0	1.0	$\hat{P}_\varepsilon^1 \cap \hat{P}_\varepsilon^0$
3	1.0	1.5	$\hat{P}_\varepsilon^1 \cap \hat{P}_\varepsilon^{0-}$
4	0.5	1.25	$\hat{P}_\varepsilon^1 \cap \hat{P}_\varepsilon^{+-}$

Table 2.3: Example problems.

(2.4.2). This will verify computationally Theorems 2.5.1 and 2.5.2. It will also demonstrate experimentally that the other methods resolve the layers that are present in the solutions of the corresponding problem classes. To this end we consider the following problem posed on the domain $\hat{\Omega}_L$. Note that we take $T = 1$.

Problem Class 2.6.1.

$$\begin{aligned} (\varepsilon u_{\xi\xi} + u_\xi - u_t - u)(x,t) &= -\xi - 1 \quad in \quad \hat{\Omega}_L, \\ u(\xi,0) &= 1 - \xi^2, \quad \xi \in [0,1], \\ u(-m_1 t, t) = 1, \quad u(1 - m_2 t, t) &= 0, \quad t \in (0,1]. \end{aligned}$$

We can construct a problem from each of the four subclasses using this problem posed on various (similar) domains. This will show quite explicitly that the nature of the layers present in the solution of a problem from Problem Class 2.2.1 depends critically on the geometry of the domain. In Table 2.3 we show appropriate values of m_1 and m_2 that give us an example problem from each of the subclasses.

To generate approximate solutions to each of the examples we apply the appropriate numerical method given in Table 2.2. We let $N_x = N_t = N$ and tabulate the computed errors, E_ε^N, and the computed ε-uniform errors, E^N, for a variety of values of ε and N for each of the examples given. As we do not have an exact solution for any of the problems we use the piecewise bilinear interpolant of the numerical solution generated by the appropriate method on the finest available mesh, *viz.* $\overline{U}^{1024}$, as our approximation to the exact solution. Thus we define E_ε^N and E^N as follows

$$E_\varepsilon^N = \max_{0 \le i,j \le N} |U^N(x_i,t_j) - \overline{U}^{1024}(x_i,t_j)|, \quad E^N = \max_{\varepsilon = 1, 2^{-1}, \ldots, 2^{-32}} E_\varepsilon^N.$$

The values of these quantities for each of the numerical methods applied to the appropriate example problems are shown in Tables 2.4-2.7. Note that the vertical dot notation indicates that in each column the errors have stabilised and remain essentially constant for each of the values of ε omitted. In each table we see that the values of E_ε^N for each fixed ε decrease with increasing N. *A fortiori* the values of E^N decrease with increasing N indicating that the convergence is uniform with respect to ε. These results indicate that each of the methods are layer-resolving for the corresponding example problems.

We also present graphs of some representative numerical solutions generated by each of the numerical methods applied to the corresponding examples for particular values of ε and N. We choose to plot these graphs on the original domain as it illustrates more clearly the effect of the geometry.

2.7 More complicated domains

In this section we will look at some problems where the boundary of the domain is more complicated than those considered thus far. Assume that the sides of the original domain are parallel. That is we will assume that $\hat{\Omega} = \hat{\Omega}_P$ is a domain bounded by the lines

$$\phi_1(t) = \phi(t), \quad \phi_2(t) = 1 + \phi(t), \quad \forall t \in [0, T],$$

where ϕ is sufficiently regular. The resulting transformed problem class, P_ε^2 is

Problem Class 2.7.1.

$$\begin{aligned} L_\varepsilon u(x,t) \equiv (\varepsilon u_{xx} + a u_x - b u_t - d u)(x,t) = f(x,t) \quad & in \ \ \Omega, \\ u(x,t) = g(x,t) \quad & on \ \ \Gamma, \end{aligned}$$

where

$$\begin{aligned} a(x,t) = \hat{a}(\xi,t) + \hat{b}(\xi,t)\phi'(t), \quad b(x,t) = \hat{b}(\xi,t), \quad d(x,t) = \hat{d}(\xi,t), \\ f(x,t) = \hat{f}(\xi,t), \quad g(x,t) = \hat{g}(\xi,t), \quad \xi = \xi(x,t) \equiv x + \phi(t). \end{aligned}$$

ε	Number of Intervals N					
	8	16	32	64	128	256
1	3.11e-02	1.82e-02	1.01e-02	5.21e-03	2.52e-03	1.10e-03
2^{-1}	1.29e-02	7.48e-03	3.94e-03	1.97e-03	9.34e-04	4.04e-04
2^{-2}	1.51e-02	8.01e-03	4.03e-03	1.98e-03	9.28e-04	3.99e-04
2^{-3}	3.03e-02	1.59e-02	8.07e-03	3.96e-03	1.86e-03	8.01e-04
2^{-4}	6.30e-02	3.04e-02	1.35e-02	5.85e-03	2.75e-03	1.19e-03
2^{-5}	8.86e-02	4.69e-02	2.35e-02	1.12e-02	5.06e-03	2.08e-03
2^{-6}	1.04e-01	5.80e-02	3.03e-02	1.52e-02	7.18e-03	3.08e-03
2^{-7}	1.13e-01	6.49e-02	3.51e-02	1.83e-02	8.98e-03	3.98e-03
2^{-8}	1.18e-01	6.88e-02	3.84e-02	2.07e-02	1.05e-02	4.81e-03
2^{-9}	1.21e-01	7.12e-02	4.06e-02	2.24e-02	1.18e-02	5.55e-03
2^{-10}	1.22e-01	7.26e-02	4.19e-02	2.36e-02	1.27e-02	6.14e-03
2^{-11}	1.23e-01	7.34e-02	4.27e-02	2.43e-02	1.33e-02	6.55e-03
2^{-12}	1.23e-01	7.39e-02	4.32e-02	2.48e-02	1.36e-02	6.81e-03
2^{-13}	1.23e-01	7.41e-02	4.34e-02	2.50e-02	1.38e-02	6.96e-03
2^{-14}	1.23e-01	7.42e-02	4.36e-02	2.51e-02	1.39e-02	7.03e-03
2^{-15}	1.24e-01	7.43e-02	4.36e-02	2.52e-02	1.40e-02	7.07e-03
2^{-16}	1.24e-01	7.43e-02	4.37e-02	2.52e-02	1.40e-02	7.10e-03
2^{-17}	1.24e-01	7.44e-02	4.37e-02	2.52e-02	1.40e-02	7.11e-03
2^{-18}	1.24e-01	7.44e-02	4.37e-02	2.52e-02	1.40e-02	7.11e-03
2^{-19}	1.24e-01	7.44e-02	4.37e-02	2.53e-02	1.40e-02	7.11e-03
2^{-20}	1.24e-01	7.44e-02	4.37e-02	2.53e-02	1.40e-02	7.11e-03
2^{-21}	1.24e-01	7.44e-02	4.37e-02	2.53e-02	1.40e-02	7.12e-03
2^{-22}	1.24e-01	7.44e-02	4.37e-02	2.53e-02	1.40e-02	7.12e-03
2^{-23}	1.24e-01	7.44e-02	4.37e-02	2.53e-02	1.40e-02	7.12e-03
2^{-24}	1.24e-01	7.44e-02	4.37e-02	2.53e-02	1.40e-02	7.12e-03
$\vdots$	$\vdots$	$\vdots$	$\vdots$	$\vdots$	$\vdots$	$\vdots$
2^{-32}	1.24e-01	7.44e-02	4.37e-02	2.53e-02	1.40e-02	7.12e-03
E^N	1.24e-01	7.44e-02	4.37e-02	2.53e-02	1.40e-02	7.12e-03

Table 2.4: Computed errors, E_ε^N, and computed ε-uniform errors, E^N, for appropriate method chosen from Table 2.2 applied to example 1.

ε	Number of Intervals N					
	8	16	32	64	128	256
1	2.93e-02	1.70e-02	9.10e-03	4.64e-03	2.22e-03	9.67e-04
2^{-1}	2.56e-02	1.27e-02	6.26e-03	3.03e-03	1.41e-03	6.05e-04
2^{-2}	3.58e-02	1.81e-02	9.01e-03	4.38e-03	2.05e-03	8.78e-04
2^{-3}	3.82e-02	1.96e-02	9.81e-03	4.78e-03	2.24e-03	9.61e-04
2^{-4}	4.14e-02	2.09e-02	1.03e-02	4.96e-03	2.32e-03	9.93e-04
2^{-5}	4.92e-02	2.40e-02	1.17e-02	5.59e-03	2.60e-03	1.11e-03
2^{-6}	5.44e-02	2.63e-02	1.26e-02	5.98e-03	2.77e-03	1.18e-03
2^{-7}	6.25e-02	2.91e-02	1.35e-02	6.29e-03	2.89e-03	1.23e-03
2^{-8}	6.44e-02	3.41e-02	1.48e-02	6.69e-03	3.01e-03	1.27e-03
2^{-9}	6.49e-02	4.00e-02	1.99e-02	7.38e-03	3.18e-03	1.31e-03
2^{-10}	6.55e-02	4.02e-02	2.47e-02	1.11e-02	3.70e-03	1.39e-03
2^{-11}	6.59e-02	4.03e-02	2.47e-02	1.16e-02	4.53e-03	1.64e-03
2^{-12}	6.62e-02	4.03e-02	2.49e-02	1.14e-02	4.42e-03	1.50e-03
2^{-13}	6.64e-02	4.04e-02	2.49e-02	1.15e-02	4.42e-03	1.50e-03
2^{-14}	6.65e-02	4.04e-02	2.49e-02	1.15e-02	4.43e-03	1.51e-03
2^{-15}	6.66e-02	4.05e-02	2.50e-02	1.15e-02	4.43e-03	1.51e-03
2^{-16}	6.67e-02	4.05e-02	2.50e-02	1.15e-02	4.43e-03	1.51e-03
2^{-17}	6.67e-02	4.05e-02	2.50e-02	1.15e-02	4.43e-03	1.51e-03
2^{-18}	6.68e-02	4.05e-02	2.50e-02	1.15e-02	4.43e-03	1.51e-03
2^{-19}	6.68e-02	4.05e-02	2.50e-02	1.15e-02	4.43e-03	1.51e-03
2^{-20}	6.68e-02	4.06e-02	2.50e-02	1.15e-02	4.43e-03	1.51e-03
2^{-21}	6.68e-02	4.06e-02	2.50e-02	1.15e-02	4.43e-03	1.51e-03
2^{-22}	6.68e-02	4.06e-02	2.50e-02	1.15e-02	4.43e-03	1.51e-03
2^{-23}	6.68e-02	4.06e-02	2.50e-02	1.15e-02	4.43e-03	1.51e-03
2^{-24}	6.69e-02	4.06e-02	2.50e-02	1.15e-02	4.43e-03	1.51e-03
$\vdots$	$\vdots$	$\vdots$	$\vdots$	$\vdots$	$\vdots$	$\vdots$
2^{-32}	6.69e-02	4.06e-02	2.50e-02	1.15e-02	4.43e-03	1.51e-03
E^N	6.69e-02	4.06e-02	2.50e-02	1.16e-02	4.53e-03	1.64e-03

Table 2.5: Computed errors, E_ε^N, and computed ε-uniform errors, E^N, for appropriate method chosen from Table 2.2 applied to example 2.

ε	Number of Intervals N					
	8	16	32	64	128	256
1	3.35e-02	1.88e-02	9.95e-03	5.01e-03	2.39e-03	1.03e-03
2^{-1}	3.33e-02	1.72e-02	8.60e-03	4.19e-03	1.97e-03	8.44e-04
2^{-2}	3.89e-02	1.99e-02	9.99e-03	4.87e-03	2.28e-03	9.78e-04
2^{-3}	4.19e-02	2.12e-02	1.06e-02	5.14e-03	2.40e-03	1.03e-03
2^{-4}	5.70e-02	3.14e-02	1.63e-02	8.21e-03	3.90e-03	1.69e-03
2^{-5}	6.43e-02	4.78e-02	3.16e-02	1.88e-02	9.16e-03	4.00e-03
2^{-6}	7.37e-02	5.87e-02	3.74e-02	2.19e-02	1.19e-02	5.77e-03
2^{-7}	8.80e-02	7.99e-02	5.02e-02	2.74e-02	1.40e-02	6.54e-03
2^{-8}	9.59e-02	9.91e-02	6.96e-02	3.88e-02	1.83e-02	7.89e-03
2^{-9}	9.89e-02	1.10e-01	8.56e-02	5.51e-02	2.92e-02	1.25e-02
2^{-10}	9.93e-02	1.14e-01	9.43e-02	6.63e-02	3.94e-02	1.91e-02
2^{-11}	9.78e-02	1.15e-01	9.72e-02	7.14e-02	4.58e-02	2.45e-02
2^{-12}	9.53e-02	1.13e-01	9.65e-02	7.21e-02	4.78e-02	2.71e-02
2^{-13}	9.28e-02	1.11e-01	9.45e-02	7.05e-02	4.71e-02	2.73e-02
2^{-14}	9.08e-02	1.10e-01	9.26e-02	6.85e-02	4.57e-02	2.65e-02
2^{-15}	8.98e-02	1.08e-01	9.13e-02	6.70e-02	4.44e-02	2.57e-02
2^{-16}	8.91e-02	1.08e-01	9.05e-02	6.61e-02	4.37e-02	2.51e-02
2^{-17}	8.87e-02	1.07e-01	9.01e-02	6.56e-02	4.32e-02	2.47e-02
2^{-18}	8.84e-02	1.07e-01	8.99e-02	6.53e-02	4.30e-02	2.45e-02
2^{-19}	8.83e-02	1.07e-01	8.97e-02	6.52e-02	4.28e-02	2.45e-02
2^{-20}	8.82e-02	1.07e-01	8.97e-02	6.51e-02	4.28e-02	2.44e-02
2^{-21}	8.81e-02	1.07e-01	8.96e-02	6.51e-02	4.27e-02	2.44e-02
2^{-22}	8.81e-02	1.07e-01	8.96e-02	6.50e-02	4.27e-02	2.44e-02
2^{-23}	8.80e-02	1.07e-01	8.96e-02	6.50e-02	4.27e-02	2.44e-02
2^{-24}	8.80e-02	1.07e-01	8.96e-02	6.50e-02	4.27e-02	2.44e-02
$\vdots$	$\vdots$	$\vdots$	$\vdots$	$\vdots$	$\vdots$	$\vdots$
2^{-32}	8.80e-02	1.07e-01	8.96e-02	6.50e-02	4.27e-02	2.43e-02
E^N	9.93e-02	1.15e-01	9.72e-02	7.21e-02	4.78e-02	2.73e-02

Table 2.6: Computed errors, E_ε^N, and computed ε-uniform errors, E^N, for appropriate method chosen from Table 2.2 applied to example 3.

ε	Number of Intervals N					
	8	16	32	64	128	256
1	4.18e-02	2.40e-02	1.29e-02	6.52e-03	3.12e-03	1.35e-03
2^{-1}	4.11e-02	2.16e-02	1.09e-02	5.33e-03	2.50e-03	1.08e-03
2^{-2}	5.17e-02	2.66e-02	1.33e-02	6.51e-03	3.05e-03	1.31e-03
2^{-3}	6.56e-02	3.42e-02	1.72e-02	8.42e-03	3.95e-03	1.70e-03
2^{-4}	8.53e-02	4.45e-02	2.24e-02	1.10e-02	5.17e-03	2.22e-03
2^{-5}	8.32e-02	4.63e-02	2.40e-02	1.19e-02	5.62e-03	2.42e-03
2^{-6}	5.95e-02	4.12e-02	2.18e-02	1.10e-02	5.29e-03	2.30e-03
2^{-7}	8.27e-02	7.89e-02	4.67e-02	2.55e-02	1.28e-02	5.65e-03
2^{-8}	1.04e-01	1.07e-01	8.46e-02	5.31e-02	2.81e-02	1.28e-02
2^{-9}	1.17e-01	1.18e-01	8.84e-02	5.65e-02	3.34e-02	1.70e-02
2^{-10}	1.25e-01	1.26e-01	9.29e-02	5.96e-02	3.50e-02	1.78e-02
2^{-11}	1.29e-01	1.29e-01	9.54e-02	6.12e-02	3.59e-02	1.82e-02
2^{-12}	1.32e-01	1.31e-01	9.66e-02	6.20e-02	3.63e-02	1.84e-02
2^{-13}	1.33e-01	1.33e-01	9.72e-02	6.24e-02	3.65e-02	1.86e-02
2^{-14}	1.34e-01	1.33e-01	9.75e-02	6.26e-02	3.66e-02	1.86e-02
2^{-15}	1.34e-01	1.33e-01	9.76e-02	6.27e-02	3.67e-02	1.86e-02
2^{-16}	1.34e-01	1.34e-01	9.77e-02	6.28e-02	3.67e-02	1.86e-02
2^{-17}	1.34e-01	1.34e-01	9.78e-02	6.28e-02	3.67e-02	1.86e-02
2^{-18}	1.34e-01	1.34e-01	9.78e-02	6.28e-02	3.67e-02	1.87e-02
2^{-19}	1.34e-01	1.34e-01	9.78e-02	6.28e-02	3.67e-02	1.87e-02
2^{-20}	1.34e-01	1.34e-01	9.78e-02	6.28e-02	3.67e-02	1.87e-02
2^{-21}	1.34e-01	1.34e-01	9.78e-02	6.28e-02	3.67e-02	1.87e-02
2^{-22}	1.34e-01	1.34e-01	9.78e-02	6.28e-02	3.67e-02	1.87e-02
2^{-23}	1.34e-01	1.34e-01	9.78e-02	6.28e-02	3.67e-02	1.87e-02
2^{-24}	1.34e-01	1.34e-01	9.78e-02	6.28e-02	3.67e-02	1.87e-02
$\vdots$	$\vdots$	$\vdots$	$\vdots$	$\vdots$	$\vdots$	$\vdots$
2^{-32}	1.34e-01	1.34e-01	9.78e-02	6.28e-02	3.67e-02	1.87e-02
E^N	1.34e-01	1.34e-01	9.78e-02	6.28e-02	3.67e-02	1.87e-02

Table 2.7: Computed errors, E_ε^N, and computed ε-uniform errors, E^N, for appropriate method chosen from Table 2.2 applied to example 4.

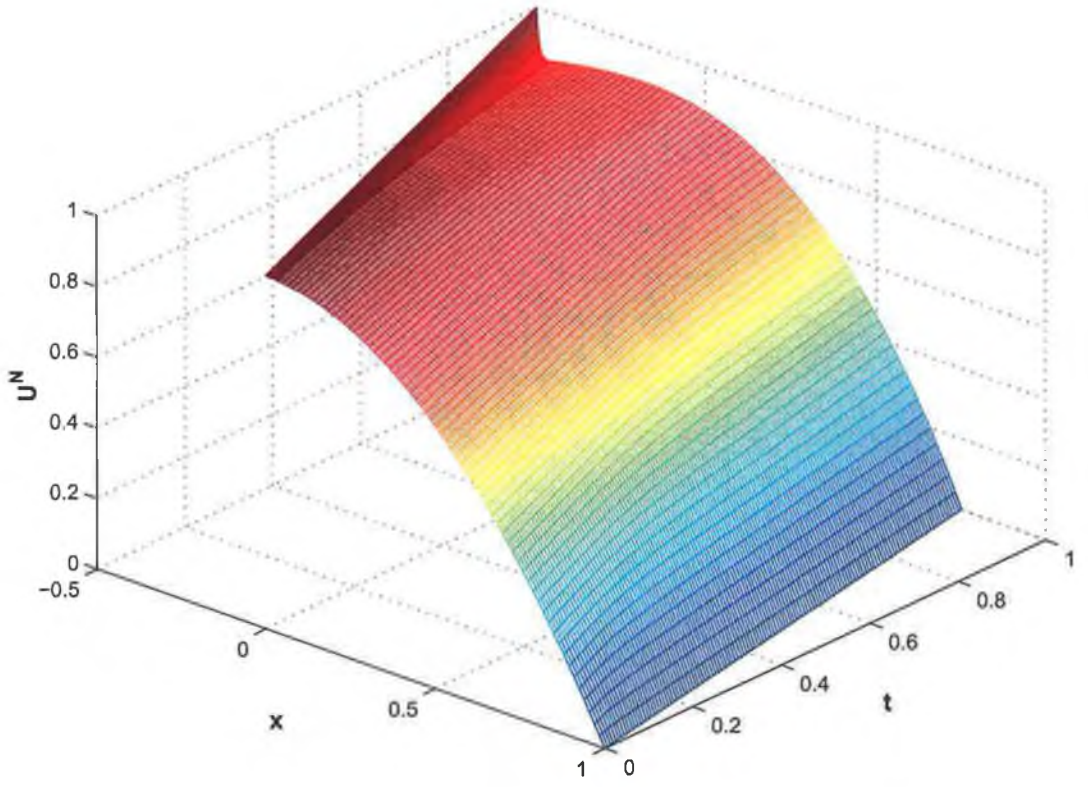

Figure 2.4: Plot of numerical solution generated by appropriate method chosen from Table 2.2 applied to example 1 with $\varepsilon = 2^{-8}$ and $N = 128$.

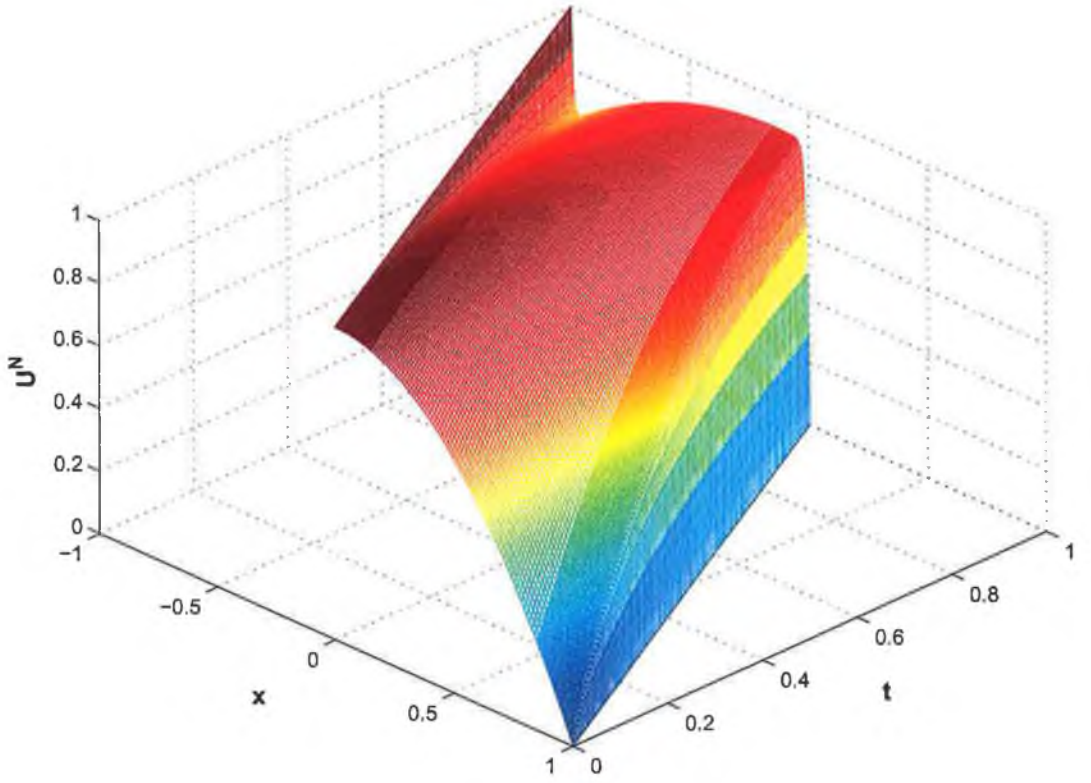

Figure 2.5: Plot of numerical solution generated by appropriate method chosen from Table 2.2 applied to example 2 with $\varepsilon = 2^{-12}$ and $N = 128$.

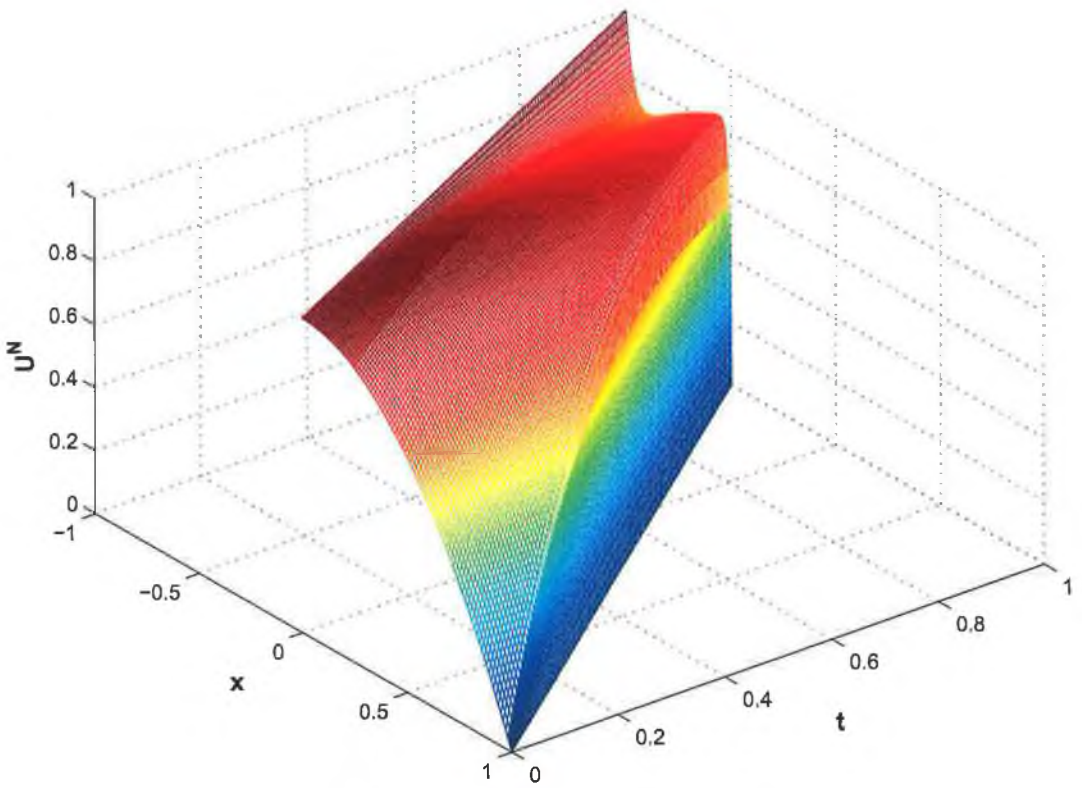

Figure 2.6: Plot of numerical solution generated by appropriate method chosen from Table 2.2 applied to example 3 with $\epsilon = 2^{-8}$ and $N = 128$.

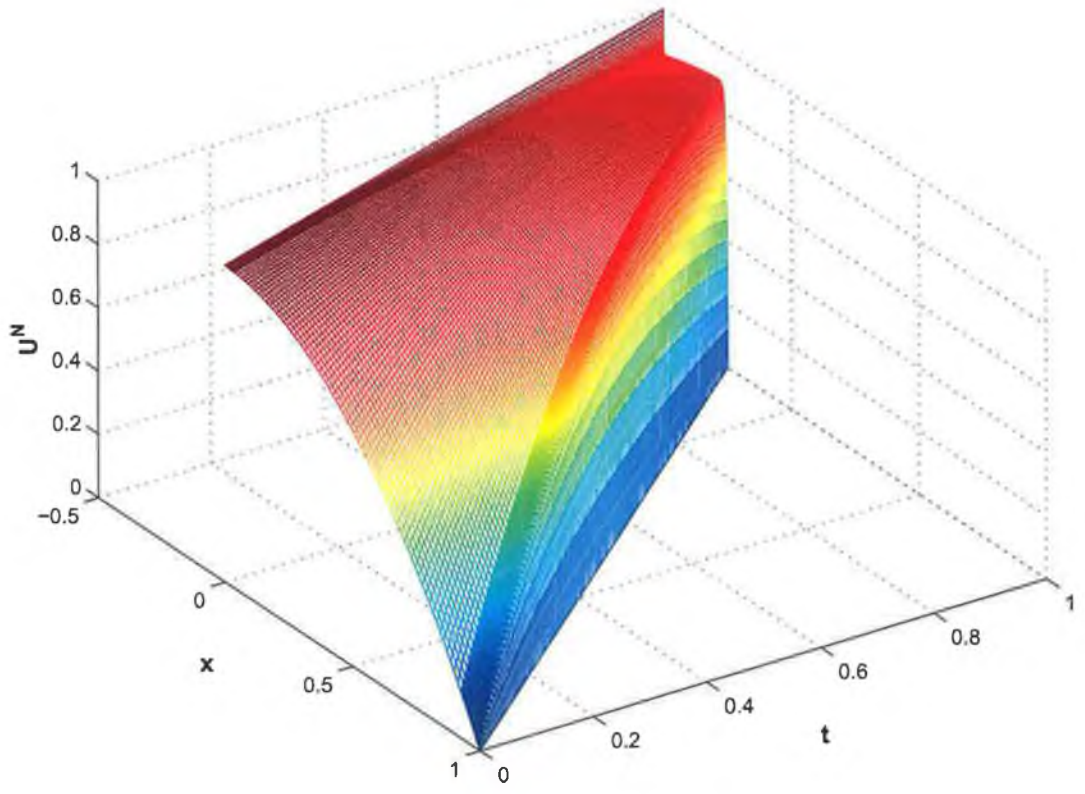

Figure 2.7: Plot of numerical solution generated by appropriate method chosen from Table 2.2 applied to example 4 with $\varepsilon = 2^{-10}$ and $N = 128$.

To determine the location and nature of the layers present in solutions of problems from this class we again consider the reduced problem (2.4.1). In this case the characteristics will in general be curves. They are given by $(\xi(s), t(s))$ where

$$\frac{d\xi}{ds} = \hat{a}, \quad \frac{dt}{ds} = -\hat{b}.$$

We introduce the following vectors

$$\mathbf{c}(\xi, t) = (-\hat{a}(\xi, t), \hat{b}(\xi, t)), \quad \mathbf{n}(t) = (-1, \phi'(t)). \tag{2.7.1}$$

The vector $\mathbf{c}(\xi, t)$ is interpreted as the characteristic direction at the point (ξ, t) and $\mathbf{n}(t)$ is an outward normal to the boundary $\xi = \phi(t)$ and an inward normal to the boundary $\xi = 1 + \phi(t)$ depending on its location. In order to be able to classify every problem in P_ε^2 into a subclass of P_ε depending on its layer behaviour we will assume the following.

Assumption 2.7.1. *The signs of the quantities* $\mathbf{c}(\phi(t), t) \cdot \mathbf{n}(t)$ *and* $\mathbf{c}(1+\phi(t), t) \cdot \mathbf{n}(t)$ *do not change as* t *varies.*

Geometrically speaking this means that the angles that all of the characteristic curves make with each of the boundaries of the domain, are of the same type for all t, i.e., always acute, right or obtuse. This rules out situations where the characteristic curves intersect the boundaries in complicated ways. For example we cannot have a characteristic curve being tangent to the boundary at one point only. In this case the layer structure of the solution of the corresponding problem would be considerably more complex than the examples considered here.

It can be seen that the signs of the quantities $\mathbf{c}(\phi(t), t).\mathbf{n}(t)$ and $\mathbf{c}(1+\phi(t), t).\mathbf{n}(t)$ determine whether the corresponding boundary is part of the inflow boundary, outflow boundary or characteristic boundary. Therefore these quantities determine the types of layers present in the solutions of problems from the original class, and therefore also the transformed class, P_ε^2. Note that the coefficient a in the transformed problem class is precisely the quantity $\mathbf{c}(\xi, t) \cdot \mathbf{n}(t)$ and hence the above assumption is equivalent to assuming that the sign of a remains the same along both sides of the domain. Therefore, under Assumption 2.7.1, any problem from P_ε^2 can be classified into one

of the subclasses of P_ε defined in §2.3.

Consider the following problem posed on the domain $\hat{\Omega}_P$. We take $T = 1$.

Problem Class 2.7.2.

$$\begin{aligned}(\varepsilon u_{\xi\xi} + (2t^2 - 1)u_\xi - u_t - u)(x,t) = -\xi - 1 \quad &\text{in } \hat{\Omega}_P,\\ u(\xi,0) = 1 - \xi^2, \quad &\xi \in [0,1],\\ u(\phi(t),t) = 1 + t^2, \quad u(1+\phi(t),t) = 0, \quad &t \in (0,1].\end{aligned}$$

where

$$\phi(t) = t - \tfrac{2}{3}t^3.$$

With this choice of boundary function ϕ it is easy to see that $\mathbf{c}(\xi,t)\cdot\mathbf{n}(t) = 0$, $\forall t$. Hence the corresponding transformed problem class is a subclass of P_ε^0 and the solutions will possess parabolic boundary layers of width $\mathcal{O}(\sqrt{\varepsilon})$ in a neighbourhood of $x = 0$ and $x = 1$. To generate numerical solutions to problems from the transformed class we apply Method 2.5.2 with the appropriate transition points

$$\tau_1 = \min\left\{\frac{1}{4}, 2\sqrt{\varepsilon}\ln N_x\right\}, \quad \tau_2 = 1 - \tau_1. \tag{2.7.2}$$

In Table 2.8 we show the computed errors, E_ε^N, and the computed ε-uniform errors, E^N, for a variety of values of ε and N. Similar to the examples considered already, the values of E_ε^N for each fixed ε decrease with increasing N and the values of E^N also decrease with increasing N indicating that the convergence is uniform with respect to ε. We also present a graph of a representative numerical solution plotted on the original domain for particular values of ε and N (Figure 2.8) and an illustration of how the piecewise-uniform fitted mesh would look on the original domain (Figure 2.9).

ε	Number of Intervals N					
	8	16	32	64	128	256
1	1.99e-02	1.21e-02	6.81e-03	3.56e-03	1.73e-03	7.55e-04
2^{-1}	1.35e-02	7.36e-03	3.79e-03	1.88e-03	8.85e-04	3.82e-04
2^{-2}	2.58e-02	1.31e-02	6.55e-03	3.21e-03	1.51e-03	6.50e-04
2^{-3}	4.21e-02	2.10e-02	1.03e-02	4.97e-03	2.32e-03	9.92e-04
2^{-4}	5.67e-02	2.72e-02	1.31e-02	6.28e-03	2.91e-03	1.25e-03
2^{-5}	6.93e-02	3.23e-02	1.53e-02	7.19e-03	3.31e-03	1.41e-03
2^{-6}	8.92e-02	3.84e-02	1.74e-02	7.99e-03	3.63e-03	1.53e-03
2^{-7}	1.12e-01	4.72e-02	2.01e-02	8.88e-03	3.94e-03	1.64e-03
2^{-8}	1.22e-01	6.53e-02	2.51e-02	1.02e-02	4.32e-03	1.76e-03
2^{-9}	1.24e-01	8.57e-02	3.27e-02	1.27e-02	4.94e-03	1.92e-03
2^{-10}	1.25e-01	8.62e-02	4.30e-02	1.75e-02	6.12e-03	2.20e-03
2^{-11}	1.26e-01	8.66e-02	4.30e-02	1.82e-02	7.12e-03	2.61e-03
2^{-12}	1.27e-01	8.68e-02	4.32e-02	1.82e-02	7.06e-03	2.62e-03
2^{-13}	1.28e-01	8.70e-02	4.33e-02	1.82e-02	7.08e-03	2.62e-03
2^{-14}	1.28e-01	8.71e-02	4.33e-02	1.83e-02	7.09e-03	2.63e-03
2^{-15}	1.28e-01	8.72e-02	4.34e-02	1.83e-02	7.10e-03	2.63e-03
2^{-16}	1.29e-01	8.73e-02	4.34e-02	1.83e-02	7.11e-03	2.63e-03
2^{-17}	1.29e-01	8.74e-02	4.34e-02	1.83e-02	7.12e-03	2.63e-03
2^{-18}	1.29e-01	8.74e-02	4.34e-02	1.83e-02	7.12e-03	2.63e-03
2^{-19}	1.29e-01	8.74e-02	4.34e-02	1.83e-02	7.12e-03	2.63e-03
2^{-20}	1.29e-01	8.74e-02	4.34e-02	1.83e-02	7.12e-03	2.63e-03
2^{-21}	1.29e-01	8.74e-02	4.34e-02	1.83e-02	7.12e-03	2.63e-03
2^{-22}	1.29e-01	8.75e-02	4.34e-02	1.83e-02	7.13e-03	2.63e-03
$\vdots$	$\vdots$	$\vdots$	$\vdots$	$\vdots$	$\vdots$	$\vdots$
2^{-32}	1.29e-01	8.75e-02	4.34e-02	1.83e-02	7.13e-03	2.63e-03
E^N	1.29e-01	8.75e-02	4.34e-02	1.83e-02	7.13e-03	2.63e-03

Table 2.8: Computed errors, E_ε^N, and computed ε-uniform errors E^N, for Method 2.5.2 with transition points given by (2.7.2) applied to Problem Class 2.7.2.

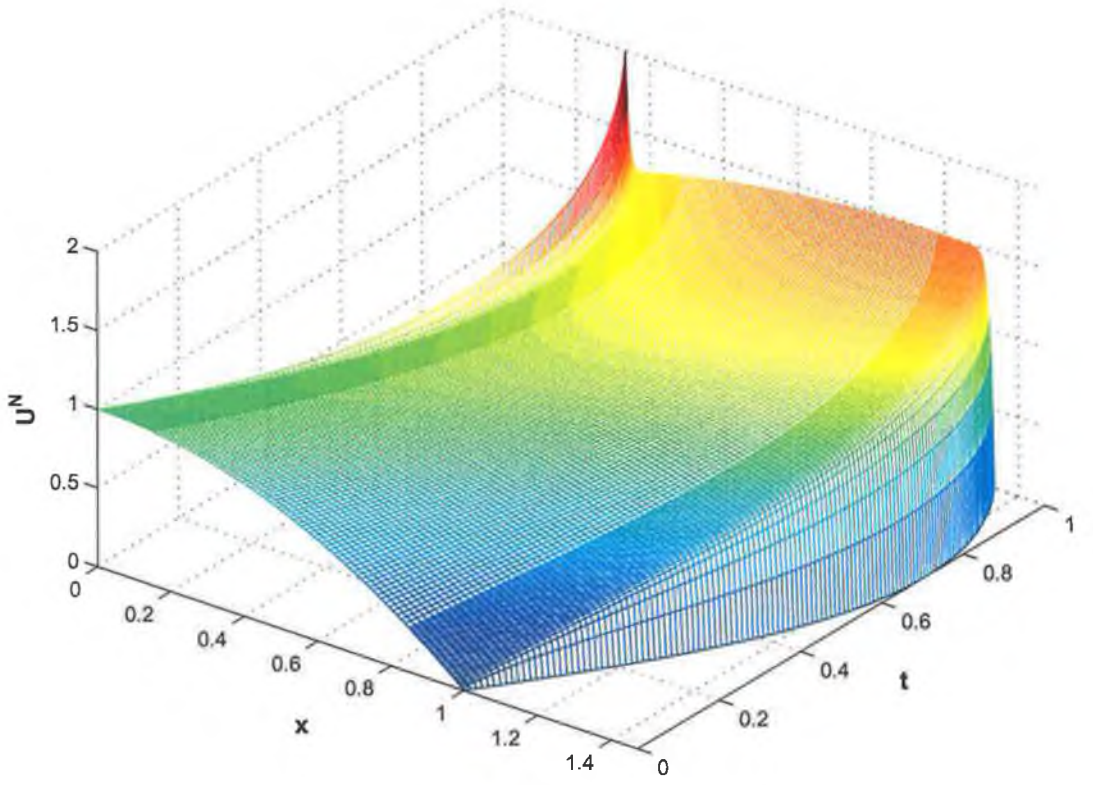

Figure 2.8: Plot of Numerical Solution generated by Method 2.5.2 with transition points given by (2.7.2) applied to the problem from Problem Class 2.7.2 with $\varepsilon = 2^{-12}$ and $N = 128$ on original domain.

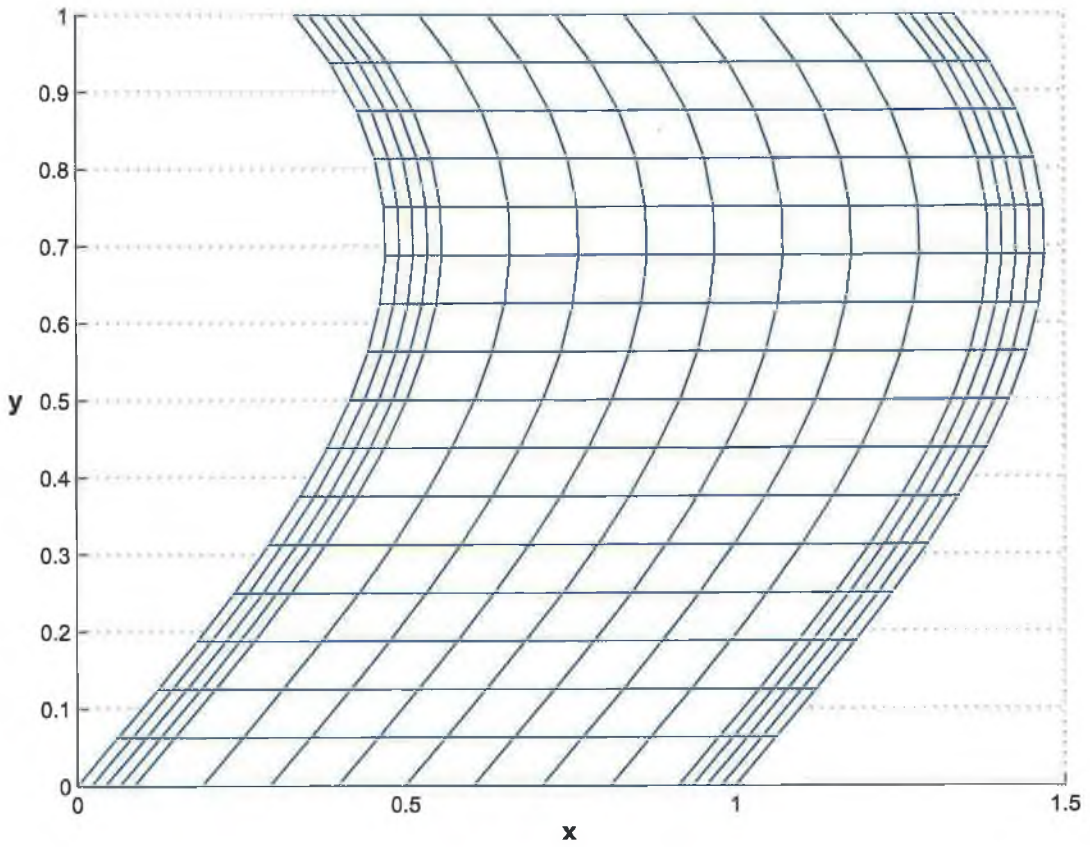

Figure 2.9: Piecewise-uniform fitted mesh for the problem from Problem Class 2.7.2 on original domain.

Chapter 3

Numerical methods for a class of singularly perturbed problems with a boundary turning point

3.1 Introduction

In this chapter we will study a class of singularly perturbed problems with a boundary turning point. As remarked in §2.4 this problem is a generalisation of a class of problems that was generated from the consideration of a suitable parabolic problem on a non-rectangular domain. The key feature of problems from this class is that the coefficient of the convective term in the differential equation becomes zero along one side of the domain. It will be seen that this means that the solutions of problems from this class possess a parabolic layer in a neighbourhood of this side of the domain.

The material in this chapter is set out as follows. In §3.2 we state precisely the class of problems we will be investigating and identify the nature and location of the boundary layers present. In §3.3 we consider some properties of the continuous problem. In particular we establish a maximum principle and bounds on the derivatives of the solution. In §3.4 we obtain sharper bounds on the derivatives through a suitable decomposition of the solution into regular and layer components. The numerical method is constructed in §3.5 and its monotonicity is proven. In §3.6 we show that the numerical solutions generated by the method converge uniformly to the solution

of the continuous problem with respect to the singular perturbation parameter. Detailed numerical results are presented in §3.7. Finally, in §3.8 we briefly consider a related problem also with a boundary turning point. Some of the material in this chapter has appeared in [12] in a slightly different form.

3.2 Statement of problem

Consider the following class of singularly perturbed parabolic problems:

Problem Class 3.2.1.

$$L_\varepsilon u(x,t) \equiv (\varepsilon u_{xx} + a u_x - b u_t - d u)(x,t) = f(x,t) \quad \text{in } \Omega, \tag{3.2.1a}$$

$$u(x,t) = g(x,t) \quad \text{on } \Gamma, \tag{3.2.1b}$$

$$a(x,t) = a_0(x,t)x^p, \quad p \geq 1, \quad a_0(x,t) \geq \alpha > 0, \quad \forall (x,t) \in \overline{\Omega}, \tag{3.2.1c}$$

$$b(x,t) \geq \beta > 0, \qquad d(x,t) \geq \delta \geq 0 \qquad \forall (x,t) \in \overline{\Omega}, \tag{3.2.1d}$$

where

$$\Omega = (0,1) \times (0,T], \quad \Gamma = \overline{\Omega} \setminus \Omega = \Gamma_L \cup \Gamma_B \cup \Gamma_R,$$
$$\Gamma_L = \{(0,t) \mid 0 \leq t \leq T\}, \quad \Gamma_B = \{(x,0) \mid 0 \leq x \leq 1\}, \quad \Gamma_R = \{(1,t) \mid 0 \leq t \leq T\}.$$

We assume that the data a_0, b, d, f and g are sufficiently regular. In particular, this means that for a to have a certain amount of regularity (for example to be in $C^3(\overline{\Omega})$) we must rule out the case when $p < 3$ and takes a non-integer value. We also assume that f and g satisfy sufficient compatibility conditions at the corners of the domain so that the solution and its regular component are sufficiently smooth for our analysis.

Problem 3.2.1 is a so-called boundary turning point problem. For $p > 1$, the turning point is called a multiple turning point. It is a parabolic partial differential equation where the coefficient of the convective term is zero along the left side of the boundary of the domain, i.e. on Γ_L. Note that we make no assertions about a steady-state solution of this problem. The corresponding reduced problem is defined

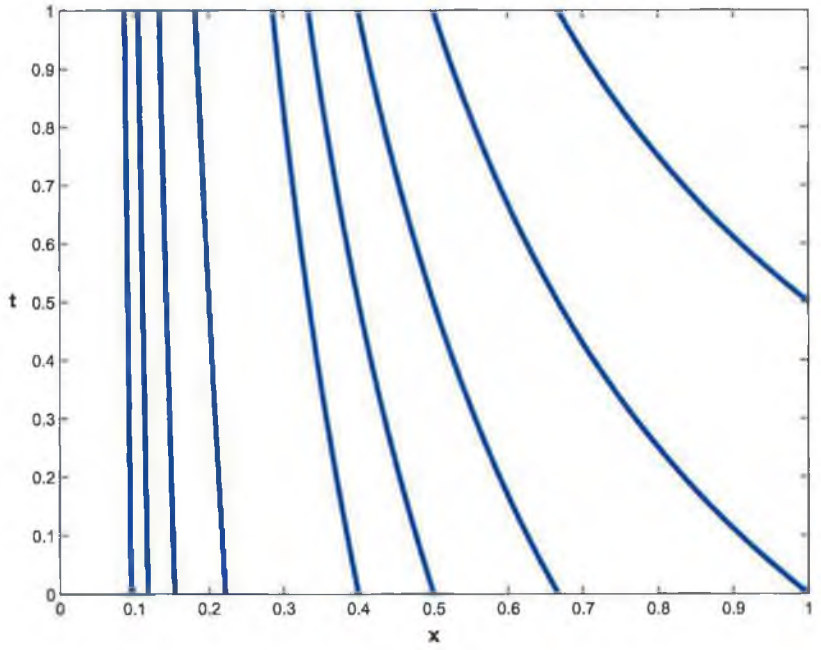

Figure 3.1: Characteristics of the reduced problem (3.2.2).

to be

$$(a(v_0)_x - b(v_0)_t - dv_0)(x,t) = f(x,t) \quad \text{in } \Omega, \tag{3.2.2a}$$

$$v_0(x,t) = g(x,t) \quad \text{on } \Gamma_B \cup \Gamma_R. \tag{3.2.2b}$$

The solution is said to have a parabolic boundary layer in a neighbourhood of Γ_L when $a(0,t) = 0$ and $b(0,t) > 0$, as the boundary $x = 0$ is then a characteristic curve of the reduced problem. The other characteristics do not intersect the boundary Γ_L, but deviate increasingly from the vertical away from the lateral boundary (Figure 3.1).

Ordinary differential equations of a form related to Problem Class 3.2.1 have been dealt with by several authors (see for example [53], [52], [32], [31] and [27]) and arise in geophysics and in modelling thermal boundary layers in laminar flow (see [52] and the references therein).

The analysis in this chapter (when p set equal to 0) is also valid for the case

$$a(x,t) \geq \alpha > 0, \quad \forall (x,t) \in \overline{\Omega}.$$

The solutions of problems from the class then possess a different type of layer than the layers examined here, *viz.* a regular layer. This class of problems has been extensively studied (see for example [47], [50], and [24]). Moreover the method of proof given can also be applied to the reaction-diffusion case, when a is identically zero (see [36]). In this case the solutions of problems from the class possess parabolic boundary layers at both $x = 0$ and $x = 1$. These facts indicate that the technique of proof can be applied to a wide variety of problems involving boundary layers. This illustrates the potential of the technique in establishing theoretical results for other classes of singularly perturbed problems.

3.3 The continuous problem

The differential operator L_ε in (3.2.1a) satisfies the following minimum principle.

Lemma 3.3.1 (Minimum Principle). *Let* $v \in C^{2,1}(\overline{\Omega})$.

$$\textit{If} \quad v(x,t) \geq 0, \quad \forall (x,t) \in \Gamma, \quad \textit{and} \quad L_\varepsilon v(x,t) \leq 0, \quad \forall (x,t) \in \Omega,$$

$$\textit{then} \quad v(x,t) \geq 0, \quad \forall (x,t) \in \overline{\Omega}.$$

Proof. Assume

$$\exists \mathbf{r} \in \overline{\Omega} \quad \text{such that} \quad v(\mathbf{r}) = \min_{\overline{\Omega}} v < 0,$$

$$\text{then} \quad \mathbf{r} \notin \Gamma, \quad \text{which implies} \quad \mathbf{r} \in \Omega.$$

Now let

$$w(x,t) = v(x,t)\, e^{\alpha x^{p+1}/2(p+1)\varepsilon}, \quad \forall (x,t) \in \overline{\Omega}.$$

Then $w(x,t) \geq 0, \quad \forall (x,t) \in \Gamma$, and $w(\mathbf{r}) < 0$. Thus the minimum of w must also be negative. Let $\mathbf{q} \in \Omega$ such that

$$w(\mathbf{q}) = \min_{\overline{\Omega}} w < 0.$$

Applying the differential operator to v gives

$$\begin{aligned} L_\varepsilon v =& L_\varepsilon(we^{-\alpha x^{p+1}/2(p+1)\varepsilon}) \\ =& \Big(\varepsilon w_{xx} + (a-\alpha x^p)w_x + \left(\frac{\alpha x^p}{2\varepsilon}\left(\frac{\alpha x^p}{2} - a\right) - \frac{\alpha p x^{p-1}}{2}\right) w \\ & - bw_t - dw\Big)(x,t)\, e^{-\alpha x^{p+1}/2(p+1)\varepsilon}. \end{aligned}$$

The argument now divides into two cases depending on the position of $\mathbf{q}$.

If $\mathbf{q} \notin \Gamma_T = \{(x,T) \mid 0 < x < 1\}$ we have

$$w_{xx}(\mathbf{q}) \geq 0, \quad w_x(\mathbf{q}) = w_t(\mathbf{q}) = 0,$$

which gives

$$L_\varepsilon v(\mathbf{q}) > 0.$$

If $\mathbf{q} \in \Gamma_T$ then

$$w_{xx}(\mathbf{q}) \geq 0, \quad w_x(\mathbf{q}) = 0, \quad w_t(\mathbf{q}) \leq 0,$$

which again gives

$$L_\varepsilon v(\mathbf{q}) > 0.$$

This is a contradiction and thus our original assumption is false and we can conclude that the minimum of v is non-negative. □

An immediate consequence of this is the following bound on the solution of any problem from Problem Class 3.2.1.

Lemma 3.3.2. *The solution u of any problem from Problem Class 3.2.1 satisfies the following bound*

$$\|u\|_{\overline{\Omega}} \leq \|g\|_\Gamma + T\,\|f\|_{\overline{\Omega}}/\beta.$$

Proof. Consider the barrier functions

$$\psi^\pm(x,t) = C_1 + C_2 t \pm u(x,t),$$

where $C_1 = \|g\|_\Gamma$ and $C_2 = \|f\|_{\overline{\Omega}}/\beta$.

These functions satisfy the hypotheses of Lemma 3.3.1 and therefore

$$\psi^{\pm}(x,t) \geq 0, \quad \forall (x,t) \in \overline{\Omega},$$

and the result follows. □

Remark 3.3.1. Note that Lemma 3.3.2 yields a time-dependent stability bound. If we impose the restriction

$$\|f/a\|_{\overline{D}} \leq C, \tag{3.3.1}$$

then by using the barrier function

$$\psi^{\pm}(x,t) = C_1 + C_2(1-x) \pm u(x,t),$$

where $C_1 = \|g\|_{\Gamma}$ and $C_2 = \|f/a\|_{\overline{D}}$ we can establish a time-independent stability bound. However, we do not wish to limit the problem class with the restriction (3.3.1).

We have the following bounds on the derivatives of any problem from Problem Class 3.2.1.

Theorem 3.3.3. *Let $u \in C^{3,\nu}(\overline{\Omega})$ be the solution of a problem from Problem Class 3.2.1. Then for all non-negative integers i, j, such that $0 \leq i + 2j \leq 3$,*

$$\left\| \frac{\partial^{i+j} u}{\partial x^i \partial t^j} \right\| \leq C\varepsilon^{-i/2}. \tag{3.3.2}$$

Proof. Transforming the variable x to the stretched variable $\tilde{x} = x/\sqrt{\varepsilon}$, Problem Class 3.2.1 becomes

Problem Class 3.3.1.

$$(\tilde{u}_{\tilde{x}\tilde{x}} + \tilde{a}\varepsilon^{\frac{p-1}{2}}\tilde{u}_{\tilde{x}} - \tilde{b}\tilde{u}_t - \tilde{d}\tilde{u})(\tilde{x},t) = \tilde{f}(\tilde{x},t) \quad \text{in } \tilde{\Omega}, \tag{3.3.3a}$$

$$\tilde{u}(\tilde{x},t) = \tilde{g}(\tilde{x},t) \quad \text{on } \tilde{\Gamma}, \tag{3.3.3b}$$

where $\tilde{\Omega} = (0, 1/\sqrt{\varepsilon}) \times (0, T]$ *and* $\tilde{\Gamma}$ *is its boundary and*

$$\tilde{u}(\tilde{x}, t) = u(x, t), \quad \tilde{a}(\tilde{x}, t) = \tilde{a}_0(\tilde{x}, t)\tilde{x}^p, \quad \tilde{a}_0(\tilde{x}, t) = a_0(x, t),$$
$$\tilde{b}(\tilde{x}, t) = b(x, t), \quad \tilde{d}(\tilde{x}, t) = d(x, t), \quad \tilde{f}(\tilde{x}, t) = f(x, t), \quad \tilde{g}(\tilde{x}, t) = g(x, t).$$

Applying the estimate (10.5) from [25, p. 352] gives, for all non-negative integers i, j, such that $0 \leq i + 2j \leq 3$,

$$\left\| \frac{\partial^{i+j}\tilde{u}}{\partial \tilde{x}^i \partial t^j} \right\|_{\tilde{N}_\delta} \leq C(1 + \|\tilde{u}\|_{\tilde{N}_{2\delta}}),$$

where for each $(\tilde{x}, t) \in \tilde{\Omega}$ and $\delta > 0$ we define

$$\tilde{N}_\delta = \tilde{N}_\delta(\tilde{x}, t) = ((\tilde{x} - \delta, \tilde{x} + \delta) \times (0, T]) \cap \overline{\tilde{\Omega}},$$

and the constant C is independent of $\tilde{N}_\delta$ and does not depend on inverse powers of the coefficient $\tilde{a}\varepsilon^{\frac{|2-1}{2}}$ or its derivatives. Returning to the original variable it follows that

$$\begin{aligned} \left\| \frac{\partial^{i+j}u}{\partial x^i \partial t^j} \right\|_{N_\delta} &\leq C\varepsilon^{-i/2}(1 + \|u\|_{N_{2\delta}}) \\ &\leq C\varepsilon^{-i/2}(1 + \|u\|_{\overline{\Omega}}) \\ &\leq C\varepsilon^{-i/2}, \end{aligned}$$

using the bound on u given in Lemma 3.3.2, where N_δ is defined in an analogous manner to $\tilde{N}_\delta$. Taking the supremum of the left-hand side over all $N_\delta \subset \Omega$ gives the required result. □

3.4 Decomposition of solution

It turns out that the above bounds on the derivatives of the solution are not sharp enough for the proof of our required result. Stronger bounds are now obtained based on a method originally contained in Shishkin [46]. This is achieved using the following

decomposition of the solution into a regular and a singular part. Let

$$u(x,t) = v(x,t) + w(x,t), \quad \forall (x,t) \in \overline{\Omega},$$

where

$$\begin{aligned} L_\varepsilon v(x,t) &= f(x,t) \quad \text{in } \Omega, && \text{(3.4.1a)} \\ v(x,t) &= u(x,t) \quad \text{on } \Gamma_B \cup \Gamma_R, && \text{(3.4.1b)} \end{aligned}$$

with the value of v on Γ_L still to be specified. Thus, w is the solution to the problem

$$\begin{aligned} L_\varepsilon w(x,t) &= 0 \quad \text{in } \Omega, && \text{(3.4.2a)} \\ w(x,t) &= 0 \quad \text{on } \Gamma_B \cup \Gamma_R, && \text{(3.4.2b)} \\ w(x,t) &= u(x,t) - v(x,t) \quad \text{on } \Gamma_L. && \text{(3.4.2c)} \end{aligned}$$

The values that v takes on Γ_L are chosen so that its first two derivatives in space are bounded independently of ε. This is aided by the further decomposition

$$v(x,t) = (v_0 + \varepsilon v_1 + \varepsilon^2 v_2)(x,t), \quad \forall (x,t) \in \overline{\Omega},$$

where v_0 is the solution to the reduced problem (3.2.2), and v_1 and v_2 are the respective solutions to the problems

$$\begin{aligned} (a\frac{\partial v_1}{\partial x} - b\frac{\partial v_1}{\partial t} - dv_1)(x,t) &= -\frac{\partial^2 v_0}{\partial x^2}(x,t) \quad \text{in } \Omega, && \text{(3.4.3a)} \\ v_1(x,t) &= 0 \text{ on } \Gamma_B \cup \Gamma_R, && \text{(3.4.3b)} \end{aligned}$$

and

$$\begin{aligned} L_\varepsilon v_2(x,t) &= -\frac{\partial^2 v_1}{\partial x^2}(x,t) \quad \text{in } \Omega, \\ v_2(x,t) &= 0 \quad \text{on } \Gamma. \end{aligned}$$

We clearly have $L_\varepsilon v(x,t) = f(x,t)$ in Ω, as required, with

$$v(x,t) = (v_0 + \varepsilon v_1)(x,t) \quad \text{on} \quad \Gamma_L.$$

Note that extra compatibility conditions must be imposed on the data at the corners of the domain so that the components v_0, v_1, v_2 and w are sufficiently regular. To establish bounds on the derivatives of v we need the following assumption about the regularity of v_0 and v_1.

Assumption 3.4.1. *Let v_0 be the solution of the problem* (3.2.2) *and v_1 be the solution of the problem* (3.4.3). *Assume that for all non-negative integers i, j, such that $0 \le i + 2j \le 3$,*

$$\left\| \frac{\partial^{i+j} v_0}{\partial x^i \partial t^j} \right\| \le C, \quad \left\| \frac{\partial^{i+j} v_1}{\partial x^i \partial t^j} \right\| \le C.$$

Theorem 3.4.2. *Let v be the solution of* (3.4.1). *Then, under Assumption 3.4.1, for all non-negative integers i, j, such that $0 \le i + 2j \le 3$,*

$$\left\| \frac{\partial^{i+j} v}{\partial x^i \partial t^j} \right\| \le C(1 + \varepsilon^{2-i/2}).$$

Proof. Clearly v_2 satisfies a problem of the same form as u, and so applying Theorem 3.3.3 we have: For all non-negative integers i, j, such that $0 \le i + 2j \le 3$,

$$\left\| \frac{\partial^{i+j} v_2}{\partial x^i \partial t^j} \right\| \le C\varepsilon^{-i/2}.$$

Combining this with the bounds on v_0 and v_1 given in Assumption 3.4.1 we have: For all non-negative integers i, j, such that $0 \le i + 2j \le 3$,

$$\begin{aligned} \left\| \frac{\partial^{i+j} v}{\partial x^i \partial t^j} \right\| &\le \left\| \frac{\partial^{i+j} v_2}{\partial x^i \partial t^j} \right\| + \varepsilon \left\| \frac{\partial^{i+j} v_2}{\partial x^i \partial t^j} \right\| + \varepsilon^2 \left\| \frac{\partial^{i+j} v_2}{\partial x^i \partial t^j} \right\| \\ &\le C + \varepsilon C + \varepsilon^2 C \varepsilon^{-i/2} \\ &\le C(1 + \varepsilon^{2-i/2}) \end{aligned}$$

as required. □

We now consider the other term in the decomposition, w. This is the part that

represents the boundary layer. For the proof of our result we just require a sharper bound on w itself and not its derivatives. This bound is given in the following theorem.

Theorem 3.4.3. *Let w be the solution of* (3.4.2). *Then*

$$|w(x,t)| \leq Ce^{-x/\sqrt{\varepsilon}}, \quad \forall (x,t) \in \overline{\Omega}.$$

Proof. Consider the barrier functions

$$\psi_1^{\pm}(x,t) = Ce^{-x/\sqrt{\varepsilon}}e^{At} \pm w(x,t),$$

where $A = \max_{\overline{\Omega}}\{0, (1-d)/b\}$. We have

$$\begin{aligned} \psi^{\pm}(x,0) &= Ce^{-x/\sqrt{\varepsilon}} \geq 0, \\ \psi^{\pm}(0,t) &= Ce^{At} \pm u(x,t) - v(x,t) \geq 0, \\ \psi^{\pm}(1,0) &= Ce^{-1/\sqrt{\varepsilon}}e^{A} \geq 0 \end{aligned}$$

if C is chosen sufficiently large. Also

$$L_\varepsilon \psi_1^{\pm}(x,t) = C(1 - a/\sqrt{\varepsilon} - bA - d)(x,t)e^{-x/\sqrt{\varepsilon}}e^{At} \leq 0. \tag{3.4.5}$$

It follows from Lemma 3.3.1 that

$$\psi_1^{\pm}(x,t) \geq 0, \quad \forall (x,t) \in \overline{\Omega},$$

and the result follows. □

3.5 Numerical method

We now introduce the appropriate discretisation that we will use for generating numerical approximations to problems from the class $P_{\varepsilon,p}$. This consists of a standard upwind finite difference operator on a fitted piecewise uniform mesh. The difference operator L_ε^N, on a mesh Ω^N, is defined for any mesh function Z^N, as

$$L_\varepsilon^N Z^N(x_i,t_j) \equiv (\varepsilon\delta_x^2 Z^N + aD_x^+ Z^N - bD_t^- Z^N - dZ^N)(x_i,t_j), \quad \forall (x_i,t_j) \in \Omega^N.$$

Define the mesh, $\overline{\Omega}^{N_t}$, that discretises $[0,T]$ with N_t uniform mesh elements, as

$$\overline{\Omega}^{N_t} = \{t_j \mid t_j = Tj/N_t, \quad 0 \le j \le N_t\},$$

and the piecewise-uniform mesh, $\overline{\Omega}_\sigma^{N_x}$, that discretises $[0,1]$ with N_x mesh elements, as

$$\overline{\Omega}_\sigma^{N_x} = \left\{ x_i \middle| x_i = \begin{cases} 2i\sigma/N_x, & 0 \le i \le N_x/2 \\ \sigma + 2(i - N_x/2)(1-\sigma)/N_x, & N_x/2 < i \le N_x \end{cases} \right\},$$

where

$$\sigma = \min\left\{\frac{1}{2}, \sqrt{\varepsilon}\ln N_x\right\}.$$

It can be seen that $\Omega_\sigma^{N_x}$ consists of two uniform meshes, with $N_x/2$ mesh elements in each, joined together at the transition point σ. When $\sigma = 1/2$ the mesh is uniform, otherwise the mesh condenses near Γ_L. We use the notation $N = (N_x, N_t)$ and define the resulting piecewise uniform fitted mesh to be the tensor product

$$\Omega_\sigma^N = \Omega_\sigma^{N_x} \times \Omega^{N_t},$$

and its boundary points Γ_σ^N are $\Gamma_\sigma^N = \overline{\Omega}_\sigma^N \cap \Gamma$. The resulting fitted mesh finite difference method is

Method 3.5.1.

$$L_\varepsilon^N U^N(x_i,t_j) = f(x_i,t_j) \quad in \ \Omega_\sigma^N, \tag{3.5.1a}$$

$$U^N(x_i,t_j) = g(x_i,t_j) \quad on \ \Gamma_\sigma^N. \tag{3.5.1b}$$

The following Lemma gives a discrete analogue of the minimum principle given in Lemma 3.3.1. Its proof is standard.

Lemma 3.5.1 (Discrete Minimum Principle). *Let Z^N be any mesh function defined on $\overline{\Omega}_\sigma^N$.*

$$\textit{If} \quad Z^N(x_i,t_j) \ge 0, \quad \forall (x_i,t_j) \in \Gamma_\sigma^N, \quad \textit{and} \quad L_\varepsilon^N Z^N(x_i,t_j) \le 0, \quad \forall (x_i,t_j) \in \Omega_\sigma^N,$$

$$\textit{then} \quad Z^N(x_i,t_j) \ge 0, \quad \forall (x_i,t_j) \in \overline{\Omega}_\sigma^N.$$

A consequence of this is the following stability property of the finite difference operator L_ε^N.

Lemma 3.5.2. *Let Z^N be any mesh function defined on $\overline{\Omega}_\sigma^N$.*

$$\text{If} \quad Z^N(x_i,t_j) \geq 0, \quad \forall (x_i,t_j) \in \Gamma_\sigma^N,$$

$$\text{then} \quad \left|Z^N(x_i,t_j)\right| \leq \max_{\Gamma_\sigma^N} \left|Z^N\right| + T' \max_{\Omega_\sigma^N} \left|L_\varepsilon^N Z^N\right|/\beta, \quad \forall (x_i,t_j) \in \overline{\Omega}_\sigma^N.$$

Proof. Consider the discrete barrier functions

$$\psi^{\pm}(x_i,t_j) = C_1 + C_2 t_j \pm Z^N(x_i,t_j),$$

where $C_1 = \max_{\Gamma_\sigma^N} \left|Z^N\right|$ and $C_2 = \max_{\Omega_\sigma^N} \left|L_\varepsilon^N Z^N\right|/\beta$.

These functions satisfy the hypotheses of Lemma 3.5.1 and therefore

$$\psi^{\pm}(x_i,t_j) \geq 0, \quad \forall (x_i,t_j) \in \overline{\Omega}_\sigma^N,$$

and the result follows. □

In the next section we will need the following bound on the local truncation error of Method 3.5.1 whose proof is standard.

Lemma 3.5.3 (Truncation Error). *Let u be the solution of* (3.2.1) *and U^N be the solution of the discrete problem* (3.5.1) *defined on $\overline{\Omega}_\sigma^N$. Then the following gives a bound on the local truncation error*

$$\begin{aligned} \left|L_\varepsilon^N (U^N - u)(x_i,t_j)\right| \quad &\leq \quad \frac{\varepsilon}{3}(x_{i+1} - x_{i-1}) \left\| \frac{\partial^3 u}{\partial x^3} \right\| + \frac{a(x_i,t_j)}{2}(x_{i+1} - x_i) \left\| \frac{\partial^2 u}{\partial x^2} \right\| \\ &+ \quad \frac{b(x_i,t_j)}{2}(t_j - t_{j-1}) \left\| \frac{\partial^2 u}{\partial t^2} \right\|. \end{aligned}$$

3.6 Decomposition of numerical solution and error estimates

In an analogous manner to the continuous case we decompose our numerical solution into a regular and a singular component

$$U^N(x_i,t_j) = V^N(x_i,t_j) + W^N(x_i,t_j), \quad \forall (x_i,t_j) \in \overline{\Omega}_\sigma^N,$$

where V^N is the solution of the inhomogeneous problem

$$\begin{aligned} L_\varepsilon^N V^N(x_i,t_j) &= f(x_i,t_j) \quad \text{in } \Omega_\sigma^N, && \text{(3.6.1a)} \\ V^N(x_i,t_j) &= v(x_i,t_j) \quad \text{on } \Gamma_\sigma^N, && \text{(3.6.1b)} \end{aligned}$$

and therefore W^N is the solution to the problem

$$\begin{aligned} L_\varepsilon^N W^N(x_i,t_j) &= 0 \quad \text{in } \Omega_\sigma^N, && \text{(3.6.2a)} \\ W^N(x_i,t_j) &= w(x_i,t_j) \quad \text{on } \Gamma_\sigma^N. && \text{(3.6.2b)} \end{aligned}$$

The error in our numerical solution can now also be decomposed:

$$(U^N - u)(x_i,t_j) = ((V^N - v) + (W^N - w))(x_i,t_j), \quad \forall (x_i,t_j) \in \overline{\Omega}_\sigma^N,$$

and we estimate the error in the regular component and the singular component separately.

Theorem 3.6.1 (Error in the Regular Component). *Under Assumption 3.4.1 the error in the regular component satisfies the following estimate*

$$\left|(V^N - v)(x_i,t_j)\right| \leq C(N_x^{-1} + N_t^{-1}), \quad \forall (x_i,t_j) \in \overline{\Omega}_\sigma^N,$$

where V^N is the solution of (3.6.1) *and v is the solution of* (3.4.1).

Proof. We begin by considering the truncation error with respect to the regular component. From Theorem 3.5.3 this is

$$\begin{aligned}\left|L_\varepsilon^N(V^N - v)(x_i,t_j)\right| &\leq \frac{\varepsilon}{3}(x_{i+1}-x_{i-1})\left\|\frac{\partial^3 v}{\partial x^3}\right\| + \frac{a(x_i,t_j)}{2}(x_{i+1}-x_i)\left\|\frac{\partial^2 v}{\partial x^2}\right\| \\ &+ \frac{b(x_i,t_j)}{2}(t_j - t_{j-1})\left\|\frac{\partial^2 v}{\partial t^2}\right\|.\end{aligned}$$

Using the bounds on the derivatives of v given in Theorem 3.4.2 and the fact that

$$x_{i+1} - x_{i-1} \leq 4N_x^{-1}, \quad x_{i+1} - x_i \leq 2N_x^{-1}, \quad t_j - t_{j-1} = N_t^{-1},$$

we get

$$\begin{aligned}\left|L_\varepsilon^N(V^N - v)(x_i,t_j)\right| &\leq C(N_x^{-1}\varepsilon(1+\varepsilon^{1/2}) + N_x^{-1}(1+\varepsilon) + N_t^{-1}) \\ &\leq C(N_x^{-1} + N_t^{-1}), \quad \forall (x_i,t_j) \in \Omega_\sigma^N,\end{aligned}$$

and an application of Lemma 3.5.2 gives us

$$\left|(V^N - v)(x_i,t_j)\right| \leq C(N_x^{-1} + N_t^{-1}), \quad \forall (x_i,t_j) \in \overline{\Omega}_\sigma^N.$$

□

Note that the above theorem is also valid on a uniform mesh. It is only when we come to deal with the singular component that the fitted mesh is needed. In order to examine the error in the singular component we will require the following bound (see for example [15]).

$$\left(1 + \frac{2\ln M}{M}\right)^{-M/2} \leq \frac{2}{M}, \quad \forall M \geq 4. \tag{3.6.3}$$

Theorem 3.6.2 (Error in the Singular Component). *Under Assumption 3.4.1 we have, for all $N_x \geq 4$ and $N_t > \max_{\overline{\Omega}}\{0, (2-d)/b\}$, the following estimate for the error in the singular component*

$$\left|(W^N - w)(x_i,t_j)\right| \leq C(N_x^{-1}(\ln N_x)^2 + N_t^{-1}), \quad \forall (x_i,t_j) \in \overline{\Omega}_\sigma^N,$$

where W^N is the solution of (3.6.2) *and w is the solution of* (3.4.2).

Proof. We consider separately the cases $\sigma = 1/2$ and $\sigma = \sqrt{\varepsilon}\ln N_x$. In the first case the mesh is uniform and we have

$$\varepsilon^{-1} \leq 4(\ln N_x)^2. \tag{3.6.4}$$

The expression for the local truncation error is, from Theorem 3.5.3,

$$\begin{aligned} \left|L_\varepsilon^N(W^N - w)(x_i,t_j)\right| &\leq \frac{\varepsilon}{3}(x_{i+1} - x_{i-1})\left\|\frac{\partial^3 w}{\partial x^3}\right\| + \frac{a(x_i,t_j)}{2}(x_{i+1} - x_i)\left\|\frac{\partial^2 w}{\partial x^2}\right\| \\ &+ \frac{b(x_i,t_j)}{2}(t_j - t_{j-1})\left\|\frac{\partial^2 w}{\partial t^2}\right\|. \end{aligned}$$

Using the bounds on the derivatives of w (which follow from the bounds on the derivatives of u given in Theorem 3.3.3), (3.6.4), and the fact that

$$x_{i+1} - x_{i-1} = 2N_x^{-1}, \quad x_{i+1} - x_i = N_x^{-1}, \quad t_j - t_{j-1} = N_t^{-1},$$

we get

$$\begin{aligned} \left|L_\varepsilon^N(W^N - w)(x_i,t_j)\right| &\leq C(N_x^{-1}\varepsilon^{-1/2} + N_x^{-1}\varepsilon^{-1} + N_t^{-1}) \\ &\leq C(N_x^{-1}(\ln N_x)^2 + N_t^{-1}), \quad \forall (x_i,t_j) \in \Omega_\sigma^N. \end{aligned}$$

Applying Lemma 3.5.2 then gives

$$\left|(W^N - w)(x_i,t_j)\right| \leq C(N_x^{-1}(\ln N_x)^2 + N_t^{-1}), \quad \forall (x_i,t_j) \in \overline{\Omega}_\sigma^N.$$

We now consider the other case, that is when $\sigma = \sqrt{\varepsilon}\ln N_x$. The mesh is now piecewise uniform and the mesh spacing (in the x-direction) is $h = 2\sigma/N_x$ in the subinterval $(0,\sigma)$ and $H = 2(1-\sigma)/N_x$ in the subinterval $(\sigma,1)$. The argument now depends on the position of the mesh point x_i.

If $x_i \in [\sigma,1)$ then from the bound on w given in Theorem 3.4.3 we have

$$|w(x_i,t_j)| \leq Ce^{-\sigma/\sqrt{\varepsilon}} = CN_x^{-1}.$$

To derive a similar bound on W^N we introduce the mesh function Y^N which is defined as

$$Y^N_{i,j} \equiv Y^N(x_i,t_j) = \begin{cases} \left(1+\frac{h}{\sqrt{\varepsilon}}\right)^{-i}\left(1-\frac{A}{N_t}\right)^{-j}, & 0 \le i \le \frac{N_x}{2}, \\ Y^N_{N_x/2,j}\left(1+\frac{H}{\sqrt{\varepsilon}}\right)^{-(i-N_x/2)}\left(1-\frac{A}{N_t}\right)^{-j}, & \frac{N_x}{2} < i \le N_x, \end{cases}$$

where $A = \max_{\overline{\Omega}}\{0,(2-d)/b\}$. This is the discrete analogue of the barrier function used in Theorem 3.4.3.

Provided we choose N_t large enough (i.e. $N_t > A$) we have

$$Y^N(x_i,t_j) \ge 0, \quad \forall (x_i,t_j) \in \overline{\Omega}^N_\sigma.$$

Also,

$$D^+_x Y(x_i,t_j) < 0, \quad D^-_t Y(x_i,t_j) > 0, \quad \forall (x_i,t_j) \in \Omega^N_\sigma.$$

Now we apply the difference operator to Y^N:

$$\begin{aligned} L^N_\varepsilon Y^N_{i,j} &= \varepsilon\delta^2_x Y^N_{i,j} + a(x_i,t_j)D^+_x Y^N_{i,j} - b(x_i,t_j)D^-_t Y^N_{i,j} - d(x_i,t_j)Y^N_{i,j} \\ &\le \varepsilon\delta^2_x Y^N_{i,j} + a(x_i,t_j)D^+_x Y^N_{i,j}. \end{aligned}$$

Depending on the position of the mesh point x_i we get two different expressions. If $i \ne N_x/2$ we have

$$L^N_\varepsilon Y_{i,j} \le (1-Ab-d)Y^N_{i,j} \le 0, \quad \forall j.$$

While if $i = N_x/2$

$$\begin{aligned} L^N_\varepsilon Y_{N_x/2,j} &\le (N_x H - Ab - d)Y^N_{i,j} \\ &\le (2-Ab-d)Y^N_{i,j} \le 0, \quad \forall j. \end{aligned}$$

Now consider the mesh function, $CY^N - W^N$. We have

$$(CY^N - W^N)(x_i,t_j) \ge 0, \quad \forall (x_i,t_j) \in \Gamma^N_\sigma,$$

once we take $C \geq \max_{0\leq j\leq N_t} \left|W^N(0,t_j)\right|$. Also

$$\begin{aligned} L_\varepsilon^N(CY^N - W^N)(x_i,t_j) &= (CL_\varepsilon^N Y^N - L_\varepsilon^N W^N)(x_i,t_j) \\ &= CL_\varepsilon^N Y^N(x_i,t_j) \\ &\leq 0. \end{aligned}$$

Then Lemma 3.5.1 applies and we get

$$W^N(x_i,t_j) \leq CY^N(x_i,t_j), \quad \forall (x_i,t_j) \in \overline{\Omega}_\sigma^N.$$

But

$$\begin{aligned} Y^N(\sigma,t_j) &= \left(1+\frac{2\ln N_x}{N_x}\right)^{-N_x/2}\left(1-\frac{A}{N_t}\right)^{-j} \\ &\leq 2N_x^{-1}\left(1-\frac{A}{N_t}\right)^{-N_t} \\ &\leq CN_x^{-1}, \end{aligned}$$

by (3.6.3), and the fact that

$$\lim_{N_t\to\infty}\left(1-\frac{A}{N_t}\right)^{-N_t} \leq C.$$

Therefore we get

$$W^N(x_i,t_j) \leq CN_x^{-1}, \quad \forall (x_i,t_j) \in \overline{\Omega}_\sigma^N \quad s.t. \quad x_i \in [\sigma,1),$$

and the error in the singular component in this case can now be estimated as

$$\begin{aligned} \left|(W^N - w)(x_i,t_j)\right| &\leq \left|W^N(x_i,t_j)\right| + \left|w(x_i,t_j)\right| \\ &\leq CN_x^{-1}, \quad \forall (x_i,t_j) \in \overline{\Omega}_\sigma^N \quad s.t. \quad x_i \in [\sigma,1). \end{aligned}$$

If $x_i \in (0,\sigma)$ then the expression for the truncation error becomes

$$\left|L_\varepsilon^N(W^N - w)(x_i,t_j)\right| \leq C(N_x^{-1}\ln N_x + a(x_i,t_j)\varepsilon^{-1/2}N_x^{-1}\ln N_x + N_t^{-1}).$$

Now consider the discrete barrier functions

$$\psi^{\pm}(x_i,t_j) = C(\varepsilon^{-1/2}N_x^{-1}\ln N_x(\sigma - x_i) + (N_x^{-1}(\ln N_x) + N_t^{-1})t_j + N_x^{-1}) \pm (W^N - w)(x_i,t_j).$$

We have

$$\begin{aligned} \psi^{\pm}(x_i,0) &\geq 0, \qquad 0 \leq i \leq N_x/2, \\ \psi^{\pm}(0,t_j) &\geq 0, \qquad 0 \leq j \leq N_t, \\ \psi^{\pm}(\sigma,t_j) &\geq 0, \qquad 0 \leq j \leq N_t, \\ \text{and} \quad L_\varepsilon^N \psi^{\pm}(x_i,t_j) &\leq 0, \quad \forall (x_i,t_j) \in \Omega_\sigma^N \quad s.t. \quad x_i \in (0,\sigma). \end{aligned}$$

Applying Lemma 3.5.2 in the subregion of $\overline{\Omega}_\sigma^N$ bounded by $t = 0$, $x = 0$, and $x = \sigma$ we get

$$\psi_{i,j}^{\pm} \geq 0 \quad \forall (x_i,t_j) \in \overline{\Omega}_\sigma^N \quad s.t. \quad x_i \in (0,\sigma).$$

This implies that

$$\begin{aligned} \left|(W^N - w)(x_i,t_j)\right| &\leq C(N_x^{-1}(\ln N_x)\varepsilon^{-1/2}\sigma + (N_x^{-1}(\ln N_x) + N_t^{-1})t_j + N_x^{-1}) \\ &\leq C(N_x^{-1}(\ln N_x)^2 + N_t^{-1}), \quad \forall (x_i,t_j) \in \overline{\Omega}_\sigma^N \quad s.t.\ x_i \in (0,\sigma). \end{aligned}$$

Combining the estimates in each subregion gives the required result. □

The previous two theorems together give us the following ε-uniform estimate of the error in our numerical approximations at the mesh points.

Theorem 3.6.3. *Let u be any solution from Problem Class 3.2.1 and U^N be the corresponding numerical solution generated by Method 3.5.1. Then, under Assumption 3.4.1, for all $N_x \geq 4$ and $N_t > \max_{\overline{\Omega}}\{0,(2-d)/b\}$, we have*

$$\sup_{0<\varepsilon\leq 1} \left\|U^N - u\right\|_{\overline{\Omega}_\sigma^N} \leq C(N_x^{-1}(\ln N_x)^2 + N_t^{-1}),$$

where C is a constant independent of N_x, N_t and ε.

3.7 Numerical results

In this section we present numerical results that verify computationally the theoretical result of the last section. We take $T = 1$ and consider the following subclass of Problem Class 3.2.1

Problem Class 3.7.1.

$$\begin{aligned}(\varepsilon u_{xx} + x^p u_x - u_t - u)(x,t) &= x^2 - 1 \quad in \quad \Omega,\\ u(x,0) &= (1-x)^2, \quad 0 \le x \le 1,\\ u(0,t) = 1 + t^2, \quad u(1,t) &= 0, \qquad 0 \le t \le 1.\end{aligned}$$

We let $N_x = N_t = N$ and tabulate the computed errors, E_ε^N, and the computed ε-uniform errors, E^N, for a variety of values of ε and N for $p = 1.0$ (Table 3.1). For other values of p the error behaviour is analogous and so we show only the computed ε-uniform errors (Table 3.2). As we do not have an exact solution for the above problem we use the piecewise bilinear interpolant of the numerical solution generated on the finest available mesh, *viz.* $\overline{U}^{1024}$, as an approximation to the exact solution. Thus we define E_ε^N and E_ε as follows

$$E_\varepsilon^N = \max_{0 \le i,j \le N} |U^N(x_i,t_j) - \overline{U}^{1024}(x_i,t_j)|, \qquad E^N = \max_{\varepsilon = 1, 2^{-1}, \ldots, 2^{-32}} E_\varepsilon^N.$$

We also tabulate the computed ε-uniform orders of convergence q^N for each value of p considered (Table 3.3). These are calculated from the two-mesh differences defined as

$$D_\varepsilon^N = \max_{0 \le i,j \le N} |U^N(x_i,t_j) - \overline{U}^{2N}(x_i,t_j)|, \qquad D^N = \max_{\varepsilon = 1, 2^{-1}, \ldots, 2^{-32}} D_\varepsilon^N.$$

The q^N are then defined as

$$q^N = \log_2 \frac{D^N}{D^{2N}}.$$

We see from Table 3.1 that the values of E_ε^N for each fixed ε decrease with increasing N. *A fortiori* the values of E^N decrease with increasing N indicating that the convergence is uniform with respect to ε. For various values of p, ε-uniform orders

of convergence depending on N are given in Table 3.3. As N increases, the convergence order approaches 1, which corresponds to the conclusion of Theorem 3.6.3. For this particular problem, the orders of convergence (over the range of $N \in [8, 256]$) are higher than the theoretical rate given in Theorem 3.6.3 (see [15, §8.3] for some sample values). The orders tend to the order associated with $CN^{-1} \ln N$ for all values of p. In Figure 3.2 we plot the numerical solution generated by Method 3.5.1 for particular values of p, ε and N.

3.8 The case $p < 1$.

This chapter deals with the case $p \geq 1$. It is interesting to examine numerically the case $p < 1$. There are extra technical considerations to be taken into account when $p < 1$. In particular we impose the following further restrictions on the data of the problem

$$\|f/a\|_{\overline{\Omega}} \leq C, \quad \|f/b\|_{\overline{\Omega}} \leq C, \quad \|f/d\|_{\overline{\Omega}} \leq C,$$

to ensure that the solution is ε-uniformly bounded.

We can transform the independent variable x to the stretched variable $\tilde{x} = x/\varepsilon^{\frac{1}{p+1}}$ and neglect the terms containing $\varepsilon^{\frac{1-p}{1+p}}$. The resulting differential equation is independent of ε and therefore we arrive at the following assumption:

Assumption 3.8.1. *For all non-negative integers i, j, such that $0 \leq i + 2j \leq 3$,*

$$\left\| \frac{\partial^{i+j} u}{\partial x^i \partial t^j} \right\|_{\Omega} \leq C\varepsilon^{-i/(p+1)}, \quad \text{if} \quad 0 < p < 1. \tag{3.8.1}$$

In order to generate numerical solutions to problems from this new class we propose using the same numerical method as in §3.5 but with the following choice of transition parameter

$$\sigma = \min\left\{\frac{1}{2}, \left(\frac{2(p+1)\varepsilon}{\alpha} \ln N_x\right)^{\frac{1}{p+1}}\right\}.$$

This is motivated by (3.8.1).

We now demonstrate experimentally that the numerical solutions do converge.

ε	Number of Intervals N					
	8	16	32	64	128	256
1.0	3.44e-02	2.01e-02	1.15e-02	5.95e-03	2.88e-03	1.26e-03
2^{-1}	1.85e-02	9.46e-03	4.99e-03	2.54e-03	1.22e-03	5.28e-04
2^{-2}	2.89e-02	1.46e-02	7.23e-03	3.52e-03	1.64e-03	7.06e-04
2^{-3}	3.91e-02	1.99e-02	9.86e-03	4.80e-03	2.25e-03	9.64e-04
2^{-4}	4.97e-02	2.51e-02	1.25e-02	6.07e-03	2.84e-03	1.22e-03
2^{-5}	5.09e-02	3.04e-02	1.53e-02	7.44e-03	3.48e-03	1.49e-03
2^{-6}	4.93e-02	2.93e-02	1.68e-02	9.18e-03	4.29e-03	1.84e-03
2^{-7}	4.94e-02	2.81e-02	1.58e-02	8.81e-03	4.67e-03	2.28e-03
2^{-8}	5.41e-02	3.01e-02	1.53e-02	8.38e-03	4.39e-03	2.04e-03
2^{-9}	5.70e-02	3.19e-02	1.66e-02	8.22e-03	4.31e-03	2.01e-03
2^{-10}	5.90e-02	3.29e-02	1.74e-02	8.70e-03	4.27e-03	2.00e-03
2^{-11}	6.02e-02	3.37e-02	1.81e-02	9.08e-03	4.31e-03	1.99e-03
2^{-12}	6.11e-02	3.45e-02	1.85e-02	9.34e-03	4.45e-03	1.98e-03
2^{-13}	6.16e-02	3.50e-02	1.88e-02	9.51e-03	4.55e-03	1.98e-03
2^{-14}	6.20e-02	3.53e-02	1.90e-02	9.65e-03	4.62e-03	2.01e-03
2^{-15}	6.23e-02	3.55e-02	1.91e-02	9.74e-03	4.67e-03	2.03e-03
2^{-16}	6.24e-02	3.57e-02	1.92e-02	9.80e-03	4.71e-03	2.05e-03
2^{-17}	6.26e-02	3.58e-02	1.93e-02	9.84e-03	4.73e-03	2.06e-03
2^{-18}	6.26e-02	3.59e-02	1.93e-02	9.87e-03	4.75e-03	2.07e-03
2^{-19}	6.27e-02	3.59e-02	1.93e-02	9.89e-03	4.76e-03	2.08e-03
2^{-20}	6.28e-02	3.60e-02	1.94e-02	9.90e-03	4.77e-03	2.08e-03
2^{-21}	6.28e-02	3.60e-02	1.94e-02	9.91e-03	4.78e-03	2.08e-03
2^{-22}	6.28e-02	3.60e-02	1.94e-02	9.92e-03	4.78e-03	2.09e-03
2^{-23}	6.28e-02	3.60e-02	1.94e-02	9.93e-03	4.78e-03	2.09e-03
2^{-24}	6.28e-02	3.61e-02	1.94e-02	9.93e-03	4.79e-03	2.09e-03
$\vdots$	$\vdots$	$\vdots$	$\vdots$	$\vdots$	$\vdots$	$\vdots$
2^{-32}	6.29e-02	3.61e-02	1.94e-02	9.94e-03	4.79e-03	2.09e-03
E^N	6.29e-02	3.61e-02	1.94e-02	9.94e-03	4.79e-03	2.28e-03

Table 3.1: Computed errors, E_ε^N, and computed ε-uniform errors, E^N, for Method 3.5.1 applied to Problem Class 3.7.1 with $p = 1.0$.

p	Number of Intervals N					
	8	16	32	64	128	256
2.0	5.67e-02	4.09e-02	2.28e-02	1.21e-02	5.96e-03	2.64e-03
3.0	6.40e-02	4.12e-02	2.43e-02	1.33e-02	6.68e-03	2.99e-03
5.0	7.09e-02	4.60e-02	2.68e-02	1.49e-02	7.58e-03	3.43e-03
10.0	4.39e-02	3.72e-02	2.83e-02	1.65e-02	8.63e-03	4.01e-03

Table 3.2: Computed ε-uniform errors, E^N, for Method 3.5.1 applied to Problem Class 3.7.1 for various values of p.

p	Number of Intervals N					
	8	16	32	64	128	256
1.0	6.77e-01	8.11e-01	8.85e-01	9.35e-01	8.89e-01	8.97e-01
2.0	3.88e-01	7.44e-01	8.25e-01	8.95e-01	9.37e-01	9.62e-01
3.0	5.84e-01	5.80e-01	7.87e-01	8.72e-01	9.19e-01	9.51e-01
5.0	3.79e-01	6.00e-01	7.81e-01	8.04e-01	8.96e-01	9.33e-01
10.0	1.15e-01	5.11e-01	5.94e-01	7.34e-01	8.52e-01	9.07e-01

Table 3.3: Computed ε-uniform orders of convergence, q^N, for Method 3.5.1 applied to Problem Class 3.7.1 for various values of p.

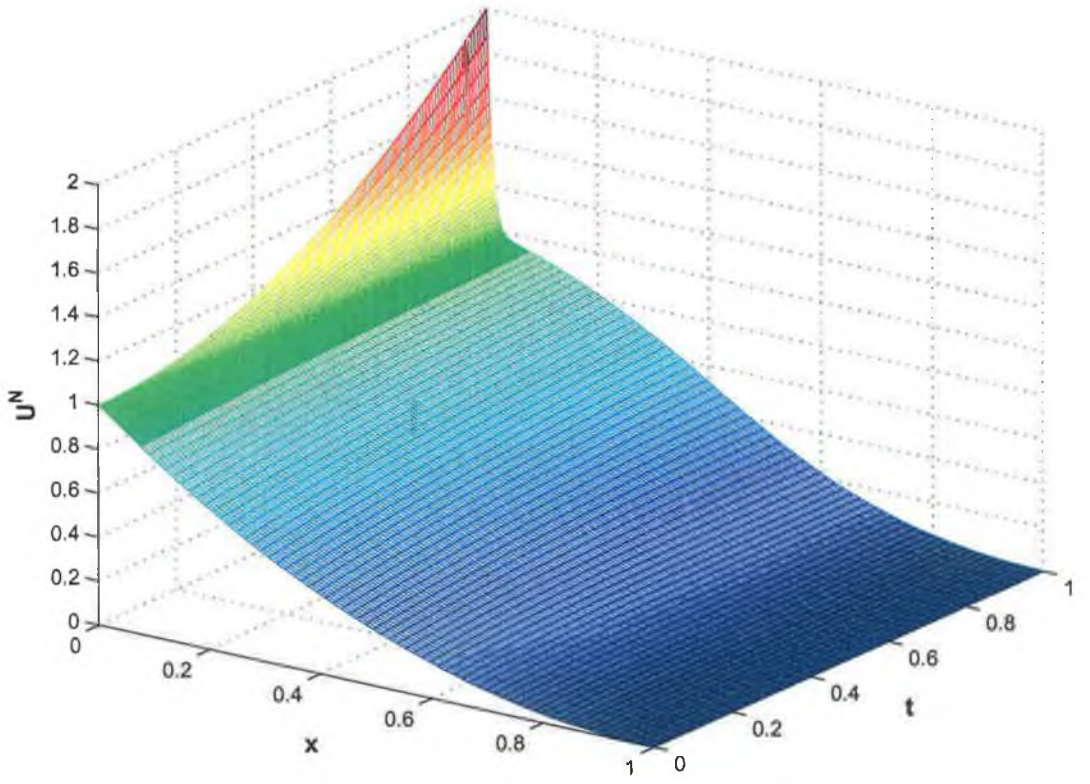

Figure 3.2: Numerical solution generated by Method 3.5.1 applied to problem from Problem Class 3.7.1 with $p = 2$, $N = 128$ and $\varepsilon = 2^{-12}$.

We consider the following problem for various values of p.

Problem Class 3.8.1.

$$\begin{aligned}(\varepsilon u_{xx} + x^p u_x - x^p u_t)(x,t) &= -2x^p \quad in\ \Omega,\\ u(0,t) = 1+t^2, \quad u(1,t) &= 0, \quad 0 \le t \le 1,\\ u(x,0) &= 1-x^2, \quad 0 \le x \le 1.\end{aligned}$$

As before we let $N_x = N_t = N$ and tabulate the computed ε-uniform orders of convergence q^N for each value of p considered (Table 3.4). The behaviour of the errors indicates that the numerical solutions converge. Of course theoretical analysis is required to establish the convergence of this numerical scheme in the case $0 < p < 1$.

	Number of Intervals N					
p	8	16	32	64	128	256
0.1	6.95e-01	7.63e-01	8.02e-01	8.48e-01	8.96e-01	9.15e-01
0.2	6.99e-01	7.61e-01	8.15e-01	8.58e-01	9.03e-01	9.37e-01
0.5	7.04e-01	7.69e-01	8.22e-01	8.69e-01	9.12e-01	9.44e-01

Table 3.4: Computed ε-uniform orders of convergence, q^N, for Problem 3.8.1 for various values of p.

Chapter 4

Numerical methods for a class of singularly perturbed elliptic problems

4.1 Introduction

In this chapter we will consider a class of singularly perturbed elliptic problems posed on a non-rectangular domain. The boundary of the domain will typically be piecewise-smooth. We assume that there exists a sufficiently regular co-ordinate transformation from the domain to the unit square. Then we will proceed to study the transformed class of problems. We restrict our attention to the case when only regular layers appear in the solutions of problems from this class. This requires some restrictions on the data of the transformed problem class.

The most interesting feature of the transformed problem class is the presence of a mixed derivative term in the differential equation. This is significant for a number of reasons. Firstly it is in sharp contrast to what happens in the parabolic case where no extra terms are introduced into the transformed problem. Thus it will be seen that the construction of an appropriate numerical method is more complicated in this case. Secondly the mixed derivative term also introduces a number of technical considerations in the analysis of the numerical method. Chief among these is the issue of the construction of a monotone difference scheme for the problem.

The material in this chapter is set out as follows. In §4.2 we introduce a class of problems posed on a non-rectangular domain and show the form of the differential equation when we transform to a rectangular domain. In §4.3 we state precisely the class of problems we will consider and establish bounds on solutions to such problems and their derivatives. In §4.4 a decomposition of the solution is constructed which enables us to establish sharper bounds on the derivatives. In §4.5 we introduce the numerical method that will be used to generate approximations to solutions of problems from the transformed problem class. In §4.6 we discuss our choice of finite difference operator paying particular attention to the requirement of monotonicity. Finally, in §4.7 we prove that the approximations generated by this method converge uniformly with respect to the singular perturbation parameter.

4.2 Statement of problem

We consider the following class of singularly perturbed elliptic problems:

Problem Class 4.2.1.

$$\hat{L}_\varepsilon \hat{u}(\xi,\eta) \equiv (\varepsilon \Delta \hat{u} + \hat{\mathbf{a}} \cdot \nabla \hat{u})(\xi,\eta) = \hat{f}(\xi,\eta) \qquad \text{in } \hat{\Omega}, \tag{4.2.1a}$$

$$\hat{u}(\xi,\eta) = \hat{g}(\xi,\eta) \qquad \text{on } \partial\hat{\Omega}, \tag{4.2.1b}$$

$$\hat{\mathbf{a}}(\xi,\eta) = (\hat{a}_1(\xi,\eta), \hat{a}_2(\xi,\eta)), \qquad \forall (\xi,\eta) \in \hat{\Omega}, \tag{4.2.1c}$$

$$\hat{\mathbf{a}} \cdot \hat{\mathbf{n}} \neq 0, \tag{4.2.1d}$$

where $\hat{\Omega} \subset \mathbb{R}^2$ *is a piecewise-smooth domain,* $\hat{\mathbf{n}}$ *denotes the unit outward normal on* $\partial\hat{\Omega}$*, and* $0 < \varepsilon \leq 1$ *is the perturbation parameter.*

We also assume that the data $\hat{a}$, $\hat{f}$, and $\hat{g}$ are sufficiently smooth and that $\hat{f}$ and $\hat{g}$ satisfy sufficient compatibility conditions at the corners of the domain.

We assume that there exists a sufficiently smooth co-ordinate transformation from $\hat{\Omega}$ to $\Omega = (0,1) \times (0,1)$:

$$x \equiv A(\xi,\eta), \quad y \equiv B(\xi,\eta), \quad u(x,y) \equiv \hat{u}(\xi,\eta). \tag{4.2.2}$$

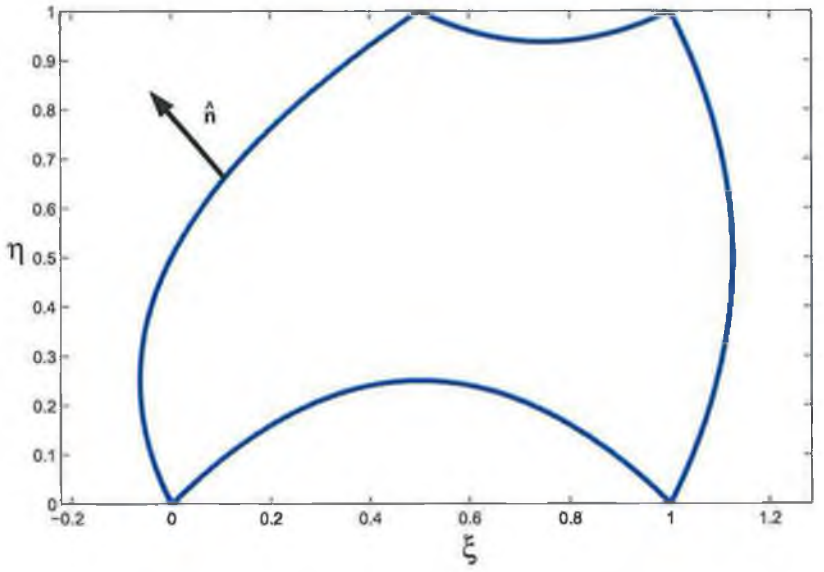

Figure 4.1: A piecewise-smooth domain $\hat{\Omega}$.

The transformed differential equation then takes the form

$$\begin{aligned}(\varepsilon((A_\xi^2 + A_\eta^2)u_{xx} + 2(A_\xi B_\xi + A_\eta B_\eta)u_{xy} + (B_\xi^2 + B_\eta^2)u_{yy}) \\ +(\hat{L}_\varepsilon A)u_x + (\hat{L}_\varepsilon B)u_y)(x,y) = f(x,y) \quad \text{in } \Omega.\end{aligned}$$

Note that to write this equation out explicitly requires that we can invert the transformation in (4.2.2) to obtain ξ and η as functions of x and y. Note also the presence of the mixed derivative of the solution in the term $2(A_\xi B_\xi + A_\eta B_\eta)u_{xy}$. The ellipticity of the differential operator is preserved once the Jacobian of the transformation (4.2.2) is non-zero. To see this we write the highest order terms in the differential equation as $au_{xx} + 2bu_{xy} + cu_{yy}$ and calculate the quantity $b^2 - ac$:

$$(A_\xi B_\xi + A_\eta B_\eta)^2 - (A_\xi^2 + A_\eta^2)(B_\xi^2 + B_\eta^2) = -(A_\xi B_\eta - A_\eta B_\xi)^2 < 0.$$

4.3 The continuous problem

Motivated by the discussion in the previous section we now state precisely the problem we are considering. It is the general second order singularly perturbed linear elliptic equation with variable coefficients and homogeneous Dirichlet boundary conditions.

Problem Class 4.3.1.

$$L_\varepsilon u(x,y) \equiv (\varepsilon(au_{xx} + 2bu_{xy} + cu_{yy}) + \mathbf{a}\cdot\nabla u)(x,y) = f(x,y) \quad \text{in } \Omega, \tag{4.3.1a}$$

$$u(x,y) = 0 \quad \text{on } \partial\Omega, \tag{4.3.1b}$$

where

$$\mathbf{a}(x,y) = (a_1(x,y), a_2(x,y)) > (\alpha_1, \alpha_2) > (0,0), \qquad \forall (x,y) \in \overline{\Omega}, \tag{4.3.1c}$$

and the coefficients a, b and c satisfy the following ellipticity conditions:
For all $(r,s) \in \mathbb{R}^2$

$$C_1(r^2+s^2) \le (ar^2 + 2brs + cs^2)(x,y) \le C_2(r^2+s^2), \quad (x,y) \in \Omega, \tag{4.3.1d}$$

where $C_1, C_2 > 0$ *are positive constants.*

Remark 4.3.1. There is no loss of generality in assuming homogeneous boundary conditions. To see this consider the problem

$$L_\varepsilon v(x,y) = f(x,y) \quad \text{in } \Omega, \qquad v(x,y) = g(x,y) \quad \text{on } \partial\Omega.$$

Assuming g is sufficiently smooth define the transformation $u = v - g^\star$, where $g^\star$ is defined to be an extension of the boundary conditions g to the whole of the domain $\overline{\Omega}$. For example we could let

$$\begin{aligned} g^\star(x,y) &= g_s(x)(1-y) + g_w(y)(1-x) + g_n(x)y + g_e(y)x \\ &- (g_s(0)(1-x)(1-y) + g_e(1)(1-x)y + g_n(1)xy + g_e(0)x(1-y)), \end{aligned}$$

where g_s, g_e, g_n and g_w are the boundary functions on the appropriate sides, and at

the four corners of the domain we have

$$g_s(0) = g_e(0), \quad g_e(1) = g_n(0), \quad g_n(1) = g_w(1), \quad g_w(0) = g_s(1).$$

Then u satisfies the problem

$$L_\varepsilon u(x,y) = f(x,y) - L_\varepsilon g^\star(x,y) \quad \text{in } \Omega, \qquad u(x,y) = 0 \quad \text{on } \partial\Omega,$$

which is of the form of Problem Class 4.3.1.

Remark 4.3.2. The conditions (4.3.1c) ensure that the solutions of problems from this class possess regular layers in a neighbourhood of the sides $x = 0$ and $y = 0$ and a corner layer in a neighbourhood of the corner $(0,0)$. We thus exclude the possibility of characteristic boundary layers.

Remark 4.3.3. The conditions (4.3.1d) obviously imply that the functions a and c are strictly positive. Another consequence of the conditions (4.3.1d) is the following familiar inequality

$$(b(x,y))^2 < a(x,y)c(x,y), \quad \text{for all } (x,y) \in \Omega. \tag{4.3.2}$$

To see this let $r = -\sqrt{c}$ and $s = \frac{b}{\sqrt{c}}$ in (4.3.1d).

The differential operator L_ε in (4.3.1a) satisfies the following minimum principle.

Lemma 4.3.1 (Minimum Principle). *Let* $v \in C^2(\overline{\Omega})$.

$$\begin{gathered} \textit{If} \quad v(x,y) \geq 0, \quad \forall (x,y) \in \partial\Omega, \quad \textit{and} \quad L_\varepsilon v(x,y) \leq 0, \quad \forall (x,y) \in \Omega, \\ \textit{then} \quad v(x,y) \geq 0, \quad \forall (x,y) \in \overline{\Omega}. \end{gathered}$$

Proof.

$$\text{Assume } \exists\, \mathbf{p} = (p_1, p_2) \in \overline{\Omega} \quad \text{such that} \quad v(\mathbf{p}) < 0,$$

$$\text{then} \quad \mathbf{p} \notin \partial\Omega, \quad \text{which implies} \quad \mathbf{p} \in \Omega.$$

Now let

$$w(x,y) = v(x,y)\, e^{\gamma_1 x/\varepsilon} e^{\gamma_2 y/\varepsilon}, \quad \forall (x,y) \in \overline{\Omega},$$

where

$$\gamma_1 = \frac{\alpha_1}{2\,\|a\|}, \quad \gamma_2 = \frac{\alpha_2}{2\,\|c\|}.$$

Then $w(x,y) \geq 0, \quad \forall (x,y) \in \partial\Omega$ and $w(\mathbf{p}) < 0$. Thus the minimum of w must also be negative. Let $\mathbf{q} = (q_1, q_2) \in \Omega$ such that

$$w(\mathbf{q}) = \min_{\overline{\Omega}} w < 0.$$

From the definition of $\mathbf{q}$ we have

$$w_x(\mathbf{q}) = w_y(\mathbf{q}) = 0, \quad w_{xx}(\mathbf{q}) \geq 0, \quad (w_{xy}(\mathbf{q}))^2 \leq w_{xx}(\mathbf{q}) w_{yy}(\mathbf{q}). \tag{4.3.3}$$

But then

$$\begin{aligned}
L_\varepsilon v(\mathbf{q}) &= (\varepsilon(a w_{xx} + 2b w_{xy} + c w_{yy})(\mathbf{q}) \\
&+ (a_1 - 2(a\gamma_1 + b\gamma_2)) w_x(\mathbf{q}) + (a_2 - 2(b\gamma_1 + c\gamma_2)) w_y(\mathbf{q}) \\
&+ \varepsilon^{-1} \left(a\gamma_1^2 + 2b\gamma_1\gamma_2 + c\gamma_2^2 - a_1\gamma_1 - a_2\gamma_2\right) w(\mathbf{q})\big) \, e^{-\gamma_1 q_1/\varepsilon} e^{-\gamma_2 q_2/\varepsilon} \\
&\geq \Bigg(\varepsilon(a w_{xx} - 2\,\mathrm{sgn}(b(q_1,q_2)) b \sqrt{w_{xx} w_{yy}} + c w_{yy})(\mathbf{q}) \\
&+ \frac{1}{4\varepsilon}\left(\frac{a\alpha_1^2}{\|a\|^2} + \frac{2b\alpha_1\alpha_2}{\|a\|\,\|c\|} + \frac{\alpha_2^2}{\|c\|^2} - \frac{2a_1\alpha_1}{\|a\|} - \frac{2a_2\alpha_2}{\|c\|}\right) w(\mathbf{q})\Bigg) \, e^{-\gamma_1 q_1/\varepsilon} e^{-\gamma_2 q_2/\varepsilon} \\
&\geq \Bigg(\varepsilon(a w_{xx} - 2\,\mathrm{sgn}(b(q_1,q_2)) b \sqrt{w_{xx} w_{yy}} + c w_{yy})(\mathbf{q}) \\
&+ \frac{1}{4\varepsilon}\Bigg(\frac{\alpha_1}{\|a\|^2}(a\alpha_1 - \|a\|\, a_1) + \frac{\alpha_2}{\|c\|^2}(c\alpha_2 - \|c\|\, a_2) \\
&- \frac{1}{\|a\|\,\|c\|}\left(\|a\|\, a_2\alpha_2 - 2b\alpha_1\alpha_2 + \|c\|\, a_1\alpha_1\right)\Bigg) w(\mathbf{q})\Bigg) \, e^{-\gamma_1 q_1/\varepsilon} e^{-\gamma_2 q_2/\varepsilon} \\
&\geq \Bigg(\varepsilon(a w_{xx} - 2\,\mathrm{sgn}(b(q_1,q_2)) b \sqrt{w_{xx} w_{yy}} + c w_{yy})(\mathbf{q}) \\
&+ \frac{1}{4\varepsilon}\Bigg(\frac{\alpha_1}{\|a\|^2}(a\alpha_1 - \|a\|\, a_1) + \frac{\alpha_2}{\|c\|^2}(c\alpha_2 - \|c\|\, a_2) \\
&- \frac{1}{\|a\|\,\|c\|}\left(a\alpha_2^2 - 2b\alpha_1\alpha_2 + c\alpha_1^2\right)\Bigg) w(\mathbf{q})\Bigg) \, e^{-\gamma_1 q_1/\varepsilon} e^{-\gamma_2 q_2/\varepsilon} > 0
\end{aligned}$$

where we have used the inequalities (4.3.1c), the ellipticity condition (4.3.1d), the

definition of γ_1 and γ_2 and (4.3.3). This is a contradiction and thus our original assumption is false and we conclude that the minimum of v is non-negative. The result follows. □

An immediate consequence of this is the following bound on the solution of problems from Problem Class 4.3.1.

Corollary 4.3.2. *The solution u of any problem from Problem Class 4.3.1 satisfies the following bound*

$$\|u\| \leq \|f\| / \alpha,$$

where $\alpha = \max\{\alpha_1, \alpha_2\}$.

Proof. Consider the functions

$$\psi^{\pm}(x,y) = \frac{\|f\|}{\alpha_1}(1-x) \pm u(x,y), \quad (x,y) \in \overline{\Omega}.$$

Now,

$$\begin{aligned} L_\varepsilon \psi^{\pm}(x,y) &= -\frac{\|f\|}{\alpha_1} a_1(x,y) \pm f(x,y) \\ &\leq -\|f\| \pm f(x,y) \\ &\leq 0. \end{aligned}$$

Also,

$$\psi^{\pm}(x,y) = \frac{\|f\|}{\alpha_1}(1-x) \geq 0, \quad (x,y) \in \partial\Omega.$$

It follows from the minimum principle that

$$|u(x,y)| \leq \frac{\|f\|}{\alpha_1}(1-x) \leq \frac{\|f\|}{\alpha_1}, \quad (x,y) \in \overline{\Omega}.$$

Similarly it can be shown that

$$|u(x,y)| \leq \frac{\|f\|}{\alpha_2}, \quad (x,y) \in \overline{\Omega},$$

and the result follows. □

We now state some assumptions regarding the smoothness of the solutions of problems from Problem Class 4.3.1.

Assumption 4.3.3. *Assume that the functions a, b, c, a_1 and a_2 are smooth. Let $f \in C^{1,\nu}(\overline{\Omega})$ for some $\nu \in (0,1)$. Assume that f satisfies the compatibility conditions*

$$f(0,0) = f(1,0) = f(0,1) = f(1,1) = 0. \tag{4.3.4}$$

Assume also that f is sufficiently regular and that the data of the problem satisfy additional compatibility conditions so that $u \in C^{3,\nu}(\overline{\Omega})$ for some $\nu \in (0,1)$.

Remark 4.3.4. With the previous assumption we are ruling out the existence of any corner singularities in the solutions of our problems. The solutions to elliptic problems on non-smooth domains are in general not as smooth as their data and additional conditions need to be imposed to ensure their regularity. The conditions (4.3.4) are sufficient in the case when $b \equiv 0$ (see [18].) These are local conditions on the function f. Unfortunately for the Problem Class 4.3.1 it seems that such local conditions cannot be derived. This necessitates the introduction of this assumption as we require that $u \in C^{3,\nu}(\overline{\Omega})$ in the following analysis. This issue is discussed further in §1.5 in the Introduction.

We now establish some classical bounds on the derivatives of problems from Problem Class 4.3.1 where the inhomogeneous term in the differential equation can depend on ε.

Theorem 4.3.4. *Assume that a, b, c, a_1, a_2, $f \in C^{1,\nu}(\overline{\Omega})$ for some $\nu \in (0,1)$. Let $u \in C^{3,\nu}(\overline{\Omega})$ be the solution of a problem from Problem Class 4.3.1. Then if $\|f\|_\nu \leq C\varepsilon^{-1}$ we have*

$$|u|_k \leq C\varepsilon^{-k}, \quad \text{for} \quad k = 0,1,2,3,$$

and if $\|f\|_\nu \leq C\varepsilon^{-2}$ we have

$$|u|_k \leq C\varepsilon^{-(k+1)}, \quad \text{for} \quad k = 0,1,2,3.$$

Proof. We follow the proof given in [28, Theorem 3.2]. Transforming the variables

(x, y) to the stretched variables

$$\tilde{x} = \frac{x}{\varepsilon}, \quad \tilde{y} = \frac{y}{\varepsilon},$$

we see that Problem Class 4.3.1 becomes

Problem Class 4.3.2.

$$(\tilde{a}\tilde{u}_{\tilde{x}\tilde{x}} + 2\tilde{b}u_{\tilde{x}\tilde{y}} + \tilde{c}u_{\tilde{y}\tilde{y}} + \tilde{a}_1\tilde{u}_{\tilde{x}} + \tilde{a}_2\tilde{u}_{\tilde{y}})(\tilde{x}, \tilde{y}) = \tilde{f}(\tilde{x}, \tilde{y}) \quad in \ \tilde{\Omega}, \tag{4.3.5a}$$

$$\tilde{u}(\tilde{x}, \tilde{y}) = 0 \quad on \ \partial\tilde{\Omega}, \tag{4.3.5b}$$

where $\tilde{\Omega} = (0, 1/\varepsilon) \times (0, 1/\varepsilon)$ and $\partial\tilde{\Omega}$ is its boundary and

$$\begin{aligned} \tilde{u}(\tilde{x}, \tilde{y}) &= u(x, y), \quad \tilde{a}(\tilde{x}, \tilde{y}) = a(x, y), \quad \tilde{b}(\tilde{x}, \tilde{y}) = b(x, y), \quad \tilde{c}(\tilde{x}, \tilde{y}) = c(x, y), \\ \tilde{a}_1(\tilde{x}, \tilde{y}) &= a_1(x, y), \quad \tilde{a}_2(\tilde{x}, \tilde{y}) = a_2(x, y), \quad \tilde{f}(\tilde{x}, \tilde{y}) = \varepsilon f(x, y). \end{aligned}$$

The differential equation in (4.3.5a) is independent of ε. Thus from [26, p. 110] (which can be extended to the square using the techniques of [51]) we have, for all $\tilde{N}_\delta$,

$$|\tilde{u}|_{1,\tilde{N}_\delta} \leq |\tilde{u}|_{1,\nu,\tilde{N}_\delta} \leq C(\|\tilde{f}\|_{\nu,\tilde{N}_{2\delta}} + \|\tilde{u}\|_{\tilde{N}_{2\delta}}),$$

and, for $k = 0, 1$,

$$|\tilde{u}|_{k+2,\tilde{N}_\delta} \leq |\tilde{u}|_{k+2,\nu,\tilde{N}_\delta} \leq C(\|\tilde{f}\|_{k,\nu,\tilde{N}_{2\delta}} + \|\tilde{u}\|_{\tilde{N}_{2\delta}}),$$

where for each $(\tilde{x}, \tilde{y}) \in \overline{\tilde{\Omega}}$ we define

$$\tilde{N}_\delta = \tilde{N}_\delta(\tilde{x}, \tilde{y}) = ((\tilde{x} - \delta, \tilde{x} + \delta) \times (\tilde{y} - \delta, \tilde{y} + \delta)) \cap \overline{\tilde{\Omega}},$$

and the constant C is independent of $\tilde{N}_\delta$, ν and ε. Returning to the original variables it follows that

$$\begin{aligned} \varepsilon\,|u|_{1,N_\delta} &\leq C(\varepsilon\,\|f\|_{\nu,N_{2\delta}} + \|u\|_{N_{2\delta}}) \\ &\leq C(\varepsilon\,\|f\|_\nu + \|u\|), \end{aligned}$$

where N_δ is defined in an analogous manner to $\bar{N}_\delta$. Therefore we have

$$|u|_{1,N_\delta} \leq C(\|f\|_\nu + \varepsilon^{-1}\|u\|).$$

Now if $\|f\|_\nu \leq C\varepsilon^{-1}$ we get

$$|u|_{1,N_\delta} \leq C\varepsilon^{-1}, \tag{4.3.6}$$

where we have used the bound on u given in Corollary 4.3.2. While if $\|f\|_\nu \leq C\varepsilon^{-2}$ we get

$$|u|_{1,N_\delta} \leq C\varepsilon^{-2}. \tag{4.3.7}$$

Also for $k = 0, 1$

$$\begin{aligned} \varepsilon^{k+2}|u|_{k+2,N_\delta} &\leq C\left(\sum_{i=0}^{k}\varepsilon^{i+1}|f|_{i,\nu,N_{2\delta}} + \|u\|_{N_{2\delta}}\right) \\ &\leq C\left(\sum_{i=0}^{k}\varepsilon^{i+1}|f|_{i,\nu} + \|u\|\right). \end{aligned}$$

Therefore we have

$$|u|_{k+2,N_\delta} \leq C\left(\sum_{i=0}^{k}\varepsilon^{i-k-1}|f|_{i,\nu} + \varepsilon^{-k-2}\|u\|\right).$$

And if $\|f\|_\nu \leq C\varepsilon^{-1}$ we get

$$|u|_{k+2,N_\delta} \leq C\varepsilon^{-(k+2)}, \tag{4.3.8}$$

where we have again used the bound on u. While if $\|f\|_\nu \leq C\varepsilon^{-2}$ we get

$$|u|_{k+2,N_\delta} \leq C\varepsilon^{-(k+3)}. \tag{4.3.9}$$

Taking the supremum of the left-hand sides of (4.3.6), (4.3.7), (4.3.8) and (4.3.9) over all $N_\delta \subset \Omega$ gives the required results. □

4.4 Decomposition of solution

The bounds on derivatives given in the previous section are not adequate for the analysis of our numerical method. In this section we will establish sharper bounds on the derivatives by constructing a decomposition of the solution into regular and singular components.

Firstly we shall construct the regular component of the decomposition. This is done in the following way. We introduce an auxiliary problem defined on some extended domain. Through a careful decomposition of the solution to this problem we show that we can specify boundary conditions that ensure that the solution and its first two derivatives are bounded independently of ε. We then define our regular component as the solution to this problem restricted to the original domain. To this end define the extended domain $\Omega^* = (-d, 1) \times (-d, 1)$, where $d > 0$ is an arbitrary constant independent of ε. Consider the class of "extended" problems

Problem Class 4.4.1.

$$L_\varepsilon^* v^*(x,y) \equiv (\varepsilon M^* v^* + \mathbf{a}^* \cdot \nabla v^*)(x,y) = f^*(x,y) \quad in \ \ \Omega^*, \tag{4.4.1a}$$

$$v^*(x,y) = g^*(x,y) \quad on \ \ \partial\Omega^*, \tag{4.4.1b}$$

where

$$M^* v^*(x,y) \equiv (a^* v^*_{xx} + 2b^* v^*_{xy} + c^* v^*_{yy})(x,y), \tag{4.4.1c}$$

$$\mathbf{a}^*(x,y) = (a_1^*(x,y), a_2^*(x,y)), \quad a_1^*|_{\overline{\Omega}} = a_1, \quad a_2^*|_{\overline{\Omega}} = a_2, \tag{4.4.1d}$$

$$a^*|_{\overline{\Omega}} = a, \quad b^*|_{\overline{\Omega}} = b, \quad c^*|_{\overline{\Omega}} = c, \quad f^*|_{\overline{\Omega}} = f, \quad g^*|_{\partial\Omega_I^*} = 0. \tag{4.4.1e}$$

The coefficient functions in the differential equation (4.4.1a) have been constructed so that when they are restricted to the original domain they coincide with the respective functions in (4.3.1a). To define them in the rest of Ω^* we continuously extend each function in such a way that if $a_1 \in C^{k,\nu}(\overline{\Omega})$ then $a_1^* \in C^{k,\nu}(\overline{\Omega}^*)$ with similar statements for the other functions *mutatis mutandis*. In addition we define f^* in such a way that at $(-d, 1)$ and $(1, -d)$ it satisfies the following compatibility conditions

$$\partial^i f^*(-d, 1) = \partial^i f^*(1, -d) = 0,$$

for all multi-indices i such that $|i| = 0, \ldots, 4$.

The boundary data g^* is defined to be 0 on the inflow boundary $\partial\Omega_I^*$ so that it coincides with the boundary values of the original problem on $\partial\Omega_I$. We will define g^* on the outflow boundary $\partial\Omega_O^*$ appropriately later.

We further decompose v^* into the following sum

$$v^* = v_0^* + \varepsilon v_1^* + \varepsilon^2 v_2^*, \tag{4.4.2a}$$

where

$$\begin{aligned}
\mathbf{a}^* \cdot \nabla v_0^*(x,y) &= f^*(x,y) \quad \text{in } \Omega^*, \qquad v_0^* = 0 \quad \text{on } \partial\Omega_I^*, && \text{(4.4.2b)}\\
\mathbf{a}^* \cdot \nabla v_1^*(x,y) &= -M^* v_0^*(x,y) \quad \text{in } \Omega^*, \qquad v_1^* = 0 \quad \text{on } \partial\Omega_I^*, && \text{(4.4.2c)}\\
L_\varepsilon^* v_2^*(x,y) &= -M^* v_1^*(x,y) \quad \text{in } \Omega^*, \qquad v_2^* = g^* \quad \text{on } \partial\Omega^*. && \text{(4.4.2d)}
\end{aligned}$$

It can be easily verified that v^* defined in this way satisfies the differential equation in (4.4.1a). We need the following assumption.

Assumption 4.4.1. *Assume that g^* can be chosen on $\partial\Omega_O^*$ so that the data of the problem 4.4.2d satisfy additional compatibility conditions so that $v_2^* \in C^{3,\nu}(\overline{\Omega^*})$ for some $\nu \in (0,1)$.*

Theorem 4.4.2. *Assume 4.4.1 and that a^*, b^*, c^*, a_1^* and a_2^* are smooth, $f^* \in C^{5,\nu}(\overline{\Omega^*})$ and that $g^* \in C^{3,\nu}(\partial\Omega^*)$ for some $\nu \in (0,1)$. Suppose that f^* satisfies the following additional compatibility conditions at the inflow corner $(1,1)$*

$$\partial^i f^*(1,1) = 0,$$

for all multi-indices i such that $|i| = 0, \ldots, 4$. Then $v^* \in C^{3,\nu}(\overline{\Omega^*})$ and

$$|v^*|_k \leq C(1 + \varepsilon^{2-k}) \quad \text{for} \quad k = 0, \ldots, 3.$$

Proof. From [28] we have $v_0^* \in C^{5,\nu}(\overline{\Omega^*})$ and therefore $M^* v_0^* \in C^{3,\nu}(\overline{\Omega^*})$. Also

$$\partial^i v_0^*(1,1) = 0,$$

for all multi-indices i such that $|i| = 0, \ldots, 5$, and from [28] we have $v_1^* \in C^{3,\nu}(\overline{\Omega}^*)$ and therefore $M^* v_1^* \in C^{1,\nu}(\overline{\Omega}^*)$. Also

$$\partial^i v_1^*(1,1) = 0,$$

for all multi-indices i such that $|i| = 0, \ldots, 3$. This implies that in particular

$$M^* v_1^*(1,1) = 0.$$

We also have $M^* v_1^*(-d,1) = M^* v_1^*(1,-d) = 0$.

From Assumption 4.4.1 we have $v_2^* \in C^{3,\nu}(\overline{\Omega}^*)$ and we can apply a similar theorem to Theorem 4.3.4 to get

$$|v_2^*|_k \leq C\varepsilon^{-k}, \quad \text{for} \quad k = 0, \ldots, 3.$$

Since the equations defining v_0^* and v_1^* are independent of ε we have

$$|v_0^*|_k \leq C, \quad |v_1^*|_k \leq C, \quad \text{for} \quad k = 0, \ldots, 3,$$

and the result follows. □

We now introduce the following decomposition of the solution of Problem Class 4.3.1 into regular and singular components

$$u(x,y) = v(x,y) + w(x,y), \quad (x,y) \in \overline{\Omega}, \tag{4.4.3}$$

where v is defined as the restriction of v^* to $\overline{\Omega}$

$$v = v^*|_{\overline{\Omega}}, \tag{4.4.4}$$

and the singular component satisfies the following homogeneous problem

$$\begin{aligned} L_\varepsilon w(x,y) &= 0 && \text{in } \Omega, && (4.4.5a)\\ w(x,y) &= 0 && \text{on } \partial\Omega_I, && (4.4.5b)\\ w(x,y) &= -v(x,y) && \text{on } \partial\Omega_O. && (4.4.5c) \end{aligned}$$

We now proceed to prove the required sharper bounds on the derivatives of w. It is convenient to introduce the exponential functions

$$\begin{aligned} e_1(x,y) &= e^{-A_1(0,y)x/\varepsilon}, \\ e_2(x,y) &= e^{-A_2(x,0)y/\varepsilon}, \\ e(x,y) &= e_1(x,y) + e_2(x,y) - e_1(x,0)e_2(0,y). \end{aligned}$$

where

$$A_1(x,y) = \frac{a_1(x,y)}{a(x,y)}, \qquad A_2(x,y) = \frac{a_2(x,y)}{c(x,y)}.$$

Theorem 4.4.3. *Let w be the solution of* (4.4.5). *Then w can be decomposed into the following sum*

$$w(x,y) = w_L(x,y) + w_B(x,y) + w_C(x,y), \quad (x,y) \in \overline{\Omega}, \tag{4.4.6}$$

where, for all $(x,y) \in \Omega$ we have the following bounds

$$\begin{aligned} |w_L(x,y)| &\leq Ce^{-\gamma_1 x/2\varepsilon}, \\ |w_B(x,y)| &\leq Ce^{-\gamma_2 y/2\varepsilon}, \\ |w_C(x,y)| &\leq Ce^{-\gamma_1 x/2\varepsilon}e^{-\gamma_2 y/2\varepsilon}, \end{aligned}$$

and for all i,j, $1 \leq i+j \leq 3$ we have

$$\begin{aligned} \left|\frac{\partial^{i+j} w_L}{\partial x^i \partial y^j}(x,y)\right| &\leq C\varepsilon^{-i}(e_1(x,y) + \varepsilon^{1-j}), \\ \left|\frac{\partial^{i+j} w_B}{\partial x^i \partial y^j}(x,y)\right| &\leq C\varepsilon^{-j}(e_2(x,y) + \varepsilon^{1-i}), \\ \left|\frac{\partial^{i+j} w_C}{\partial x^i \partial y^j}(x,y)\right| &\leq C\varepsilon^{-(i+j)}, \end{aligned}$$

where

$$\gamma_1 = \min_{(x,y)\in\overline{\Omega}} \left\{ \frac{a_1(x,y)}{a(x,y)} \right\}, \quad \gamma_2 = \min_{(x,y)\in\overline{\Omega}} \left\{ \frac{a_2(x,y)}{c(x,y)} \right\}. \tag{4.4.7}$$

Remark 4.4.1. The key feature of the bounds on the derivatives of the layer components w_L and w_B, is that the magnitudes of the derivatives in the directions normal

to the layers, have an extra positive power of ε. This will be crucial in the analysis of the error in the singular component in §4.7.

Proof. Initially we use the decomposition $w = w_0 + \varepsilon w_1$ where w_0 satisfies an inhomogeneous differential equation, but the same boundary conditions as w, and w_1 satisfies homogeneous boundary conditions and an appropriate inhomogeneous differential equation. This was originally used in [35]. We choose w_0 in the following way. Extend the boundary data of (4.4.5) defined on $\partial\Omega$ to a function $\phi \in C^{3,\nu}(\overline{\Omega})$ for some $\nu \in (0,1)$. Note that we do not need to specify additional compatibility conditions at the corners $(0,1)$ and $(1,0)$ as $v \in C^{3,\nu}(\overline{\Omega})$ for some $\nu \in (0,1)$. Define w_0 as $w_0 = \phi e$. Since $e = 1$ on $\partial\Omega_O$ it is clear that w_0 satisfies the same boundary conditions as w. Note also that ϕ and its derivatives are independent of ε.

As a consequence of the definition of w_0 we see that w_1 satisfies the following problem

$$\begin{aligned} L_\varepsilon w_1(x,y) &= -\frac{1}{\varepsilon} L_\varepsilon w_0(x,y) \quad \text{in } \Omega, \\ w_1(x,y) &= 0 \quad \text{on } \partial\Omega. \end{aligned}$$

Noting that

$$L_\varepsilon w_0 = L_\varepsilon(\phi e) = L_\varepsilon(\phi e_1(x,y)) + L_\varepsilon(\phi e_2(x,y)) - L_\varepsilon(\phi e_1(x,0)e_2(0,y)),$$

we define a further decomposition of w_1 by

$$w_1 = z_1 + z_2 + z_{1,2},$$

where

$$L_\varepsilon z_1(x,y) = -\frac{1}{\varepsilon} L_\varepsilon(\phi e_1)(x,y) \quad \text{in } \Omega, \qquad z_1 = 0 \quad \text{on } \partial\Omega, \tag{4.4.8a}$$

$$L_\varepsilon z_2(x,y) = -\frac{1}{\varepsilon} L_\varepsilon(\phi e_2)(x,y) \quad \text{in } \Omega, \qquad z_2 = 0 \quad \text{on } \partial\Omega, \tag{4.4.8b}$$

$$L_\varepsilon z_{1,2}(x,y) = -\frac{1}{\varepsilon} L_\varepsilon(\phi e_1(x,0)e_2(0,y)) \quad \text{in } \Omega, \qquad z_{1,2} = 0 \quad \text{on } \partial\Omega. \tag{4.4.8c}$$

We now bound z_1, z_2, $z_{1,2}$ and their respective derivatives separately. To accomplish this it is necessary to bound the inhomogeneous terms in (4.4.8). Starting with the equation for z_1 we have

$$\begin{aligned} L_\varepsilon(\phi e_1)(x,y) &= (L_\varepsilon\phi)e_1(x,y) + \phi(L_\varepsilon e_1(x,y)) \\ &+ 2\varepsilon(a\phi_x(e_1)_x + b(\phi_x(e_1)_y + \phi_y(e_1)_x) + c\phi_y(e_1)_y)(x,y). \end{aligned}$$

Since ϕ and its derivatives are independent of ε we have

$$|L_\varepsilon(\phi e_1)(x,y)| \le C\left(e_1(x,y) + |L_\varepsilon e_1(x,y)| + \varepsilon \max\left\{\left|\frac{\partial e_1}{\partial x}(x,y)\right|, \left|\frac{\partial e_1}{\partial y}(x,y)\right|\right\}\right).$$

It can be verified that

$$\max\left\{\left|\frac{\partial e_1}{\partial x}(x,y)\right|, \left|\frac{\partial e_1}{\partial y}(x,y)\right|\right\} \le \frac{C}{\varepsilon}e_1(x,y), \tag{4.4.9}$$

and it remains to estimate $|L_\varepsilon e_1(x,y)|$. We have

$$\begin{aligned} L_\varepsilon e_1(x,y) &= \left[\varepsilon\left(a(x,y)\left(\frac{A_1(0,y)}{\varepsilon}\right)^2 + 2b(x,y)\left(\frac{xA_1(0,y)(A_1(0,y))_y}{\varepsilon^2} - \frac{(A_1(0,y))_y}{\varepsilon}\right)\right.\right. \\ &+ c(x,y)\left(\left(\frac{x(A_1(0,y))_y}{\varepsilon}\right)^2 - \frac{x(A_1(0,y))_{yy}}{\varepsilon}\right)\Bigg) \\ &- \left.\frac{a_1(x,y)A_1(0,y)}{\varepsilon} - \frac{xa_2(x,y)(A_1(0,y))_y}{\varepsilon}\right] e_1(x,y) \\ &= \frac{1}{\varepsilon}\left[a(x,y)A_1(0,y)(A_1(0,y) - A_1(x,y))\right. \\ &+ 2b(x,y)(xA_1(0,y)(A_1(0,y))_y - \varepsilon(A_1(0,y))_y) \\ &+ \left.c(x,y)((x(A_1(0,y))_y)^2 - \varepsilon x(A_1(0,y))_{yy}) - xa_2(x,y)(A_1(0,y))_y\right] e_1(x,y). \end{aligned}$$

Since

$$A_1(0,y) - A_1(x,y) = -x\frac{\partial A_1}{\partial x}(x',y), \quad 0 < x' < x,$$

we have

$$|L_\varepsilon e_1(x,y)| \le C\left(1 + \frac{x}{\varepsilon}\right)e_1(x,y) \le 2C\sqrt{e_1(x,y)}.$$

Using this and (4.4.9) we obtain

$$|L_\varepsilon \phi e_1(x,y)| \leq C\sqrt{e_1(x,y)}. \tag{4.4.10}$$

In an analogous manner we get

$$|L_\varepsilon(\phi e_2)(x,y)| \leq C\sqrt{e_2(x,y)}. \tag{4.4.11}$$

Now,

$$\begin{aligned} L_\varepsilon(\phi e_1(x,0)e_2(0,y)) &= (L_\varepsilon\phi)e_1(x,0)e_2(0,y) + \phi(L_\varepsilon e_1(x,0)e_2(0,y)) \\ &+ 2\varepsilon\Big(a(x,y)\phi_x(e_1(x,0)e_2(0,y))_x + b(x,y)(\phi_x(e_1(x,0)e_2(0,y))_y \\ &+ \phi_y(e_1(x,0)e_2(0,y))_x) + c(x,y)\phi_y(e_1(x,0)e_2(0,y))_y\Big). \end{aligned}$$

Since ϕ and its derivatives are independent of ε we have

$$\begin{aligned} |L_\varepsilon(\phi e_1(x,0)e_2(0,y))| &\leq C\Big(e_1(x,0)e_2(0,y) + |L_\varepsilon e_1(x,0)e_2(0,y)| \\ &+ \varepsilon \max\left\{|e_2(0,y)|\left|\frac{\partial}{\partial x}(e_1(x,0))\right|, |e_1(x,0)|\left|\frac{\partial}{\partial y}(e_2(0,y))\right|\right\}\Big). \end{aligned}$$

It is easily seen that

$$\max\left\{|e_2(0,y)|\left|\frac{\partial}{\partial x}(e_1(x,0))\right|, |e_1(x,0)|\left|\frac{\partial}{\partial y}(e_2(0,y))\right|\right\} \leq \frac{C}{\varepsilon}e_1(x,0)e_2(0,y), \tag{4.4.12}$$

and it remains to estimate $|L_\varepsilon e_1(x,0)e_2(0,y)|$. We have

$$\begin{aligned}
L_\varepsilon e_1(x,0)e_2(0,y) &= (L_\varepsilon e_1(x,0))e_2(0,y) + e_1(x,0)(L_\varepsilon e_2(0,y)) \\
&+ 2\varepsilon b(x,y)(e_1(x,0))_x(e_2(0,y))_y \\
&= \frac{1}{\varepsilon}\Big(a(x,y)(A_1(0,0))^2 - a_1(x,y)A_1(0,0) + 2b(x,y)A_1(0,0)A_2(0,0) \\
&+ c(x,y)(A_2(0,0))^2 - a_2(x,y)A_2(0,0)\Big)e_1(x,0)e_2(0,y) \\
&= \frac{1}{\varepsilon}\Big(a(x,y)A_1(0,0)(A_1(0,0) - A_1(x,y)) \\
&+ 2(b(x,y) - b(0,0))A_1(0,0)A_2(0,0) + 2b(0,0)A_1(0,0)A_2(0,0) \\
&+ c(x,y)A_2(0,0)(A_2(0,0) - A_2(x,y))\Big)e_1(x,0)e_2(0,y).
\end{aligned}$$

Since

$$\begin{aligned}
A_1(0,0) - A_1(x,y) &= -x\frac{\partial A_1}{\partial x}(x',y) - y\frac{\partial A_1}{\partial y}(x,y'), \quad 0 < x' < x, \quad 0 < y' < y, \\
A_2(0,0) - A_2(x,y) &= -x\frac{\partial A_2}{\partial x}(x'',y) - y\frac{\partial A_2}{\partial y}(x,y''), \quad 0 < x'' < x, \quad 0 < y'' < y, \\
b(x,y) - b(0,0) &= x\frac{\partial b}{\partial x}(x''',y) + y\frac{\partial b}{\partial y}(x,y'''), \quad 0 < x''' < x, \quad 0 < y''' < y,
\end{aligned}$$

we have, for all $(x,y) \in \Omega$,

$$\begin{aligned}
|L_\varepsilon(e_1(x,0)e_2(0,y))| &\leq \frac{C}{\varepsilon}\Big(x + y + |b(0,0)|\Big)e_1(x,0)e_2(0,y) \\
&\leq C(1 + \varepsilon^{-1}|b(0,0)|)\sqrt{e_1(x,0)}\sqrt{e_2(0,y)}.
\end{aligned}$$

Note that the presence of the mixed derivative term introduces an extra inverse power of ε into this bound which is not present in the special case when $b(0,0) = 0$. Using this bound and (4.4.12) we obtain

$$|L_\varepsilon(\phi e_1(x,0)e_2(0,y))| \leq C(1 + \varepsilon^{-1}|b(0,0)|)\sqrt{e_1(x,0)}\sqrt{e_2(0,y)}. \tag{4.4.13}$$

The bounds on z_1, z_2 and $z_{1,2}$ are now obtained using the minimum principle.

Starting with z_1 we introduce the barrier function

$$\psi_1(x) = C' e^{-\gamma_1 x/2\varepsilon}.$$

Then at each point in Ω, using (4.4.7), (4.4.8a) and (4.4.10), we have

$$\begin{aligned} L_\varepsilon(\psi_1(x) \pm z_1(x,y)) &= L_\varepsilon \psi_1(x) \mp \frac{1}{\varepsilon} L_\varepsilon(\phi e_1)(x,y) \\ &\leq \frac{1}{\varepsilon}\left(\frac{C'\gamma_1 a(x,y)}{4}\left(\gamma_1 - 2\frac{a_1(x,y)}{a(x,y)}\right) + C\right) e^{-\gamma_1 x/2\varepsilon} \\ &\leq 0, \end{aligned}$$

if C' is chosen sufficiently large. Also at each point on $\partial\Omega$

$$(\psi_1 \pm z_1) = \psi_1 \geq 0.$$

It follows from the minimum principle that $(\psi_1 \pm z_1) \geq 0$ in $\overline{\Omega}$ and so at each point in $\overline{\Omega}$ we have

$$|z_1(x,y)| \leq C' e^{-\gamma_1 x/2\varepsilon}. \tag{4.4.14}$$

In an analogous manner we can use (4.4.7), (4.4.8b) and (4.4.11) to get the bound on z_2

$$|z_2(x,y)| \leq C' e^{-\gamma_2 y/2\varepsilon}. \tag{4.4.15}$$

To bound $z_{1,2}$ we use the barrier function

$$\psi_{1,2}(x,y) = C'(1 + \varepsilon^{-1}|b(0,0)|) e^{-\gamma_1 x/2\varepsilon} e^{-\gamma_2 y/2\varepsilon}.$$

Then at each point in Ω, using (4.4.7), (4.4.8c), (4.4.13), the inequalities (4.3.1c) and

the ellipticity conditions (4.3.1d), we have

$$\begin{aligned}
L_\varepsilon(\psi_{1,2} \pm z_{1,2}) &= L_\varepsilon\psi_{1,2}(x,y) \pm \frac{1}{\varepsilon}L_\varepsilon(\phi e_1(x,0)e_2(0,y)) \\
&\leq \frac{\varepsilon + |b(0,0)|}{\varepsilon^2}\left(\frac{C'}{4}\left(a(x,y)\gamma_1^2 + 2b(x,y)\gamma_1\gamma_2 + c(x,y)\gamma_2^2\right.\right. \\
&- \left.\left. 2a_1(x,y)\gamma_1 - 2a_2(x,y)\gamma_2\right) + C\right)e^{-\gamma_1 x/2\varepsilon}e^{-\gamma_2 y/2\varepsilon} \\
&= \frac{\varepsilon + |b(0,0)|}{\varepsilon^2}\left(\frac{C'}{4}\left(a(x,y)\gamma_1\left(\gamma_1 - \frac{a_1(x,y)}{a(x,y)}\right)\right.\right. \\
&+ c(x,y)\gamma_2\left(\gamma_2 - \frac{a_2(x,y)}{c(x,y)}\right) \\
&- \left.\left.\left(a_1(x,y)\gamma_1 - 2b(x,y)\gamma_1\gamma_2 + a_2(x,y)\gamma_2\right)\right) + C\right)e^{-\gamma_1 x/2\varepsilon}e^{-\gamma_2 y/2\varepsilon} \\
&\leq \frac{\varepsilon + |b(0,0)|}{\varepsilon^2}\left(\frac{C'}{4}\left(a(x,y)\gamma_1\left(\gamma_1 - \frac{a_1(x,y)}{a(x,y)}\right)\right.\right. \\
&+ c(x,y)\gamma_2\left(\gamma_2 - \frac{a_2(x,y)}{c(x,y)}\right) \\
&- \left.\left.\left(a(x,y)\gamma_1^2 - 2b(x,y)\gamma_1\gamma_2 + c(x,y)\gamma_2^2\right)\right) + C\right)e^{-\gamma_1 x/2\varepsilon}e^{-\gamma_2 y/2\varepsilon} \\
&\leq 0,
\end{aligned}$$

if C' is chosen sufficiently large. Also at each point on $\partial\Omega$

$$(\psi_{1,2} \pm z_{1,2}) = \psi_{1,2} \geq 0.$$

It follows from the minimum principle (4.3.1) that $(\psi_{1,2} \pm z_{1,2}) \geq 0$ in $\overline{\Omega}$ and so at each point in $\overline{\Omega}$ we have

$$|z_{1,2}(x,y)| \leq C'(1 + \varepsilon^{-1}|b(0,0)|)e^{-\gamma_1 x/2\varepsilon}e^{-\gamma_2 y/2\varepsilon}. \tag{4.4.16}$$

To bound the derivatives of z_1, z_2 and $z_{1,2}$ we note that z_1, z_2 and $z_{1,2}$ are solutions of problems from Problem Class 4.3.1 and therefore we can apply Theorem 4.3.4. The inhomogeneous terms in equations (4.4.8a) and (4.4.8b) defining z_1 and z_2 are

bounded by $C\varepsilon^{-1}$. Therefore we have

$$|z_1|_k \leq C\varepsilon^{-k}, \quad |z_1|_k \leq C\varepsilon^{-k}, \quad \text{for} \quad k = 1, 2, 3. \tag{4.4.17}$$

The inhomogeneous term in the equation (4.4.8c) defining $z_{1,2}$ is bounded by $C\varepsilon^{-2}$. Therefore

$$|z_{1,2}|_k \leq C\varepsilon^{-(k+1)}, \quad \text{for} \quad k = 1, 2, 3. \tag{4.4.18}$$

Setting

$$\begin{aligned} w_L &= \phi e_1 + \varepsilon z_1, \\ w_B &= \phi e_2 + \varepsilon z_2, \\ w_C &= -\phi e_1 e_2 + \varepsilon z_{1,2}, \end{aligned}$$

taking appropriate derivatives, and using (4.4.14), (4.4.15), (4.4.16), (4.4.17) and (4.4.18) we get the desired result. □

4.5 Numerical method

We now introduce a numerical method that will generate approximations to solutions of problems from Problem Class 4.3.1. It comprises an upwind finite difference operator on a fitted piecewise-uniform mesh. The difference operator L_ε^N, on a mesh Ω^N, is defined for any mesh function Z^N, as

$$L_\varepsilon^N Z_{i,j}^N \equiv (\varepsilon(a\delta_x^2 + 2(\tilde{b}^+\delta_{xy}^+ + \tilde{b}^-\delta_{xy}^-) + c\delta_y^2) + a_1 D_x^+ + a_2 D_y^+) Z^N(x_i, y_j), \quad \forall (x_i, y_j) \in \Omega^N, \tag{4.5.1}$$

where

$$\tilde{b}^+(x_i, y_j) = \begin{cases} 0.5(b(x_i, y_j) + |b(x_i, y_j)|), & i < N_x/2,\ j < N_y/2, \\ 0, & \text{otherwise}, \end{cases},$$

$$\tilde{b}^-(x_i, y_j) = \begin{cases} 0.5(b(x_i, y_j) - |b(x_i, y_j)|), & i < N_x/2,\ j < N_y/2, \\ 0, & \text{otherwise}, \end{cases},$$

$$\delta^+_{xy} Z^N(x_i, y_j) = \frac{D^+_x D^+_y + D^-_x D^-_y}{2} Z^N(x_i, y_j), \tag{4.5.2a}$$

and

$$\delta^-_{xy} Z^N(x_i, y_j) = \frac{D^+_x D^-_y + D^-_x D^+_y}{2} Z^N(x_i, y_j). \tag{4.5.2b}$$

Clearly, at each mesh point, at most one of $\tilde{b}^+$ and $\tilde{b}^-$ can be non-zero. We defer a discussion of our choice of difference scheme until §4.6.

We use N_x mesh intervals in the x co-ordinate direction and N_y mesh intervals in the y co-ordinate direction where N_x and N_y are both even integers greater than 4. We discretise the domain $\overline{\Omega}$ with the tensor product mesh $\overline{\Omega}^N_\sigma = \overline{\Omega}^{N_x}_{\sigma_1} \times \overline{\Omega}^{N_y}_{\sigma_2}$, where

$$\overline{\Omega}^{N_x}_{\sigma_1} = \{x_i \mid 0 \le i \le N_x\}, \quad \text{and} \quad \overline{\Omega}^{N_y}_{\sigma_2} = \{y_j \mid 0 \le j \le N_y\},$$

with

$$x_i = \begin{cases} 2i\sigma_1/N_x, & 0 \le i \le N_x/2 \\ \sigma_1 + 2(i - N_x/2)(1-\sigma_1)/N_x, & N_x/2 < i \le N_x \end{cases},$$

$$y_j = \begin{cases} 2j\sigma_2/N_y, & 0 \le j \le N_y/2 \\ \sigma_2 + 2(j - N_y/2)(1-\sigma_2)/N_y, & N_y/2 < j \le N_y \end{cases},$$

and

$$\sigma_1 = \min\left\{\frac{1}{2}, \frac{\varepsilon}{\gamma_1}\ln(N_x N_y)\right\}, \quad \sigma_2 = \min\left\{\frac{1}{2}, \frac{\varepsilon}{\gamma_2}\ln(N_x N_y)\right\}. \tag{4.5.3}$$

Note that when $b \equiv 0$ and $N_x = N_y$ we have an appropriate choice of σ_1 and σ_2 in the standard case (see, for example [15]). For later convenience we shall define the following mesh widths

$$h_i = x_i - x_{i-1}, \quad \hbar_i = (h_i + h_{i+1})/2, \quad h = \frac{2\sigma_1}{N_x}, \quad H = \frac{2(1-\sigma_1)}{N_x}, \tag{4.5.4a}$$

$$k_j = y_j - y_{j-1}, \quad \bar{k}_j = (k_j + k_{j+1})/2, \quad k = \frac{2\sigma_2}{N_y}, \quad K = \frac{2(1-\sigma_2)}{N_y}. \tag{4.5.4b}$$

Setting $\partial\Omega^N_\sigma = \overline{\Omega}^N_\sigma \cap \partial\Omega$, the resulting fitted mesh finite difference method is

Method 4.5.1.

$$\begin{aligned} L_\varepsilon^N U^N(x_i, y_j) &= f(x_i, y_j) \quad \text{in } \Omega_\sigma^N, \\ U^N(x_i, y_j) &= 0 \quad \text{on } \partial\Omega_\sigma^N. \end{aligned}$$

The finite difference operator L_ε^N in (4.5.1) satisfies the following discrete minimum principle on $\overline{\Omega}_\sigma^N$.

Theorem 4.5.1 (Discrete Minimum Principle). *Let Z^N be any mesh function defined on $\overline{\Omega}_\sigma^N$.*

$$\begin{gathered} \text{If } \; Z^N(x_i, y_j) \geq 0, \quad \forall (x_i, y_j) \in \partial\Omega_\sigma^N, \quad L_\varepsilon^N Z^N(x_i, y_j) \leq 0, \quad \forall (x_i, y_j) \in \Omega_\sigma^N, \\ \text{and } N_x \text{ and } N_y \text{ satisfy the inequalities } \; \frac{|b_{i,j}|}{c_{i,j}} \leq \frac{\sigma_1 N_y}{\sigma_2 N_x} \leq \frac{a_{i,j}}{|b_{i,j}|}, \quad \forall (x_i, y_j) \in \Omega_\sigma^N, \\ \text{such that } \; 0 < i < N_x/2, \quad 0 < j < N_y/2, \\ \text{then } \; Z^N(x_i, y_j) \geq 0, \quad \forall (x_i, y_j) \in \overline{\Omega}_\sigma^N. \end{gathered}$$

Proof. This follows from the fact that the associated system matrix is an M-matrix (see [15, §2.3]). To see this we need only examine those rows of the matrix that correspond to the bottom left hand corner region, i.e., the set of mesh points (x_i, y_j) for which $i < N_x/2$ and $j < N_y/2$. In all other rows the M-matrix structure is guaranteed by the choice of the upwind finite difference operator (see [15, §2.4]). A typical finite difference equation for a mesh point in the corner region is as follows

$$\begin{aligned} L_\varepsilon^N Z^N(x_i, y_j) &= \frac{\varepsilon \tilde{b}_{i,j}^+}{hk} Z_{i-1,j-1}^N + \varepsilon \left(\frac{c_{i,j}}{k^2} - \frac{\tilde{b}_{i,j}^+}{hk} + \frac{\tilde{b}_{i,j}^-}{hk} \right) Z_{i,j-1}^N \\ &- \frac{\varepsilon \tilde{b}_{i,j}^-}{hk} Z_{i+1,j-1}^N + \varepsilon \left(\frac{a_{i,j}}{h^2} - \frac{\tilde{b}_{i,j}^+}{hk} + \frac{\tilde{b}_{i,j}^-}{hk} \right) Z_{i-1,j}^N \\ &- \left(2\varepsilon \left(\frac{a_{i,j}}{h^2} - \frac{\tilde{b}_{i,j}^+}{hk} + \frac{\tilde{b}_{i,j}^-}{hk} + \frac{c_{i,j}}{k^2} \right) + \frac{(a_1)_{i,j}}{h} + \frac{(a_2)_{i,j}}{k} \right) Z_{i,j}^N \\ &+ \left(\varepsilon \left(\frac{a_{i,j}}{h^2} - \frac{\tilde{b}_{i,j}^+}{hk} + \frac{\tilde{b}_{i,j}^-}{hk} \right) + \frac{(a_1)_{i,j}}{h} \right) Z_{i+1,j}^N - \frac{\varepsilon \tilde{b}_{i,j}^-}{hk} Z_{i-1,j+1}^N \end{aligned}$$

$$+ \left(\varepsilon \left(\frac{c_{i,j}}{k^2} - \frac{\tilde{b}^+_{i,j}}{hk} + \frac{\tilde{b}^-_{i,j}}{hk} \right) + \frac{(a_2)_{i,j}}{k} \right) Z^N_{i,j+1} + \frac{\varepsilon \tilde{b}^+_{i,j}}{hk} Z^N_{i+1,j+1}.$$

We will assume that $b_{i,j} > 0$ and thus $\tilde{b}^+_{i,j} = b_{i,j}$ and $\tilde{b}^-_{i,j} = 0$. The case $b_{i,j} < 0$ is analogous. It is clear that the system matrix is irreducibly diagonally dominant. Also the coefficient of $Z^N_{i,j}$ in the above expression which corresponds to the diagonal of the system matrix will be negative once the following inequality is satisfied

$$\frac{a_{i,j}}{h^2} - \frac{b_{i,j}}{hk} + \frac{c_{i,j}}{k^2} > 0.$$

This follows directly from the ellipticity conditions (4.3.1d) by setting $r = \frac{1}{h}$ and $s = -\frac{1}{k}$. All the coefficients of the other Z^N in the above expression which correspond to off-diagonal elements in the system matrix will be non-negative once the following inequalities are satisfied

$$\frac{a_{i,j}}{h^2} - \frac{b_{i,j}}{hk} \geq 0, \quad \frac{c_{i,j}}{k^2} - \frac{b_{i,j}}{hk} \geq 0.$$

Together they require that the following hold

$$\frac{b_{i,j}}{c_{i,j}} \leq \frac{h}{k} \leq \frac{a_{i,j}}{b_{i,j}}.$$

Using the expressions for the mesh widths given in (4.5.4) this becomes

$$\frac{b_{i,j}}{c_{i,j}} \leq \frac{\sigma_1 N_y}{\sigma_2 N_x} \leq \frac{a_{i,j}}{b_{i,j}}. \tag{4.5.6}$$

Depending on the values of σ_1 and σ_2 we have the following cases:

1. $\sigma_1 = \sigma_2 = 1/2$. We must have

$$\frac{b_{i,j}}{c_{i,j}} \leq \frac{N_y}{N_x} \leq \frac{a_{i,j}}{b_{i,j}}.$$

We can always find an N_x and N_y to satisfy these inequalities because from

(4.3.2) we have

$$\begin{aligned} b_{i,j}^2 &< a_{i,j}c_{i,j} \\ \Rightarrow \frac{b_{i,j}}{c_{i,j}} &< \frac{a_{i,j}}{b_{i,j}}. \end{aligned}$$

It is then trivial to ensure that the N_x and N_y so chosen are even to enable the construction of the mesh.

2. $\sigma_1 = \frac{\varepsilon}{\gamma_1}\ln(N_xN_y), \sigma_2 = 1/2$. We must have

$$\frac{\gamma_1 b_{i,j}}{\gamma_2 c_{i,j}} \leq \frac{N_y}{N_x} \leq \frac{a_{i,j}}{b_{i,j}}.$$

To ensure that these inequalities can be satisfied we must have

$$\frac{\gamma_1 b_{i,j}}{\gamma_2 c_{i,j}} < \frac{a_{i,j}}{b_{i,j}}.$$

This imposes conditions on the coefficients in the differential equation.

3. $\sigma_1 = 1/2, \sigma_2 = \frac{\varepsilon}{\gamma_2}\ln(N_xN_y)$. We must have

$$\frac{b_{i,j}}{c_{i,j}} \leq \frac{N_y}{N_x} \leq \frac{\gamma_1 a_{i,j}}{\gamma_2 b_{i,j}}.$$

To ensure that these inequalities can be satisfied we must have

$$\frac{b_{i,j}}{c_{i,j}} < \frac{\gamma_1 a_{i,j}}{\gamma_2 b_{i,j}}.$$

This imposes conditions on the coefficients in the differential equation.

4. $\sigma_1 = \frac{\varepsilon}{\gamma_1}\ln(N_xN_y), \sigma_2 = \frac{\varepsilon}{\gamma_2}\ln(N_xN_y)$. We must have

$$\frac{\gamma_1 b_{i,j}}{\gamma_2 c_{i,j}} \leq \frac{N_y}{N_x} \leq \frac{\gamma_1 a_{i,j}}{\gamma_2 b_{i,j}}. \tag{4.5.7}$$

As in case 1 the inequality (4.3.2) ensures that we can always find an N_x and N_y to satisfy these inequalities.

Thus we have shown that the system matrix corresponding to the numerical method 4.5.1 is an M-matrix and the result follows. □

Remark 4.5.1. In §4.7 we will prove that in the perturbed case the numerical solutions generated by Method 4.5.1 converge uniformly to the solution of the corresponding problem from Problem Class 4.3.1. Thus the monotonicity of our scheme depends on the inequalities in Case 4 in the preceding proof. However, in Chapter 5 when we will present numerical results demonstrating our method, it will be convenient from a practical point of view, to take $N_x = N_y = N$. In this case the appropriate inequalities are the following

$$\frac{b_{i,j}}{c_{i,j}} \leq \frac{\gamma_2}{\gamma_1} \leq \frac{a_{i,j}}{b_{i,j}},$$

and if we want to include the case when $b_{i,j} < 0$ the inequalities become

$$\frac{|b_{i,j}|}{c_{i,j}} \leq \frac{\gamma_2}{\gamma_1} \leq \frac{a_{i,j}}{|b_{i,j}|}, \tag{4.5.8}$$

In the sample problems we consider we shall ensure that these inequalities are satisfied, noting however that this restriction can be lifted if we allow N_x and N_y to be different. This issue is discussed further in §5.4.

We will need the following bound on the local truncation error of Method 4.5.1 in the next section. The proof is standard.

Lemma 4.5.2 (Truncation Error). *Let u be the solution of* (4.3.1) *and U^N be the solution of the discrete problem* (4.5.1) *defined on $\overline{\Omega}_\sigma^N$. Then the following gives a bound on the local truncation error in the corner mesh region*

$$\begin{aligned} \left|L_\varepsilon^N(U^N - u)(x_i, y_j)\right| \;\leq\; & C\left[\varepsilon\left(h\left(\left\|\frac{\partial^3 u}{\partial x^3}\right\| + \left\|\frac{\partial^3 u}{\partial x^2 \partial y}\right\|\right) + k\left(\left\|\frac{\partial^3 u}{\partial y^3}\right\| + \left\|\frac{\partial^3 u}{\partial x \partial y^2}\right\|\right)\right)\right. \\ & + \left. h\left\|\frac{\partial^2 u}{\partial x^2}\right\| + k\left\|\frac{\partial^2 u}{\partial y^2}\right\|\right]. \end{aligned}$$

And the following expression gives a bound for the local truncation error in the remainder of the mesh

$$\begin{aligned}\left|L_\varepsilon^N(U^N-u)(x_i,y_j)\right| \;\leq\; & C\left[\varepsilon\left((x_{i+1}-x_{i-1})\left\|\frac{\partial^3 u}{\partial x^3}\right\|+(y_{j+1}-y_{j-1})\left\|\frac{\partial^3 u}{\partial y^3}\right\|\right.\right.\\ & \left.\left.+\;\|b\|\left\|\frac{\partial^2 u}{\partial x\partial y}\right\|\right)+(x_{i+1}-x_i)\left\|\frac{\partial^2 u}{\partial x^2}\right\|+(y_{j+1}-y_j)\left\|\frac{\partial^2 u}{\partial y^2}\right\|\right].\end{aligned}$$

Remark 4.5.2. The latter expression contains the quantity $\|b\|\left\|\frac{\partial^2 u}{\partial x\partial y}\right\|$ which is due to the fact that our numerical method does not approximate the mixed derivative term outside the corner region.

4.6 Finite difference operators for the approximation of mixed derivatives

In this section we discuss the approximation of a mixed derivative with a finite difference operator. In particular we shall examine the issue of deriving a discrete comparison principle similar to the one for the continuous operator (see Lemma 4.3.1). This is important as the derivation of our error estimates in §4.7 depends crucially on the fact that the difference operator used is monotone. This however, is a non-trivial task, and there is a large literature devoted to this subject (see [42], [33] and the references therein). Monotone schemes have been constructed for a large class of elliptic equations with mixed derivatives, but these schemes are designed for classical equations. Hence, uniform meshes are used in each co-ordinate direction, and there are restrictions on the ratio of the mesh widths.

The numerical method that we introduced in the previous section is based upon a tensor product of two piecewise-uniform meshes. Therefore the above schemes cannot be used. To construct a difference operator that satisfies a comparison principle (see Theorem 4.5.1) it was necessary to employ an inconsistent operator to approximate the mixed derivative. This is because in regions of our mesh where the mesh widths in each co-ordinate direction vary in magnitude (i.e. in the regions $i < N_x/2$, $j > N_y/2$ and $i > N_x/2$, $j < N_y/2$ where the mesh is fine in one dimension and coarse in the other) the M-matrix structure of the associated system matrix breaks down. To see

this consider the region $i < N_x/2$, $j > N_y/2$ and assume that we have approximated the mixed derivative term in the entirety of the mesh. In this region the mesh widths in the x and y co-ordinate directions are h and K respectively, with h and K defined as in (4.5.4). When ε is small the magnitude of the former is significantly smaller than that of the latter. So, for example, the coefficient of the $Z^N_{i,j-1}$ term in a typical finite difference equation in this region is (assuming $b_{i,j} > 0$)

$$\varepsilon\left(\frac{c_{i,j}}{K^2} - \frac{b_{i,j}}{hK}\right).$$

We need this quantity to be positive for our system matrix to be an M-matrix. Therefore, we must have

$$c_{i,j}h > b_{i,j}K,$$

which will not hold if ε is small.

Note that this is not to say that a method based on a consistent finite difference operator will not be monotone just that its associated system matrix will not be an M-matrix. However numerical experiments have shown that this is indeed the case. We investigate the numerical performance of such a method in §5.4.1.

One further point that should be made is that the actual form of the discretisation of the mixed derivative (whether the scheme is consistent or not) seems to be unimportant. Any other simple choice for the discretisation would have suited our purposes just as well provided that we could prove a discrete comparison principle.

4.7 Decomposition of numerical solution and error estimates

In an analogous manner to the continuous case we decompose our numerical solution into a regular and singular component

$$U^N(x_i, y_j) = V^N(x_i, y_j) + W^N(x_i, y_j), \quad (x_i, y_j) \in \overline{\Omega}^N_\sigma,$$

where V^N is the solution of the inhomogeneous problem

$$\begin{aligned} L_\varepsilon^N V^N(x_i, y_j) &= f(x_i, y_j) \quad \text{in } \Omega_\sigma^N, && \text{(4.7.1a)} \\ V^N(x_i, y_j) &= v(x_i, y_j) \quad \text{on } \partial\Omega_\sigma^N, && \text{(4.7.1b)} \end{aligned}$$

and therefore W^N is the solution of the problem

$$\begin{aligned} L_\varepsilon^N W^N(x_i, y_j) &= 0 \quad \text{in } \Omega_\sigma^N, && \text{(4.7.2a)} \\ W^N(x_i, y_j) &= w(x_i, y_j) \quad \text{on } \partial\Omega_\sigma^N. && \text{(4.7.2b)} \end{aligned}$$

The error in our numerical solution can now also be decomposed

$$(U^N - u)(x_i, y_j) = ((V^N - v) + (W^N - w))(x_i, y_j), \quad (x_i, y_j) \in \overline{\Omega}_\sigma^N,$$

and the error in the regular component and the singular component can be estimated separately.

Assumption 4.7.1. *For convenience we set $N_x = N_y = N$ and assume that the inequalities* (4.5.8) *hold. Also we shall assume that $\varepsilon \leq N^{-1}$. This implies that*

$$\sigma_1 = 2\frac{\varepsilon}{\gamma_1} \ln N, \quad \sigma_2 = 2\frac{\varepsilon}{\gamma_2} \ln N. \tag{4.7.3}$$

Theorem 4.7.2 (Error in the Regular Component). *Under Assumption 4.7.1 the error in the smooth component satisfies the following ε-uniform error estimate*

$$\left|(V^N - v)(x_i, y_j)\right| \leq CN^{-1}, \quad (x_i, y_j) \in \overline{\Omega}_\sigma^N,$$

where V^N is the solution of (4.7.1) *and v is given by* (4.4.4).

Proof. We begin by considering the local truncation error with respect to the regular component. We first consider the case when $i < N/2$, and $j < N/2$. The expression

for the local truncation error from Theorem 4.5.2 is

$$\begin{aligned}\left|L_\varepsilon^N(V^N-v)(x_i,y_j)\right| &\leq C\left[\varepsilon\left(h\left(\left\|\frac{\partial^3 v}{\partial x^3}\right\|+\left\|\frac{\partial^3 v}{\partial x^2\partial y}\right\|\right)+k\left(\left\|\frac{\partial^3 v}{\partial y^3}\right\|+\left\|\frac{\partial^3 v}{\partial x\partial y^2}\right\|\right)\right)\right.\\ &+ \left. h\left\|\frac{\partial^2 v}{\partial x^2}\right\|+k\left\|\frac{\partial^2 v}{\partial y^2}\right\|\right].\end{aligned}$$

Using the bounds on the derivatives of v given in Theorem 4.4.2 and the fact that $h \leq N^{-1}$, $k \leq N^{-1}$, we get

$$\left|L_\varepsilon^N(V^N-v)(x_i,y_j)\right| \leq CN^{-1},$$

and applying the discrete minimum principle given in Theorem 4.5.1 and a standard barrier function the required result follows.

At all other points in Ω_σ^N the truncation error is from Theorem 4.5.2

$$\begin{aligned}\left|L_\varepsilon^N(V^N-v)(x_i,y_j)\right| &\leq C\left[\varepsilon\left((x_{i+1}-x_{i-1})\left\|\frac{\partial^3 v}{\partial x^3}\right\|+(y_{j+1}-y_{j-1})\left\|\frac{\partial^3 v}{\partial y^3}\right\|\right.\right.\\ &+ \left.\left.\|b\|\left\|\frac{\partial^2 v}{\partial x\partial y}\right\|\right)+(x_{i+1}-x_i)\left\|\frac{\partial^2 v}{\partial x^2}\right\|+(y_{j+1}-y_j)\left\|\frac{\partial^2 v}{\partial y^2}\right\|\right].\end{aligned}$$

Again using the bounds on v given in Theorem 4.4.2 and the fact that $x_{i+1}-x_{i-1} \leq CN^{-1}$, $x_{i+1}-x_i \leq CN^{-1}$, $y_{j+1}-y_{j-1} \leq CN^{-1}$ and $y_{j+1}-y_j \leq CN^{-1}$ we get

$$\begin{aligned}\left|L_\varepsilon^N(V^N-v)(x_i,y_j)\right| &\leq C(N^{-1}+\varepsilon\|b\|)\\ &\leq CN^{-1},\end{aligned}$$

since $\varepsilon \leq N^{-1}$. The result follows as before. □

In order to estimate the error in the singular component we require the following Lemma.

Lemma 4.7.3. *The mesh function $A_{i,j}$, defined on $\overline{\Omega}_\sigma^N$, given by*

$$A_{i,j}=\begin{cases}\left(1+\frac{\gamma_1 h}{2\varepsilon}\right)^{-i}, & 0\leq i\leq N/2, \quad 0\leq j\leq N,\\ A_{N/2,j}\left(1+\frac{\gamma_1 H}{2\varepsilon}\right)^{-(i-N/2)}, & N/2+1\leq i\leq N, \quad 0\leq j\leq N,\end{cases} \tag{4.7.4}$$

has the following properties, for all $0 \le j \le N$,

$$\begin{aligned}
A_{i,j} &> 0, \qquad 0 \le i \le N, && \text{(4.7.5a)}\\
D_x^+ A_{i,j} &= -\frac{\gamma_1}{2\varepsilon} A_{i+1} \le 0, \qquad 0 \le i \le N-1, && \text{(4.7.5b)}\\
D_y^+ A_{i,j} &= 0, \qquad 0 \le i \le N, && \text{(4.7.5c)}\\
\varepsilon \delta_x^2 A_{i,j} &= \frac{\gamma_1^2}{4\varepsilon} \frac{h_{i+1}}{\hbar} A_{i+1,j}, \qquad 1 \le i \le N-1, && \text{(4.7.5d)}\\
L_\varepsilon^N A_{i,j} &< 0, \qquad 1 \le i \le N-1, && \text{(4.7.5e)}\\
A_{N/2,j} &\le 2N^{-1}, && \text{(4.7.5f)}\\
A_{i,j} &\le 2A_{i+1,j}, \qquad 0 \le i \le N/2-1. && \text{(4.7.5g)}
\end{aligned}$$

Proof. The first four properties are obvious and can be verified by computation. Using these we have

$$\begin{aligned}
L_\varepsilon^N A_{i,j} &= -\frac{\gamma_1 a_{i,j}}{2\varepsilon} \left(\frac{(a_1)_{i,j}}{a_{i,j}} - \gamma_1 \frac{h_{i+1}}{2\hbar_i} \right) A_{i+1,j}\\
&\le -\frac{\gamma_1 a_{i,j}}{2\varepsilon} \left(\frac{(a_1)_{i,j}}{a_{i,j}} - \gamma_1 \right) A_{i+1,j}\\
&< 0,
\end{aligned}$$

where we have also used the definitions of h_i and $\hbar_i$ given in (4.5.4), the definition of γ_1 given in (4.4.7) and the positivity of a_1 given in (4.3.1c).

Now

$$\begin{aligned}
A_{N/2,j} &= \left(1 + \frac{\gamma_1 h}{2\varepsilon}\right)^{-N/2}\\
&\le \left(1 + \frac{2\ln N}{N}\right)^{-N/2}\\
&\le 2N^{-1},
\end{aligned}$$

using (3.6.3).

Finally for $0 < i \leq N/2 - 1$ we have

$$\begin{aligned} A_{i,j} &= \left(1 + \frac{\gamma_1 h}{2\varepsilon}\right) A_{i+1,j} \\ &= \left(1 + \frac{2\ln N}{N}\right) A_{i+1,j} \\ &\leq 2A_{i+1,j}. \end{aligned}$$

□

Theorem 4.7.4 (Error in Singular Component). *Under Assumption 4.7.1 the error in the singular component satisfies the following ε-uniform error estimate*

$$\left|(W^N - w)(x_i, y_j)\right| \leq CN^{-1}(\ln N)^2, \quad (x_i, y_j) \in \overline{\Omega}_\sigma^N,$$

where W^N is the solution of (4.7.2) *and w is the solution of* (4.4.5).

Proof. We introduce the following decomposition of W^N into separate layer components, which is analogous to the decomposition of w given in (4.4.6).

$$W^N(x_i, y_j) = W_L^N(x_i, y_j) + W_B^N(x_i, y_j) + W_C^N(x_i, y_j), \quad (x_i, y_j) \in \overline{\Omega}_\sigma^N,$$

where

$$\begin{aligned} L_\varepsilon^N W_L(x_i, y_j) &= 0 \quad \text{in } \Omega_\sigma^N, & W_L^N(x_i, y_j) &= w_L(x_i, y_j) \quad \text{on } \partial\Omega_\sigma^N, \\ L_\varepsilon^N W_B(x_i, y_j) &= 0 \quad \text{in } \Omega_\sigma^N, & W_B^N(x_i, y_j) &= w_B(x_i, y_j) \quad \text{on } \partial\Omega_\sigma^N, \\ L_\varepsilon^N W_C(x_i, y_j) &= 0 \quad \text{in } \Omega_\sigma^N, & W_C^N(x_i, y_j) &= w_C(x_i, y_j) \quad \text{on } \partial\Omega_\sigma^N. \end{aligned}$$

The error in the singular component can therefore be written as

$$(W^N - w)(x_i, y_j) = ((W_L^N - w_L) + (W_B^N - w_B) + (W_C^N - w_C))(x_i, y_j), \quad (x_i, y_j) \in \overline{\Omega}_\sigma^N,$$

and the error in each layer component can be estimated separately.

Firstly consider the term $(W_L^N - w_L)$. We will give separate proofs depending on the location of the mesh point x_i. Suppose that $x_i \in [\sigma_1, 1]$. Using the triangle

inequality we get

$$\left|(W_L^N - w_L)(x_i, y_j)\right| \leq \left|W_L^N(x_i, y_j)\right| + \left|w_L(x_i, y_j)\right|,$$

and we shall estimate the two terms on the right-hand-side of the inequality separately. Using the bound on w_L given in Theorem 4.4.3 and the formula for σ given in (4.7.3) we get

$$\begin{aligned} |w_L(x_i, y_j)| &\leq Ce^{-\gamma_1 x_i/2\varepsilon} \\ &\leq Ce^{-\gamma_1 \sigma_1/2\varepsilon} \\ &\leq CN^{-1}. \end{aligned}$$

To establish a similar bound on $\left|W_L^N(x_i, y_j)\right|$ we introduce the mesh function

$$\psi_{i,j}^{\pm} = C_1 A_{i,j} \pm W_L^N(x_i, y_j), \quad \text{where} \quad C_1 = \|\phi\|_{\Gamma_L \cup \Gamma_B}.$$

$$\begin{aligned} \text{Now,} \quad \psi_{i,N}^{\pm} &= C_1 A_{i,N} \geq 0, \\ \psi_{N,j}^{\pm} &= C_1 A_{N,j} \geq 0, \\ \psi_{0,j}^{\pm} &= C_1 \pm \phi(0, y_j) \geq 0, \\ \psi_{i,0}^{\pm} &= C_1 A_{i,0} \pm \phi(x_i, 0) e_1(x_i, 0) \geq 0, \\ \text{and} \quad L_\varepsilon^N \psi_{i,j}^{\pm} &= C_1 L_\varepsilon^N A_{i,j} \leq 0. \end{aligned}$$

It follows from the discrete minimum principle in Theorem 4.5.1 that

$$\psi_{i,j}^{\pm} \geq 0, \quad (x_i, y_j) \in \overline{\Omega}_\sigma^N.$$

This implies that, for $x_i \geq \sigma_1$,

$$\begin{aligned} |W_L(x_i, y_j)| &\leq C_1 A_{i,j} \\ &\leq C_1 A_{N/2,j} \\ &\leq CN^{-1}, \end{aligned}$$

as required.

Now suppose that $x_i \in [0, \sigma_1)$. If $y_j \in [\sigma_2, 1)$ the expression for the local truncation error from Theorem 4.5.2 becomes

$$\begin{aligned} \left|L_\varepsilon^N(W_L^N - w_L)(x_i, y_j)\right| &\leq C\left[\varepsilon\left(h\left\|\frac{\partial^3 w_L}{\partial x^3}\right\| + K\left\|\frac{\partial^3 w_L}{\partial y^3}\right\| + \left\|\frac{\partial^2 w_L}{\partial x \partial y}\right\|\right)\right. \\ &+ \left. h\left\|\frac{\partial^2 w_L}{\partial x^2}\right\| + K\left\|\frac{\partial^2 w_L}{\partial y^2}\right\|\right]. \end{aligned} \tag{4.7.6}$$

If $y_j \in (0, \sigma_2)$ the expression for the local truncation error from Theorem 4.5.2 becomes

$$\begin{aligned} \left|L_\varepsilon^N(W_L^N - w_L)(x_i, y_j)\right| &\leq C\left[\varepsilon\left(h\left(\left\|\frac{\partial^3 w_L}{\partial x^3}\right\| + \left\|\frac{\partial^3 w_L}{\partial x^2 \partial y}\right\|\right)\right.\right. \\ &+ \left.\left. k\left(\left\|\frac{\partial^3 w_L}{\partial y^3}\right\| + \left\|\frac{\partial^3 w_L}{\partial x \partial y^2}\right\|\right)\right) + h\left\|\frac{\partial^2 w_L}{\partial x^2}\right\| + k\left\|\frac{\partial^2 w_L}{\partial y^2}\right\|\right]. \end{aligned}$$

The quantity on the right-hand-side of (4.7.6) is the largest and therefore we will assume that the truncation error in the whole region satisfies this bound.

Using the bounds on w_L given in Theorem 4.4.3 and the definitions of h and K given in (4.5.4) we have

$$\left|L_\varepsilon^N(W_L^N - w_L)(x_i, y_j)\right| \leq C(\sigma_1 \varepsilon^{-2} N^{-1} + \varepsilon^{-1} N^{-1} + 1).$$

For all $0 \leq i \leq N/2$ and $0 \leq j \leq N$ we introduce the mesh functions

$$\psi_{i,j}^{\pm} = C_2((\sigma_1 - x_i)(\sigma_1 \varepsilon^{-2} N^{-1} + \varepsilon^{-1} N^{-1} + 1) + N^{-1}) \pm (W_L^N - w_L)(x_i, y_j).$$

Now,

$$\begin{aligned} \psi_{0,j}^{\pm} &= C_2(\sigma_1(\sigma_1 \varepsilon^{-2} N^{-1} + \varepsilon^{-1} N^{-1} + 1) + N^{-1}) > 0, \\ \psi_{i,0}^{\pm} &= \psi_{i,N}^{\pm} = C_2((\sigma_1 - x_i)(\sigma_1 \varepsilon^{-2} N^{-1} + \varepsilon^{-1} N^{-1} + 1) + N^{-1}) > 0, \\ \psi_{N/2,j}^{\pm} &\geq C_2 N^{-1} - C N^{-1} \geq 0, \end{aligned}$$

if C_2 is chosen sufficiently large. Also

$$\begin{aligned} L_\varepsilon^N \psi_{i,j}^{\pm} &\leq -C_2(a_1)_{i,j}(\sigma_1\varepsilon^{-2}N^{-1} + \varepsilon^{-1}N^{-1} + 1) + C(\sigma_1\varepsilon^{-2}N^{-1} + \varepsilon^{-1}N^{-1} + 1) \\ &\leq 0, \end{aligned}$$

again if C_2 is chosen sufficiently large. Applying the discrete minimum principle in the region defined by $0 \leq i \leq N/2$ and $0 \leq j \leq N$ yields

$$\psi_{i,j}^{\pm} \geq 0, \qquad 0 \leq i \leq N/2, \quad 0 \leq j \leq N.$$

This implies that

$$\begin{aligned} \left|(W_L^N - w_L)(x_i, y_j)\right| &\leq C_2((\sigma_1 - x_i)(\sigma_1\varepsilon^{-2}N^{-1} + \varepsilon^{-1}N^{-1} + 1) + N^{-1}) \\ &\leq C_2(\sigma_1^2\varepsilon^{-2}N_x^{-1} + \sigma_1\varepsilon^{-1}N^{-1} + \sigma_1 + N^{-1}) \\ &\leq C(N^{-1}(\ln N)^2 + N^{-1}\ln N + \varepsilon \ln N + N^{-1}) \\ &\leq CN^{-1}(\ln N)^2 \end{aligned}$$

since $\varepsilon \leq N^{-1}$.

In an analogous manner it can be shown that

$$\left|(W_B^N - w_B)(x_i, y_j)\right| \leq CN^{-1}(\ln N)^2.$$

Finally we consider the term $(W_C^N - w_C)$. We will provide separate proofs in the corner region and outside the corner region. First suppose $(x_i, y_j) \notin [0, \sigma_1) \times [0, \sigma_2)$. Using the triangle inequality we get

$$\left|(W_C^N - w_C)(x_i, y_j)\right| \leq \left|W_C^N(x_i, y_j)\right| + \left|w_C(x_i, y_j)\right|,$$

and we estimate the two terms on the right-hand-side of the inequality separately. Using the bound on w_L given in Theorem 4.4.3, the formulae for σ_1 and σ_2 given in

(4.7.3) and the fact that either $x_i \geq \sigma_1$ or $y_j \geq \sigma_2$ we get

$$\begin{aligned} |w_C(x_i, y_j)| &\leq Ce^{-\gamma_1 x_i/2\varepsilon} e^{-\gamma_2 y_j/2\varepsilon} \\ &\leq C_1 e^{-\gamma_1 \sigma_1/2\varepsilon} \quad (C_1 e^{-\gamma_2 \sigma_2/2\varepsilon}), \qquad x_i \geq \sigma \quad (y_j \geq \sigma) \\ &\leq CN^{-1}. \end{aligned}$$

To establish a similar bound on $\left|W_C^N(x_i, y_j)\right|$ we introduce the mesh function

$$Z_{i,j} = A_{i,j} B_{i,j}, \qquad 0 \leq i \leq N_x, \quad 0 \leq j \leq N_y,$$

where $A_{i,j}$ is given in (4.7.4) and $B_{i,j}$ is analogously defined as

$$B_{i,j} = \begin{cases} \left(1 + \frac{\gamma_2 k}{2\varepsilon}\right)^{-j}, & 0 \leq i \leq N, \quad 0 \leq j \leq N/2, \\ B_{N/2} \left(1 + \frac{\gamma_2 K}{2\varepsilon}\right)^{-(j-N/2)}, & 0 \leq i \leq N, \quad N/2+1 \leq j \leq N. \end{cases}$$

It can be shown that $B_{i,j}$ satisfies analogous properties to those satisfied by $A_{i,j}$ given in Lemma 4.7.3. Specifically we have, for all $0 \leq i \leq N$,

$$B_{i,j} > 0, \qquad 0 \leq j \leq N, \tag{4.7.7a}$$

$$D_y^+ B_{i,j} = -\frac{\gamma_2}{2\varepsilon} B_{i,j+1} \leq 0, \qquad 0 \leq j \leq N-1, \tag{4.7.7b}$$

$$D_x^+ B_{i,j} = 0, \qquad 0 \leq j \leq N, \tag{4.7.7c}$$

$$\varepsilon \delta_y^2 B_{i,j} = \frac{\gamma_2^2}{4\varepsilon} \frac{k_{i+1}}{\bar{k}} B_{i,j+1}, \qquad 1 \leq j \leq N-1, \tag{4.7.7d}$$

$$L_\varepsilon^N B_{i,j} < 0, \qquad 1 \leq j \leq N-1, \tag{4.7.7e}$$

$$B_{i,N/2} \leq 2N^{-1}, \tag{4.7.7f}$$

$$B_{i,j} \leq 2B_{i,j+1}, \qquad 0 \leq j \leq N/2-1. \tag{4.7.7g}$$

We shall assume that $b_{i,j} > 0$ so that $b_{i,j}^+ = b_{i,j}$ and $b_{i,j}^- = 0$. The case when $b_{i,j} < 0$ can be handled in a similar manner. Now for all $(x_i, y_j) \notin [0, \sigma_1) \times [0, \sigma_2)$ we have

$$\begin{aligned} L_\varepsilon^N Z_{i,j} &= L_\varepsilon^N A_{i,j} B_{i,j} \\ &= (L_\varepsilon^N A_{i,j}) B_{i,j} + A_{i,j} (L_\varepsilon^N B_{i,j}) < 0, \end{aligned}$$

using (4.7.5a), (4.7.5c), (4.7.5e), (4.7.7a), (4.7.7c) and (4.7.7e). And for $(x_i, y_j) \in [0, \sigma_1) \times [0, \sigma_2)$ we have

$$\begin{aligned}
L_\varepsilon^N Z_{i,j} &= L_\varepsilon^N A_{i,j} B_{i,j} \\
&= (L_\varepsilon^N A_{i,j}) B_{i,j} + A_{i,j} (L_\varepsilon^N B_{i,j}) + \varepsilon b_{i,j}^+ (D_x^+ A_{i,j} D_y^+ B_{i,j} + D_x^- A_{i,j} D_y^- B_{i,j}) \\
&= \frac{\gamma_1}{2\varepsilon} \left(\frac{a_{i,j}\gamma_1}{2} - (a_1)_{i,j} \right) A_{i+1,j} B_{i,j} + \frac{\gamma_2}{2\varepsilon} \left(\frac{c_{i,j}\gamma_2}{2} - (a_2)_{i,j} \right) A_{i,j} B_{i,j+1} \\
&+ \frac{b_{i,j}^+ \gamma_1 \gamma_2}{4\varepsilon} (A_{i+1,j} B_{i,j+1} + A_{i,j} B_{i,j}) \\
&= \frac{1}{4\varepsilon} \left(\frac{a_{i,j}\gamma_1^2}{2} + 2b_{i,j}^+ \gamma_1 \gamma_2 + \frac{c_{i,j}\gamma_2^2}{2} - (a_1)_{i,j}\gamma_1 - (a_2)_{i,j}\gamma_2 \right) A_{i,j} B_{i,j} \\
&< \frac{1}{4\varepsilon} \left(a_{i,j}\gamma_1^2 + 2b_{i,j}^+ \gamma_1 \gamma_2 + c_{i,j}\gamma_2^2 - (a_1)_{i,j}\gamma_1 - (a_2)_{i,j}\gamma_2 \right) A_{i,j} B_{i,j} \\
&< 0,
\end{aligned}$$

where we have used the definitions of γ_1 and γ_2 given in (4.4.7). Therefore for all $(x_i, y_j) \in \Omega_\sigma^N$ we have $L_\varepsilon^N Z_{i,j} \leq 0$.

We introduce the mesh functions

$$\psi_{i,j}^\pm = C_1 Z_{i,j} \pm W_C^N(x_i, y_j), \quad \text{where} \quad C_1 = \|\phi\|_{\Gamma_L \cup \Gamma_B}.$$

Now,

$$\begin{aligned}
\psi_{i,N}^\pm &= C_1 Z_{i,N} \geq 0, \\
\psi_{N,j}^\pm &= C_1 Z_{N,j} \geq 0, \\
\psi_{0,j}^\pm &= C_1 B_{0,j} \mp \phi(0, y_j) e_2(0, y_j) \geq 0, \\
\psi_{i,0}^\pm &= C_1 A_{i,0} \mp \phi(x_i, 0) e_1(x_i, 0) \geq 0,
\end{aligned}$$

and

$$L_\varepsilon^N \psi_{i,j}^\pm = C_1 L_\varepsilon^N Z_{i,j} \leq 0.$$

It follows from the discrete minimum principle that

$$\psi_{i,j}^\pm \geq 0, \quad (x_i, y_j) \in \overline{\Omega}_\sigma^N.$$

Using the fact that either $x_i \geq \sigma_1$ or $y_j \geq \sigma_2$, this implies that

$$\begin{aligned} |W_C(x_i, y_j)| &\leq C_1 Z_{i,j} \\ &\leq C_1 A_{i,j} B_{i,j} \\ &\leq C_1 A_{N/2,j} \quad (C_1 B_{i,N/2}), \qquad x_i \geq \sigma_1 \quad (y_j \geq \sigma_2) \\ &\leq CN^{-1}, \end{aligned}$$

as required.

Now suppose that $(x_i, y_j) \in [0, \sigma_1) \times [0, \sigma_2)$. The expression for the local truncation error from Theorem 4.5.2 becomes

$$\begin{aligned} \left|L_\varepsilon^N (W_C^N - w_C)(x_i, y_j)\right| &\leq C \left[\varepsilon \left(h \left(\left\| \frac{\partial^3 w_C}{\partial x^3} \right\| + \left\| \frac{\partial^3 w_C}{\partial x^2 \partial y} \right\|\right)\right.\right. \\ &+ \left.\left. k \left(\left\| \frac{\partial^3 w_C}{\partial y^3} \right\| + \left\| \frac{\partial^3 w_C}{\partial x \partial y^2} \right\|\right)\right) + h \left\| \frac{\partial^2 w_C}{\partial x^2} \right\| + k \left\| \frac{\partial^2 w_C}{\partial y^2} \right\|\right]. \end{aligned}$$

Using the bounds on w_C given in Theorem 4.4.3 and the definitions of the mesh widths h and k given in (4.5.4) we get

$$\left|L_\varepsilon^N (W_C^N - w_C)(x_i, y_j)\right| \leq C\varepsilon^{-2} N^{-1} (\sigma_1 + \sigma_2).$$

For all $0 \leq i \leq N_x/2$ and $0 \leq j \leq N_y/2$ we introduce the mesh functions

$$\psi_{i,j}^{\pm} = C_3 N^{-1} (\varepsilon^{-2} (\sigma_1 (\sigma_1 - x_i) + \sigma_2 (\sigma_2 - y_j)) + 1) \pm (W_C^N - w_C)(x_i, y_j).$$

Now,

$$\begin{aligned} \psi_{0,j}^{\pm} &= C_3 N^{-1} (\varepsilon^{-2} (\sigma_1^2 + \sigma_2 (\sigma_2 - y_j)) + 1) > 0, \\ \psi_{i,0}^{\pm} &= C_3 N^{-1} (\varepsilon^{-2} (\sigma_1 (\sigma_1 - x_i) + \sigma_2^2) + 1) > 0, \\ \psi_{N_x/2,j}^{\pm} &\geq C_3 N^{-1} (\varepsilon^{-2} \sigma_2 (\sigma_2 - y_j) + 1) - CN^{-1} \geq 0, \\ \psi_{i,N_y/2}^{\pm} &\geq C_3 N^{-1} (\varepsilon^{-2} \sigma_1 (\sigma_1 - x_i) + 1) - CN^{-1} \geq 0, \end{aligned}$$

if C_3 is chosen sufficiently large. Also

$$\begin{aligned} L_\varepsilon^N \psi_{i,j}^{\pm} &\leq -C_3 \varepsilon^{-2} N^{-1}((a_1)_{i,j}\sigma_1 + (a_2)_{i,j}\sigma_2) + C\varepsilon^{-2}N^{-1}(\sigma_1+\sigma_2) \\ &\leq 0, \end{aligned}$$

if C_3 is again chosen sufficiently large. Applying the discrete minimum principle given in Theorem 4.5.1 in the region defined by $0 \leq i \leq N/2$ and $0 \leq j \leq N/2$ yields

$$\psi_{i,j}^{\pm} \geq 0, \qquad 0 \leq i \leq N/2, \quad 0 \leq j \leq N/2.$$

This implies that in the corner region

$$\begin{aligned} \left|(W_C^N - w_C)(x_i, y_j)\right| &\leq C_3 N^{-1}(\varepsilon^{-2}(\sigma_1(\sigma_1 - x_i) + \sigma_2(\sigma_2 - y_j)) + 1) \\ &\leq C_3 N^{-1}(\varepsilon^{-2}(\sigma_1^2 + \sigma_2^2) + 1) \\ &\leq CN^{-1}(\ln N)^2. \end{aligned}$$

This completes the proof. □

The previous two theorems together give us the following ε-uniform estimate of the error in our numerical approximations at the mesh points.

Theorem 4.7.5. *Let u be any solution from Problem Class 4.3.1 and U^N be the corresponding numerical solution generated by Method 4.5.1. Then, under Assumption 4.7.1, for all $N \geq 4$, we have*

$$\sup_{0<\varepsilon\leq 1} \left\|U^N - u\right\|_{\overline{\Omega}_\sigma^N} \leq CN^{-1}(\ln N)^2,$$

where C is a constant independent of N and ε.

Chapter 5

Numerical results for elliptic problems

5.1 Introduction

In this chapter we present extensive numerical results for the method introduced in Chapter 4 applied to some sample problems from Problem Class 4.3.1. These problems will be generated, of course, from the consideration of suitable problems from Problem Class 4.2.1. Various choices for the non-rectangular domain will be considered. The numerical results presented will include a validation of the theoretical result proved in Chapter 4.

This chapter is organised as follows. In §5.2 we introduce some special cases of domains for Problem Class 4.2.1 and show what form the transformed Problem Class 4.3.1 takes. In §5.3 we present detailed numerical results for some sample problems posed on parallelograms. In §5.4 we discuss some important practical issues concerning the application of our method. Finally, in §5.5 we consider more complicated geometries and present some sample numerical results.

All computations in this chapter were performed using MATLAB. The linear systems generated were solved using the Unsymmetric MultiFrontal PACKage (UMFPACK) [7]. This is a direct LU based solver which is chosen in preference to an iterative solver due to memory restrictions.

5.2 Special cases of non-rectangular domains

We consider the subclass of Problem Class 4.2.1 where the domain $\hat{\Omega} = \hat{\Omega}_P$ is a domain bounded by the lines

$$\xi = \phi(\eta), \quad \xi = 1 + \phi(\eta), \tag{5.2.1}$$

$$\eta = 0, \quad \eta = 1, \tag{5.2.2}$$

where $\phi(\eta)$ is sufficiently smooth. In this case the co-ordinate transformation (4.2.2) takes the simple form

$$x \equiv \xi - \phi(\eta), \quad y \equiv \eta, \quad u(x,y) \equiv \hat{u}(\xi,\eta). \tag{5.2.3}$$

Also in this case the inverse transformation can be easily found to be

$$\xi = x + \phi(y), \quad \eta = y.$$

So the transformed differential equation becomes

$$(\varepsilon((1+(\phi')^2)u_{xx} - 2(\phi')^2 u_{xy} + u_{yy}) + a_1 u_x + a_2 u_y)(x,y) = f(x,y) \quad \text{in } \Omega,$$

where

$$a_1(x,y) = \hat{a}_1(x+\phi(y),y) - \hat{a}_2(x+\phi(y),y)\phi'(y) - \varepsilon\phi''(y), \quad a_2(x,y) = \hat{a}_2(x+\phi(y),y). \tag{5.2.4}$$

We now introduce the corresponding Problem Class.

Problem Class 5.2.1.

$$(\varepsilon((1+(\phi')^2)u_{xx} - 2\phi' u_{xy} + u_{yy}) + a_1 u_x + a_2 u_y)(x,y) = f(x,y) \quad \textit{in } \Omega, \tag{5.2.5}$$

$$u(x,y) = 0 \quad \textit{on } \partial\Omega, \tag{5.2.6}$$

where a_1 and a_2 are given by (5.2.4) *and satisfy*

$$a_1(x,y) > 0, \quad a_2(x,y) > 0, \qquad \forall (x,y) \in \overline{\Omega}. \tag{5.2.7}$$

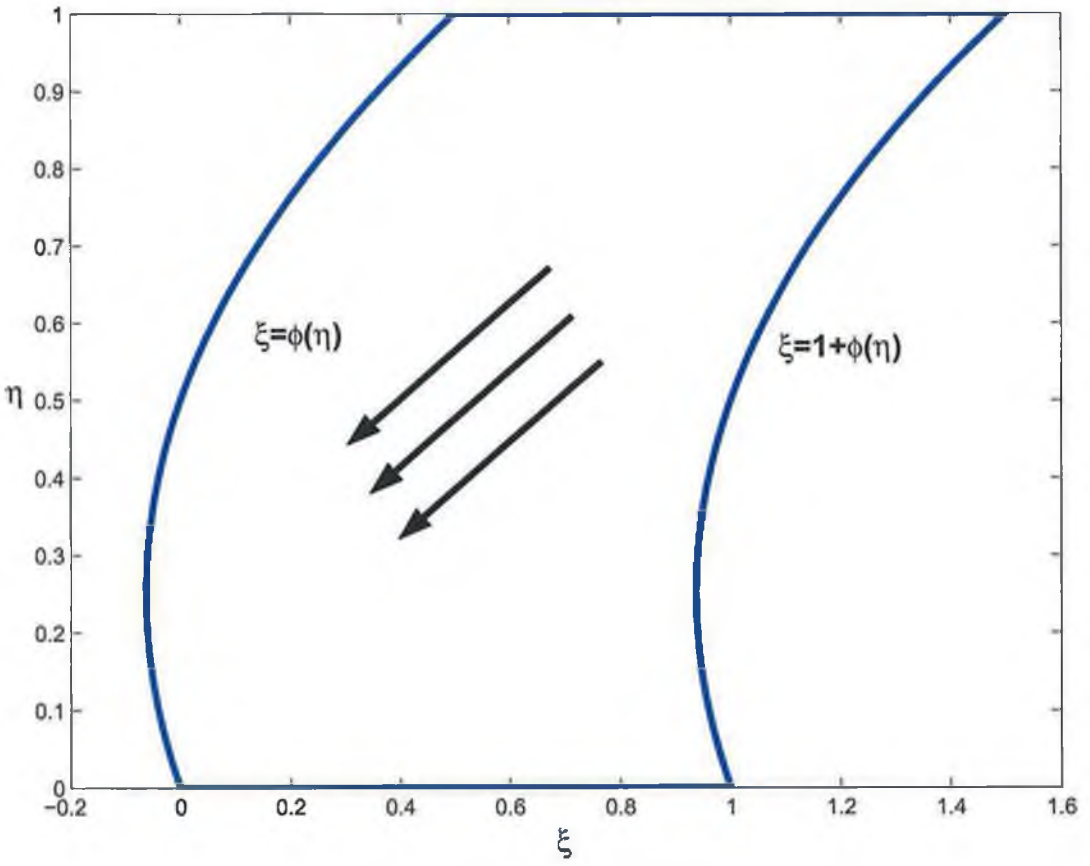

Figure 5.1: The domain $\hat{\Omega}_P$.

Remark 5.2.1. The sign of the mixed derivative term in (5.2.5) is governed by the curvature of the boundary wall $\xi = \phi(\eta)$.

Remark 5.2.2. The conditions (5.2.7) impose restrictions on the convective terms in the original equation which necessarily depend on the geometry of the original domain. For small ε, the larger the curvature of the boundary wall is the bigger $\hat{a}_1$ must be relative to $\hat{a}_2$. This is illustrated in Figure 5.1 where the arrows indicate the direction of the convective term $\hat{\mathbf{a}}$.

One particularly simple choice for the function specifying the boundary is $\phi(\eta) = -m\eta$, where m is a constant. In this case the domain is a parallelogram. This is

illustrated in Figure 5.2. The angle θ satisfies

$$\tan(\theta - \pi/2) = m \quad \text{if} \quad m \geq 0, \quad \tan\theta = 1/m \quad \text{if} \quad m < 0.$$

For simplicity we shall also assume that the convective terms in the original equation have constant coefficients. That is, $\hat{a}_1 = \alpha_1$ and $\hat{a}_2 = \alpha_2$. For all calculations in this chapter we will take $f(x,y) = 16x(1-x)y(1-y)$ as the inhomogeneous term. This choice guarantees that the compatibility conditions (4.3.4) are satisfied. The corresponding transformed Problem Class is

Problem Class 5.2.2.

$$\begin{aligned}(\varepsilon((1+m^2)u_{xx} + 2mu_{xy} + u_{yy}) + (\alpha_1 + m\alpha_2)u_x + \alpha_2 u_y)(x,y) = f(x,y) \quad &\text{in } \Omega, \\ u(x,y) = 0 \quad &\text{on } \partial\Omega,\end{aligned}$$

where

$$\alpha_1(x,y) + m\alpha_2(x,y) > 0, \quad \alpha_2(x,y) > 0, \qquad \forall (x,y) \in \overline{\Omega}. \tag{5.2.8}$$

5.3 Numerical results for elliptic problems on a parallelogram

In this section we present detailed numerical results for Method 4.5.1 applied to suitable sample problems from Problem Class 5.2.2 for a wide range of choices of the parameter m. Due to practical restrictions the maximum number of mesh points that we are able to generate solutions from our method is 512. To examine the performance of the method we will tabulate the computed orders of convergence, p_ε^N, and the computed ε-uniform orders of convergence, p^N. These are calculated from the two-mesh differences defined as

$$D_\varepsilon^N = \max_{0 \leq i,j \leq N} |U^N(x_i, y_j) - \overline{U}^{2N}(x_i, y_j)|, \qquad D^N = \max_{\varepsilon = 2^{-9}, \ldots, 2^{-32}} D_\varepsilon^N, \tag{5.3.1}$$

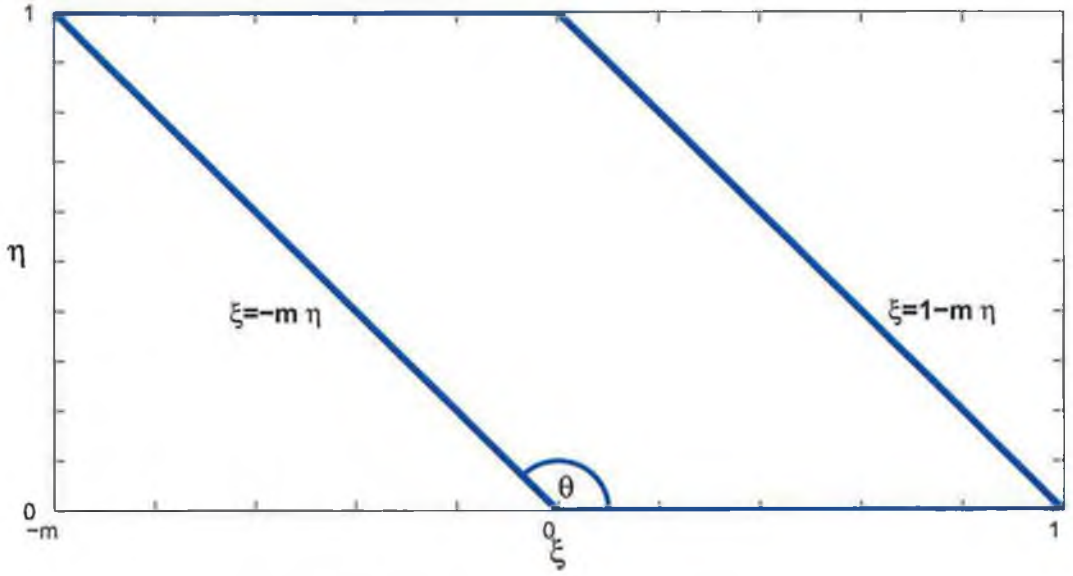

Figure 5.2: The domain $\hat{\Omega}_P$ when $\phi(\eta) = -m\eta$.

where $\overline{U}^{2N}$ indicates the piecewise bilinear interpolant of the numerical solution U^N. The p_ε^N and p^N are then defined as

$$p_\varepsilon^N = \log_2 \frac{D_\varepsilon^N}{D_\varepsilon^{2N}}, \qquad p^N = \log_2 \frac{D^N}{D^{2N}}.$$

As we are interested in the performance of our method in the perturbed case we shall assume that $\varepsilon \leq N^{-1}$ for the range of N considered. This explains the values of ε in the definition of D^N in (5.3.1). As discussed in Remark 4.5.1 and §5.4 we shall be taking $N_x = N_y = N$ and choosing our sample problems so that the inequalities (4.5.8) are satisfied. For problems from Problem Class 5.2.2 these take the form

$$\begin{aligned} m > 0: &\qquad 0 \leq \tfrac{\alpha_1}{\alpha_2} \leq \tfrac{1}{m}, \\ m < 0: &\quad -2m \leq \tfrac{\alpha_1}{\alpha_2} \leq -2m - \tfrac{1}{m}. \end{aligned} \tag{5.3.2}$$

The region defined by these inequalities is shown in Figure 5.3. Note that as the magnitude of m increases, and therefore the angle θ at the vertex of the parallelogram

deviates further from a right angle, the range of possible values of α_1 and α_2 are decreased. As mentioned in Remark 4.5.1 we can remove these restrictions if we allow the number of mesh intervals in each direction to vary and satisfy (4.5.7). So

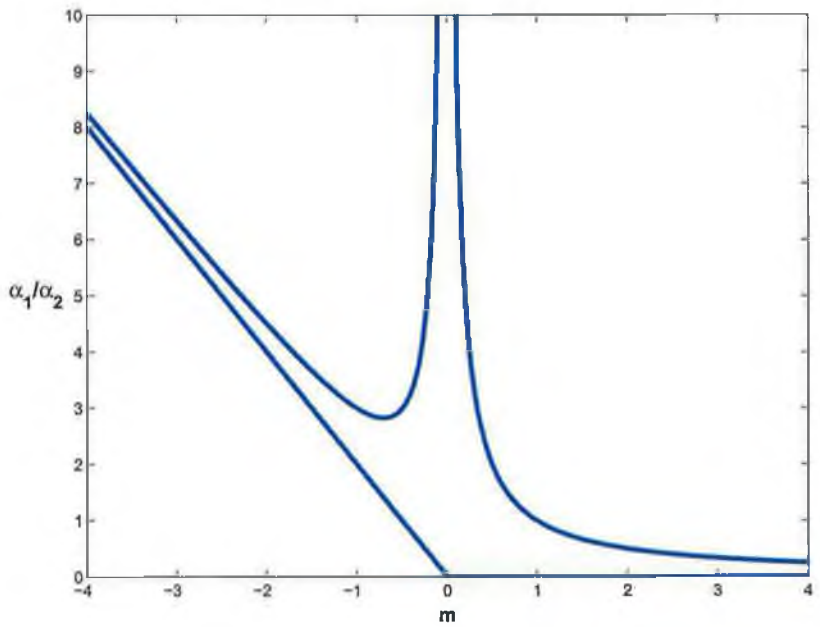

Figure 5.3: The region defined by (5.3.2).

to satisfy the inequalities (5.3.2) we will take

$$\begin{aligned} m > 0: &\quad \alpha_1 = \tfrac{1}{m}, \quad \alpha_2 = 1, \\ m = 0: &\quad \alpha_1 = 1, \quad \alpha_2 = 1, \\ m < 0: &\quad \alpha_1 = -2m, \quad \alpha_2 = 1. \end{aligned} \tag{5.3.3}$$

Note that with these choices of α_1 and α_2 the conditions (5.2.8) are also satisfied. We now define the subclass of Problem Class 5.2.2 that we will be using for our sample problems.

Problem Class 5.3.1.

$$(\varepsilon((1+m^2)u_{xx}+2mu_{xy}+u_{yy})+(\alpha_1+m\alpha_2)u_x+\alpha_2 u_y)(x,y)=f(x,y) \quad \text{in } \Omega,$$
$$u(x,y)=0 \quad \text{on } \partial\Omega,$$

where α_1 *and* α_2 *are given by* (5.3.3).

In Tables 5.1 and 5.2 we present the computed orders of convergence, p_ε^N, and the computed ε-uniform orders of convergence, p^N, for $m=1$, and $m=-2$, respectively. We see that, for the range of ε considered, the p_ε^N are essentially independent of ε, and are approaching 1, as N is increased. For other values of m the ε-uniform orders of convergence are shown in Table 5.3 which indicates that our method performs uniformly well for all values of m considered. These results validate Theorem 4.7.5. For these particular problems, the orders of convergence (over the range of $N \in [8,128]$) are higher than the theoretical rate given in Theorem 4.7.5 (see [15, §8.3] for some sample values). The orders tend to the order associated with $CN^{-1}\ln N$ for all values of p.

We also include graphs of some representative numerical solutions (see Figures 5.4 and 5.5), plotted on the original domain to better illustrate the interaction of the layers and the geometry of the problem.

5.4 Computational issues

In this section we investigate some issues of practical importance concerning the application of Method 4.5.1. In particular we will look at the following:

1. Consistent versus inconsistent difference schemes.
2. Using different number of mesh intervals in each co-ordinate direction.
3. The effect of the mixed derivative term on the layer structure.

To examine these points in detail we shall consider some problems from Problem Class 5.2.2.

	Number of Intervals N				
ε	8	16	32	64	128
2^{-9}	0.72	0.75	0.75	0.81	0.84
2^{-10}	0.71	0.75	0.74	0.81	0.84
2^{-11}	0.70	0.75	0.74	0.80	0.84
2^{-12}	0.70	0.75	0.74	0.80	0.84
2^{-13}	0.70	0.75	0.74	0.80	0.84
2^{-14}	0.70	0.75	0.74	0.80	0.84
2^{-15}	0.70	0.75	0.74	0.80	0.84
2^{-16}	0.70	0.75	0.74	0.80	0.84
2^{-17}	0.70	0.75	0.74	0.80	0.84
2^{-18}	0.70	0.75	0.74	0.80	0.84
2^{-19}	0.70	0.75	0.74	0.80	0.84
2^{-20}	0.70	0.75	0.74	0.80	0.84
p^N	0.70	0.75	0.74	0.80	0.84

Table 5.1: Computed orders of convergence, p_ε^N, and computed ε-uniform orders of convergence, p^N, for Method 4.5.1 applied to Problem Class 5.3.1 with $m = 1$.

	Number of Intervals N				
ε	8	16	32	64	128
2^{-9}	0.73	0.75	0.75	0.82	0.84
2^{-10}	0.72	0.75	0.74	0.81	0.84
2^{-11}	0.71	0.75	0.74	0.81	0.84
2^{-12}	0.70	0.75	0.74	0.80	0.84
2^{-13}	0.70	0.75	0.74	0.80	0.84
2^{-14}	0.70	0.75	0.74	0.80	0.84
2^{-15}	0.70	0.75	0.74	0.80	0.84
2^{-16}	0.70	0.75	0.74	0.80	0.84
2^{-17}	0.70	0.75	0.74	0.80	0.84
2^{-18}	0.70	0.75	0.74	0.80	0.84
2^{-19}	0.70	0.75	0.74	0.80	0.84
2^{-20}	0.70	0.75	0.74	0.80	0.84
p^N	0.70	0.75	0.74	0.80	0.84

Table 5.2: Computed orders of convergence, p_ε^N, and computed ε-uniform orders of convergence, p^N, for Method 4.5.1 applied to Problem Class 5.3.1 with $m = -2$.

m	Number of Intervals N				
	8	16	32	64	128
−3.00	0.86	0.80	0.76	0.83	0.84
−2.75	0.85	0.77	0.76	0.83	0.84
−2.50	0.83	0.76	0.76	0.82	0.84
−2.25	0.76	0.76	0.75	0.81	0.84
−2.00	0.70	0.75	0.74	0.80	0.84
−1.75	0.66	0.72	0.74	0.79	0.84
−1.50	0.66	0.73	0.73	0.78	0.83
−1.25	0.57	0.67	0.74	0.79	0.83
−1.00	0.53	0.63	0.67	0.73	0.79
−0.75	0.60	0.71	0.78	0.78	0.83
−0.50	0.70	0.75	0.74	0.80	0.84
−0.25	0.89	0.81	0.78	0.80	0.82
0.00	0.53	0.64	0.68	0.74	0.80
0.25	0.90	0.81	0.78	0.79	0.82
0.50	0.83	0.76	0.76	0.82	0.84
0.75	0.72	0.75	0.75	0.81	0.84
1.00	0.70	0.75	0.74	0.80	0.84
1.25	0.71	0.75	0.75	0.80	0.84
1.50	0.74	0.76	0.75	0.81	0.84
1.75	0.78	0.77	0.75	0.81	0.84
2.00	0.83	0.76	0.76	0.82	0.84
2.25	0.85	0.76	0.76	0.83	0.84
2.50	0.86	0.79	0.76	0.83	0.84
2.75	0.86	0.80	0.77	0.83	0.84
3.00	0.87	0.81	0.77	0.83	0.83

Table 5.3: Computed ε-uniform orders of convergence, p^N, for Method 4.5.1 applied to Problem Class 5.3.1 with various values of m.

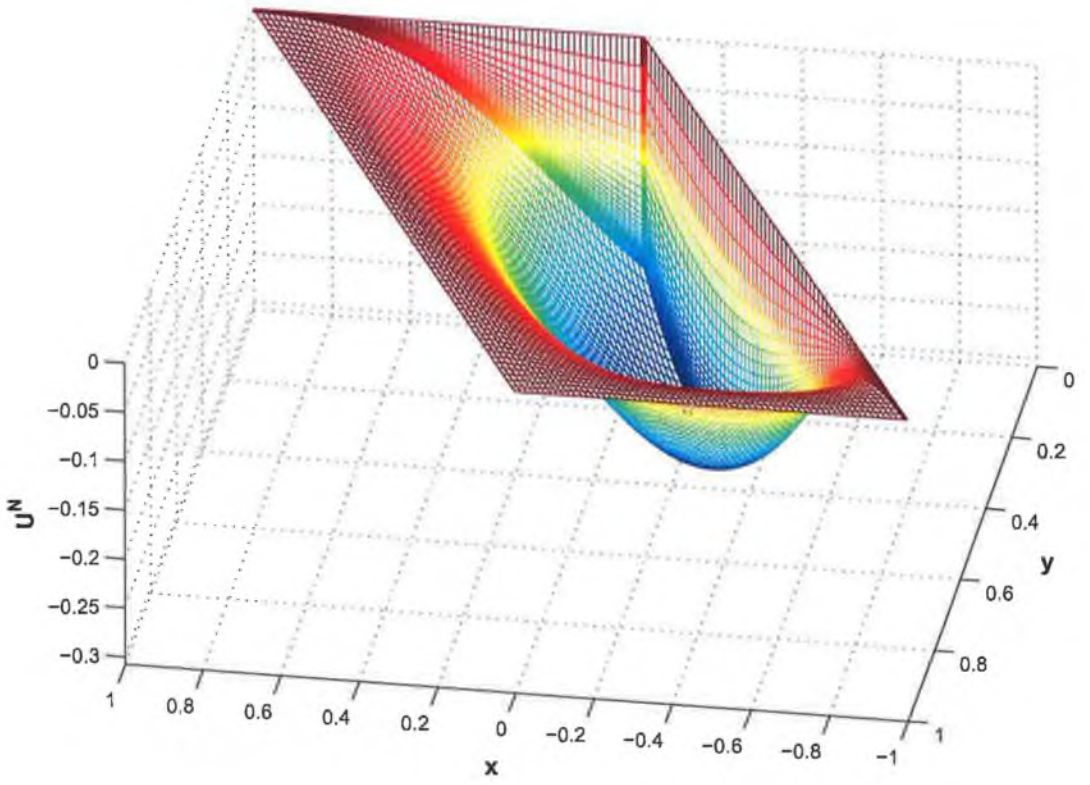

Figure 5.4: Plot of Numerical Solution generated by Method 4.5.1 applied to the problem from Problem Class 5.3.1 with $m = 1$, α_1 and α_2 given by (5.3.3), $\varepsilon = 2^{-10}$ and $N = 128$ on original domain.

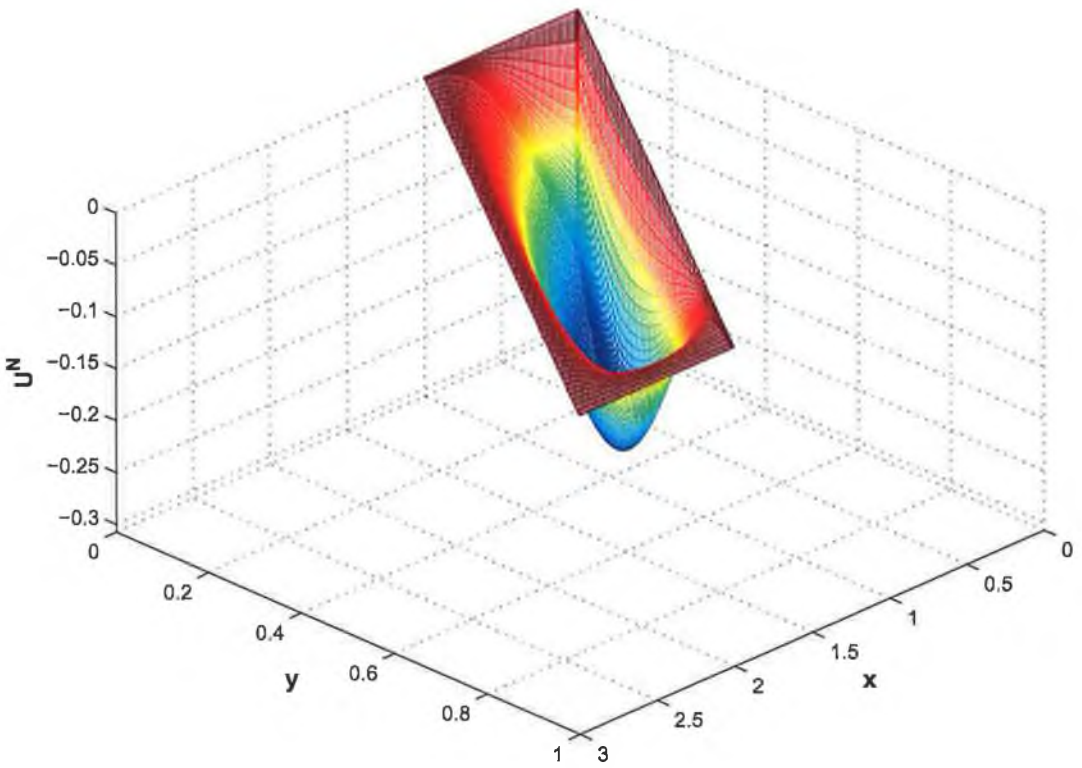

Figure 5.5: Plot of Numerical Solution generated by Method 4.5.1 applied to the problem from Problem Class 5.3.1 for $m = -2$, α_1 and α_2 given by (5.3.3), $\varepsilon = 2^{-10}$ and $N = 128$ on original domain.

5.4.1 Consistent versus inconsistent difference schemes

As demonstrated in the previous section Method 4.5.1 performs well when applied to problems from Problem Class 5.2.2 providing that the singular perturbation parameter is small with respect to the number of mesh intervals used. This is in accordance with the theoretical result proved in §4.7. As discussed in §4.6 this necessitates the employment of an inconsistent finite difference operator so that our method satisfies a discrete comparison principle (see Theorem 4.5.1). However if we wish to use a numerical scheme that is consistent (i.e. that approximates the mixed derivative throughout the mesh) then the theorem no longer holds. Therefore, it is interesting to investigate how a numerical method based on such a scheme performs and how the numerical solutions generated compare with those from our inconsistent scheme. This is the purpose of the present subsection. It is also convenient to include here an investigation of the performance of our inconsistent scheme for large ε.

Let Z^N be any mesh function. We define the difference operator $L^N_{\varepsilon,Con}$ as

$$L^N_{\varepsilon,Con}Z^N_{i,j} \equiv (\varepsilon(a\delta_x^2+2(b^+\delta^+_{xy}+b^-\delta^-_{xy})+c\delta_y^2)+a_1D_x^+ +a_2D_y^+)Z^N(x_i,y_j), \quad \forall (x_i,y_j)\in\Omega^N, \tag{5.4.1}$$

where

$$b^+(x_i,y_j)=\frac{b(x_i,y_j)+|b(x_i,y_j)|}{2}, \qquad b^-(x_i,y_j)=\frac{b(x_i,y_j)-|b(x_i,y_j)|}{2},$$

and δ^+_{xy} and δ^-_{xy} are defined in (4.5.2). Thus the operator $L^N_{\varepsilon,Con}$ is the consistent analogue of L^N_ε defined in (4.5.1).

The corresponding numerical method is

Method 5.4.1.

$$\begin{aligned} L^N_{\varepsilon,Con}U^N_{Con} &= f(x_i,y_j) \quad in\ \ \Omega^N_\sigma, \\ U^N_{Con}(x_i,y_j) &= 0 \quad on\ \ \partial\Omega^N_\sigma. \end{aligned}$$

To compare the performance of Methods 4.5.1 and 5.4.1 we consider the problem

from Problem Class 5.2.2 with $\alpha_1 = 1$, $\alpha_2 = 2$ and $m = 2$:

$$(\varepsilon(5u_{xx} + 2mu_{xy} + u_{yy}) + 5u_x + 2u_y)(x, y) = f(x, y) \quad \text{in } \Omega, \tag{5.4.3a}$$

$$u(x, y) = 0 \quad \text{on } \partial\Omega. \tag{5.4.3b}$$

This problem was chosen so that Method 4.5.1 will be monotone when applied to it. This can be checked by verifying that the inequalities (5.3.2) are satisfied. Of course Method 5.4.1 will not be monotone when applied to this problem (see §4.6). Therefore it is interesting to see if the numerical solutions generated by this method exhibit non-physical oscillations not present in the solutions generated by the monotone method.

In Figure 5.6 we show the solution generated by Method 5.4.1 when applied to problem (5.4.3) for particular values of ε and N. There seem to be no non-physical oscillations present. This is in contrast to what one normally finds when a non-monotone method is applied to a singularly perturbed problems, for example when the first derivative is approximated by a central difference operator. In Figure 5.7 we show the absolute difference between the numerical solutions generated by the two methods for the same problem. Observe that the largest values occur away from the corner of the domain. In Table 5.4 we show the maximum relative differences between the numerical solutions for a range of values of ε and N. The maximum relative difference is defined as

$$\frac{\max_{0\le i,j\le N} \left|U^N(x_i, y_j) - U^N_{Con}(x_i, y_j)\right|}{\max_{0\le i,j\le N} \{\left|U^N(x_i, y_j)\right|, \left|U^N_{Con}(x_i, y_j)\right|\}}.$$

We see from the table that for large ε the maximum relative differences are approximately constant while for small ε they are proportional to ε. In addition the difference between the two solutions for small ε is smaller in magnitude than the corresponding two-mesh differences for Method 4.5.1. To see this we compare the computed orders of convergence, p^N_ε, and the computed ε-uniform orders of convergence, p^N for these two methods. Note that here we have defined D^N for a wider range of values of ε than we did in (5.3.1):

$$D^N = \max_{\varepsilon=1,2^{-1},\ldots,2^{-20}} D^N_\varepsilon,$$

with the definitions of p^N_ε and p^N changed similarly. This is because we are interested

in the behaviour of both methods for large values of ε also. We see from Tables 5.6 and 5.5 that the orders are approximately the same for small ε. This is experimental justification for the choice of an inconsistent difference operator.

However, these tables also indicate that the use of a monotone operator is, in this case, really only to enable us to prove error estimates, as the non-monotone method appears to behave in an identical manner for small ε, at least for the examples we have considered. Moreover, for values of ε where our convergence result does not apply we see that Method 4.5.1 does not give acceptable results. For moderate values of ε (2^{-5} and 2^{-6}) we see that the computed orders of convergence decrease with increasing values of N, whereas it can be seen that the ε-uniform orders for the consistent scheme behave well. However, there is one drawback to the non-monotone method which explains why Table 5.6 is smaller than Table 5.5. The direct solver uses more memory when solving the linear systems associated with Method 5.4.1 than those associated with Method 4.5.1. The performance of an iterative solver has not been investigated as this would require even more memory.

5.4.2 Different number of mesh intervals in each co-ordinate direction

In §5.3 we remarked that for computational convenience we would choose sample problems from Problem Class 5.2.2 so that in order for Method 4.5.1 to be monotone it would suffice to have an equal number of mesh intervals in each co-ordinate direction. This involved taking particular choices for the convection coefficients in the original problem so that the inequalities (5.3.2) were satisfied. In this subsection we demonstrate the application of the method for problems where the coefficients are not restricted in this way. In this case the inequalities (4.5.7) must be satisfied and thus the number of mesh intervals in each direction will possibly be different. For problems from Problem Class 5.2.2 these inequalities take the form (for $m \neq 0$)

$$\operatorname{sgn}(m)\left(1+\frac{m\alpha-1}{1+m^2}\right) \leq \frac{N_y}{N_x} \leq \operatorname{sgn}(m)\left(1+\frac{\alpha}{m}\right), \tag{5.4.4}$$

where $\alpha = \alpha_1/\alpha_2$. This shows explicitly that for particular values of α_1 and α_2 the number of mesh points required for our method to be monotone depends on the

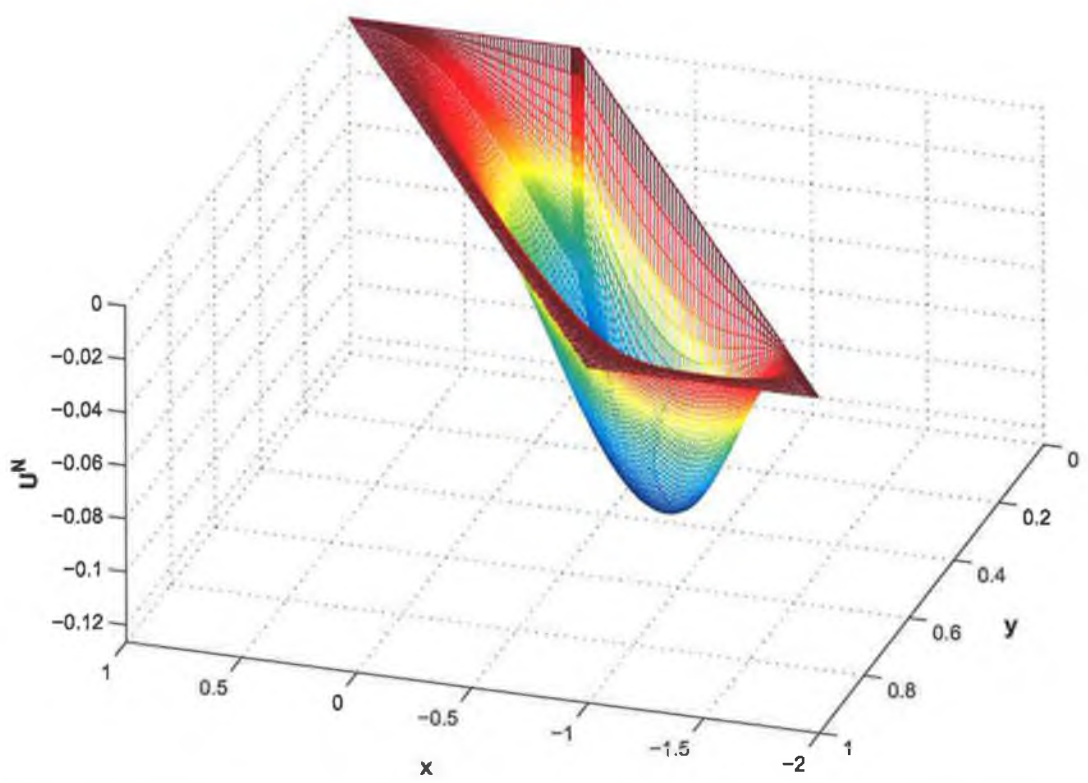

Figure 5.6: Plot of numerical solution generated by Method 5.4.1 applied to problem (5.4.3) with $\varepsilon = 2^{-8}$ and $N = 128$.

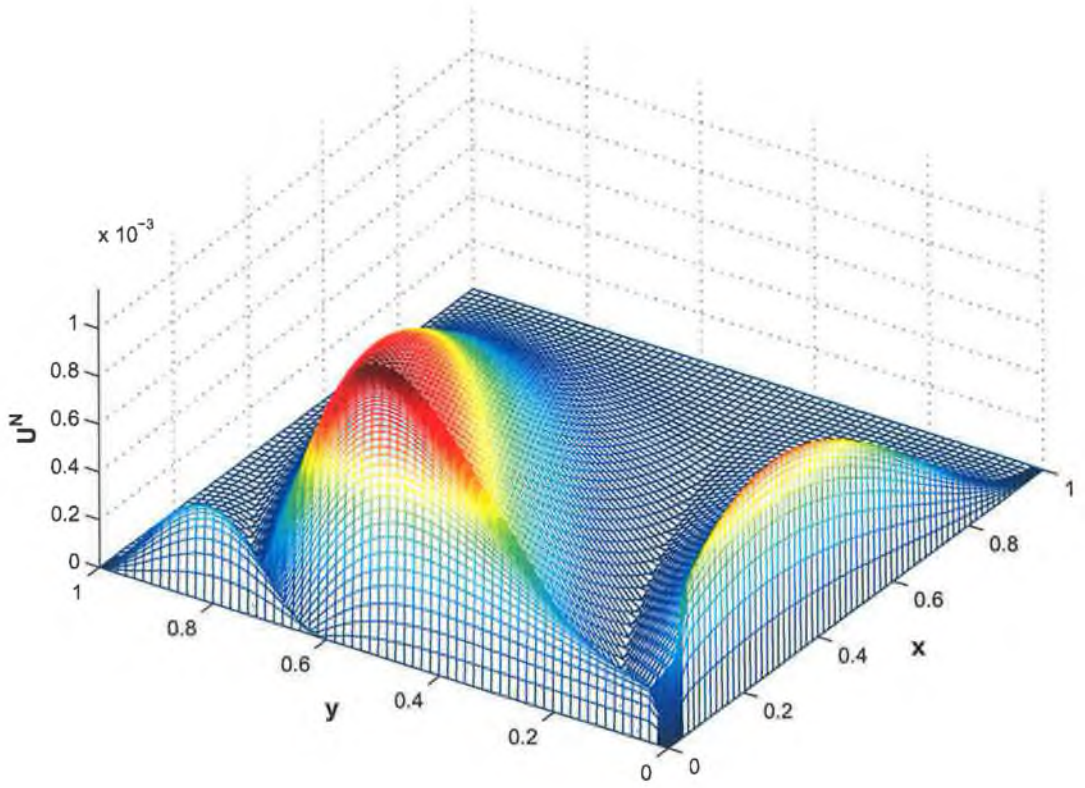

Figure 5.7: Plot of absolute difference of numerical solutions generated by Methods 4.5.1 and 5.4.1 applied to problem (5.4.3) with $\varepsilon = 2^{-8}$ and $N = 128$.

ε	Number of Intervals N					
	8	16	32	64	128	256
1	1.49e-001	1.69e-001	1.76e-001	1.80e-001	1.82e-001	1.82e-001
2^{-1}	1.45e-001	1.61e-001	1.70e-001	1.75e-001	1.78e-001	1.79e-001
2^{-2}	1.27e-001	1.45e-001	1.62e-001	1.71e-001	1.76e-001	1.78e-001
2^{-3}	9.66e-002	1.13e-001	1.32e-001	1.43e-001	1.48e-001	1.51e-001
2^{-4}	5.30e-002	7.22e-002	8.53e-002	9.49e-002	1.01e-001	1.04e-001
2^{-5}	3.24e-002	4.01e-002	4.81e-002	5.54e-002	6.00e-002	6.27e-002
2^{-6}	1.79e-002	2.25e-002	2.57e-002	3.02e-002	3.34e-002	3.53e-002
2^{-7}	9.35e-003	1.19e-002	1.35e-002	1.59e-002	1.78e-002	1.90e-002
2^{-8}	4.78e-003	6.09e-003	6.86e-003	8.22e-003	9.21e-003	9.93e-003
2^{-9}	2.42e-003	3.09e-003	3.46e-003	4.19e-003	4.70e-003	5.09e-003
2^{-10}	1.22e-003	1.55e-003	1.74e-003	2.11e-003	2.38e-003	2.58e-003
2^{-11}	6.11e-004	7.79e-004	8.72e-004	1.06e-003	1.20e-003	1.30e-003
2^{-12}	3.06e-004	3.90e-004	4.36e-004	5.31e-004	5.99e-004	6.53e-004
2^{-13}	1.53e-004	1.95e-004	2.18e-004	2.66e-004	3.00e-004	3.27e-004
2^{-14}	7.65e-005	9.76e-005	1.09e-004	1.33e-004	1.50e-004	1.64e-004
2^{-15}	3.83e-005	4.88e-005	5.46e-005	6.65e-005	7.51e-005	8.19e-005
2^{-16}	1.91e-005	2.44e-005	2.73e-005	3.33e-005	3.76e-005	4.09e-005
2^{-17}	9.57e-006	1.22e-005	1.37e-005	1.66e-005	1.88e-005	2.05e-005
2^{-18}	4.78e-006	6.10e-006	6.83e-006	8.31e-006	9.39e-006	1.02e-005
2^{-19}	2.39e-006	3.05e-006	3.41e-006	4.16e-006	4.70e-006	5.12e-006
2^{-20}	1.20e-006	1.53e-006	1.71e-006	2.08e-006	2.35e-006	2.56e-006

Table 5.4: Maximum relative differences between numerical solutions generated by Methods 4.5.1 and 5.4.1 applied to applied to problem 5.4.3 for $m = 2$.

ε	Number of Intervals N				
	8	16	32	64	128
1	0.60	0.84	0.94	0.95	0.97
2^{-1}	0.64	0.78	0.90	0.95	0.97
2^{-2}	0.57	0.71	0.84	0.91	0.95
2^{-3}	0.79	0.83	0.78	0.84	0.91
2^{-4}	0.81	0.50	0.47	0.83	0.66
2^{-5}	0.86	0.69	0.64	0.55	0.53
2^{-6}	0.86	0.78	0.75	0.78	0.58
2^{-7}	0.85	0.78	0.75	0.81	0.83
2^{-8}	0.84	0.77	0.75	0.82	0.84
2^{-9}	0.84	0.76	0.76	0.82	0.84
2^{-10}	0.83	0.76	0.76	0.82	0.84
2^{-11}	0.83	0.76	0.76	0.82	0.84
2^{-12}	0.83	0.76	0.76	0.82	0.84
2^{-13}	0.83	0.76	0.76	0.82	0.84
2^{-14}	0.83	0.76	0.76	0.82	0.84
2^{-15}	0.83	0.76	0.76	0.82	0.84
2^{-16}	0.83	0.76	0.76	0.82	0.84
2^{-17}	0.83	0.76	0.76	0.82	0.84
2^{-18}	0.83	0.76	0.76	0.82	0.84
2^{-19}	0.83	0.76	0.76	0.82	0.84
2^{-20}	0.83	0.76	0.76	0.82	0.84
p^N	0.83	0.76	0.76	0.82	0.57

Table 5.5: Computed orders of convergence, p_ε^N, and computed ε-uniform orders of convergence, p^N, for Method 4.5.1 applied to problem 5.4.3 with $m = 2$.

	Number of Intervals N			
ε	8	16	32	64
1	0.47	0.76	0.88	0.94
2^{-1}	0.59	0.81	0.91	0.95
2^{-2}	0.58	0.79	0.90	0.95
2^{-3}	0.61	0.87	0.93	0.94
2^{-4}	0.86	0.50	0.49	0.92
2^{-5}	0.80	0.72	0.74	0.77
2^{-6}	0.86	0.77	0.75	0.81
2^{-7}	0.85	0.77	0.76	0.82
2^{-8}	0.84	0.76	0.76	0.83
2^{-9}	0.84	0.76	0.76	0.82
2^{-10}	0.83	0.76	0.76	0.82
2^{-11}	0.83	0.76	0.76	0.82
2^{-12}	0.83	0.76	0.76	0.82
2^{-13}	0.83	0.76	0.76	0.82
2^{-14}	0.83	0.76	0.76	0.82
2^{-15}	0.83	0.76	0.76	0.82
2^{-16}	0.83	0.76	0.76	0.82
2^{-17}	0.83	0.76	0.76	0.82
2^{-18}	0.83	0.76	0.76	0.82
2^{-19}	0.83	0.76	0.76	0.82
2^{-20}	0.83	0.76	0.76	0.82
p^N	0.83	0.76	0.76	0.82

Table 5.6: Computed orders of convergence, p_ε^N, and computed ε-uniform orders of convergence, p^N, for Method 5.4.1 applied to problem 5.4.3 with $m = 2$.

geometry of the domain.

Consider first the case $m > 0$. Suppose that we have $\alpha = 2$. Thus, the inequalities (5.3.2) will not in general be satisfied. In this case the region defined by (5.4.4) is shown in Figure 5.8. It can be seen that for $m \geq 0.5$ the lower limit in the inequality requires that $N_y/N_x \geq 1$ and the maximum value of this ratio is approximately 1.5. Also observe that as m increases both sides of (5.4.4) tend to 1. More generally for $\alpha > 0$ as m increases the upper limit in inequality (5.4.4) decreases towards 1 and the lower limit attains its maximum value when $m = M \equiv (1 + \sqrt{1+\alpha^2})/\alpha$ and then decreases towards 1. Computing the maximum value of the lower limit in the inequality shows that when $m = M$ we must take N_y and N_x to satisfy

$$\frac{N_y}{N_x} \geq \frac{\sqrt{1+\alpha^2}}{1+M^2} + 1,$$

to guarantee the monotonicity of our scheme. So for example if $\alpha = 5$ this bound shows that we must take more than 3 times the number of mesh intervals in the y co-ordinate direction compared to the x co-ordinate direction. Thus with a maximum limit of 512 mesh intervals in each co-ordinate direction this would severely restrict the extent of any illustrative table that we could produce.

If $\alpha < 0$ the situation is reversed in that the number of mesh intervals in the x co-ordinate direction may be required to be greater than the number in the y co-ordinate direction. However the magnitude of α in this case is restricted by the fact that the conditions (5.2.8) must be satisfied. Now both sides of the inequality (5.4.4) increase with increasing m towards 1 (see Figure 5.9 which shows the situation when $\alpha = -1$). So the smaller m gets the larger N_x must be relative to N_y.

Now consider the case $m < 0$. Again the conditions (5.2.8) restrict α. Specifically we must have $\alpha > -m$. The region defined by the inequalities (5.4.4) for $\alpha = 3$ is shown in Figure 5.10. It can be seen that for values of m close to 0 we can take approximately the same number of mesh points in each co-ordinate direction. Also observe that for m with larger magnitudes both limits in the inequality tend to 0. In general the upper limit in the inequality decreases towards 0 as the magnitude of m increases. The lower limit attains its maximum value when $m = M \equiv (1-\sqrt{1+\alpha^2})/\alpha$ and then decreases towards 0. This shows that as we get closer to violating the

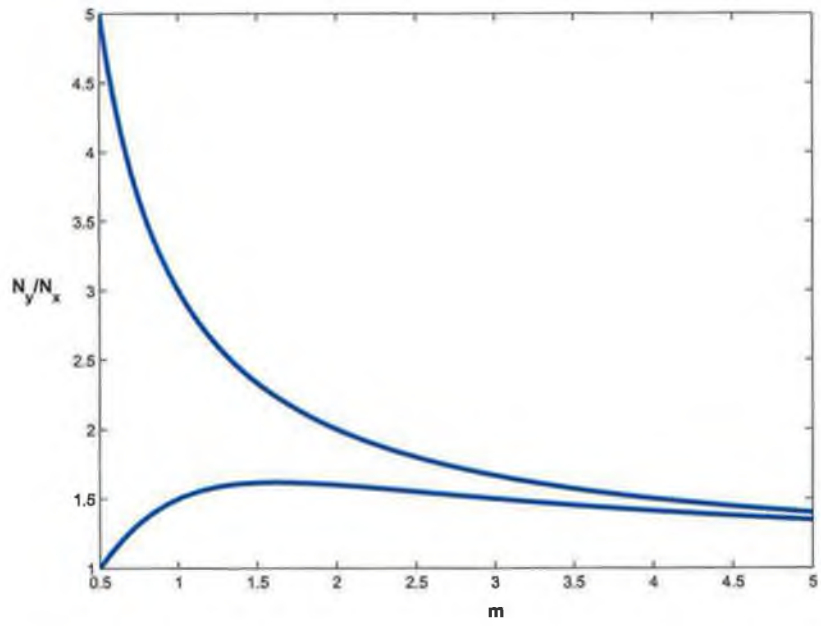

Figure 5.8: The region defined by (5.4.4) for $\alpha = 2$ and $m > 0$.

restriction $\alpha > -m$, we must take N_x to be progressively larger than N_y. Also when $m = M$ we must take N_x and N_y to satisfy

$$\frac{N_y}{N_x} \geq \frac{\sqrt{1+\alpha^2}}{1+M^2} - 1,$$

to guarantee the monotonicity of the scheme. So for example if $\alpha = 5$ this bound implies that we have to take more than twice the number of mesh intervals in the y co-ordinate direction than in the x co-ordinate direction.

To round off this subsection we present numerical results for some sample problems where it is necessary to have a different numbers of mesh points in each co-ordinate direction. Consider the following problem from Problem Class 5.2.2

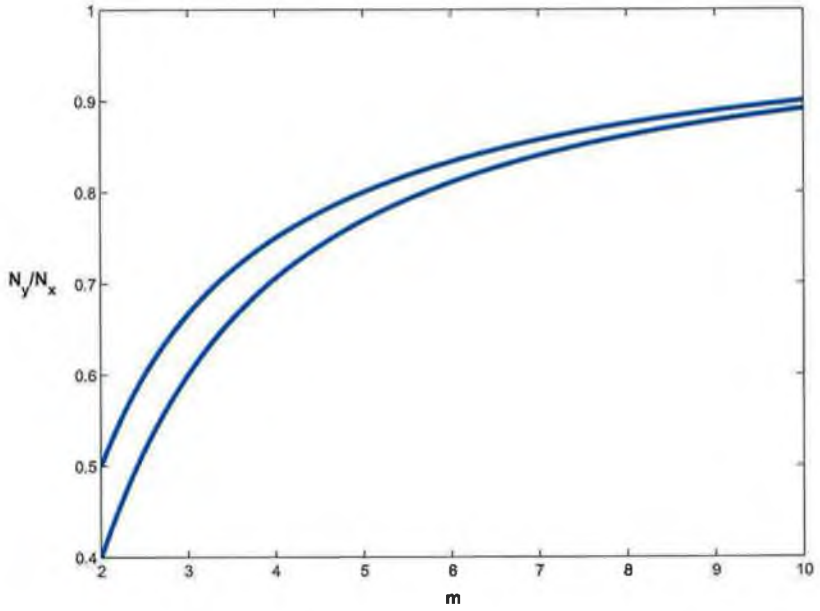

Figure 5.9: The region defined by (5.4.4) for $\alpha = -1$ and $m > 0$.

Problem Class 5.4.1.

$$(\varepsilon((1+m^2)u_{xx} + 2mu_{xy} + u_{yy}) + (3+m)u_x + u_y)(x,y) = f(x,y) \quad in \ \Omega,$$
$$u(x,y) = 0 \quad on \ \partial\Omega.$$

with $m = 2$ and $m = -2$. It is easy to see that for these choices of m the conditions (5.3.2) are not satisfied. The inequalities (5.4.4) become

$$\begin{aligned} m = 2: &\quad 2 \leq \tfrac{N_y}{N_x} \leq 2.5, \\ m = -2: &\quad 0.4 \leq \tfrac{N_y}{N_x} \leq 0.5. \end{aligned} \tag{5.4.6}$$

Thus, if we choose $N_y = 2N_x$ in the first case and $N_x = 2N_y$ in the second case Method 4.5.1 will be monotone when applied to the two problems. In Tables 5.7 and 5.8 we present numerical results for this method applied to these two problems. Note that the finest mesh that we can use here is one with 256 mesh intervals in one

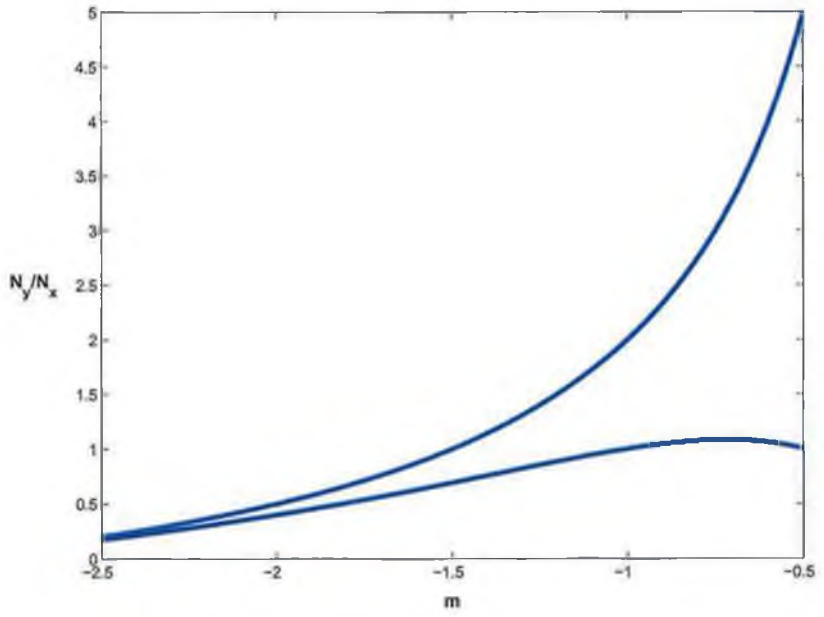

Figure 5.10: The region defined by (5.4.4) for $\alpha = 3$ and $m < 0$.

co-ordinate direction and 512 mesh intervals in the other and hence the tables shown here are smaller than those in §5.3. Nevertheless it can be seen that Method 4.5.1 used with differing number of mesh intervals in each co-ordinate direction behaves in a similar manner to the method with equal number of mesh intervals.

5.4.3 The effect of the mixed derivative on the layer structure

To conclude this survey of some of the computational issues relevant to the application of Method 4.5.1 for problems from Problem Class 4.3.1, we demonstrate numerically the effect the mixed derivative term has on the layer structure of the corresponding solutions. To this end consider the following sample problem from Problem Class

	Number of Intervals N_x			
ε	8	16	32	64
2^{-9}	0.90	0.80	0.76	0.75
2^{-10}	0.91	0.80	0.77	0.75
2^{-11}	0.91	0.81	0.77	0.75
2^{-12}	0.91	0.81	0.77	0.75
2^{-13}	0.91	0.81	0.77	0.75
2^{-14}	0.91	0.81	0.77	0.75
2^{-15}	0.91	0.81	0.77	0.75
2^{-16}	0.91	0.81	0.77	0.75
2^{-17}	0.91	0.81	0.77	0.75
2^{-18}	0.91	0.81	0.77	0.75
2^{-19}	0.91	0.81	0.77	0.75
2^{-20}	0.91	0.81	0.77	0.75
p^N	0.91	0.81	0.77	0.75

Table 5.7: Computed orders of convergence, p_ε^N, and computed ε-uniform orders of convergence, p^N, for Method 4.5.1 with $N_y = 2N_x$ applied to Problem Class 5.4.1 with $m = 2$.

	Number of Intervals N_y			
ε	8	16	32	64
2^{-9}	0.65	0.68	0.72	0.79
2^{-10}	0.63	0.67	0.71	0.78
2^{-11}	0.62	0.65	0.70	0.76
2^{-12}	0.61	0.65	0.70	0.76
2^{-13}	0.61	0.65	0.69	0.75
2^{-14}	0.61	0.64	0.69	0.75
2^{-15}	0.60	0.64	0.69	0.75
2^{-16}	0.60	0.64	0.69	0.75
2^{-17}	0.60	0.64	0.69	0.75
2^{-18}	0.60	0.64	0.69	0.75
2^{-19}	0.60	0.64	0.69	0.75
2^{-20}	0.60	0.64	0.69	0.75
p^N	0.60	0.64	0.69	0.75

Table 5.8: Computed orders of convergence, p_ε^N, and computed ε-uniform orders of convergence, p^N, for Method 4.5.1 with $N_x = 2N_y$ applied to Problem Class 5.4.1 with $m = -2$.

5.2.2

$$(\varepsilon(2u_{xx} + 2u_{xy} + u_{yy}) + 2u_x + u_y)(x, y) = f(x, y) \quad \text{in } \Omega, \tag{5.4.7a}$$

$$u(x, y) = 0 \quad \text{on } \partial\Omega, \tag{5.4.7b}$$

and the corresponding problem without a mixed derivative term

$$(\varepsilon(2u_{xx} + u_{yy}) + 2u_x + u_y)(x, y) = f(x, y) \quad \text{in } \Omega, \tag{5.4.8a}$$

$$u(x, y) = 0 \quad \text{on } \partial\Omega. \tag{5.4.8b}$$

It is easy to check that the inequalities (5.3.2) are satisfied and therefore that Method 4.5.1 will be monotone when applied to these problems. In Figure 5.11 we show the absolute difference between the numerical solutions generated by Method 4.5.1 applied to the 2 problems (a) over the whole domain and (b) in the corner mesh region for particular values of ε and N. We see that the maximum value of the difference is approximately 0.2 and this value is obtained in the corner mesh region. Outside of this region the difference is negligible in magnitude and much smaller than ε. Indeed for small values of ε we can see that the maximum value of the difference remains constant and always occurs in the corner region. This is illustrated in Table 5.9 where we have calculated the maximum value of the difference for a range of values of ε and N, and the mesh point at which this occurs. This verifies the fact that, in our analysis in Theorem 4.4.3 of the layer structure of solutions of problems from Problem Class 4.3.1, we saw that the mixed derivative term only had an influence when it came to bounding the functions associated with the corner layer.

5.5 A more complicated domain

In the final section of this thesis we present some numerical results for Method 4.5.1 applied to a problem posed on a domain that is more complicated than a parallelogram. Consider the following choice for the function ϕ in (5.2.1):

$$\phi(\eta) = -m_1\eta^2 - m_2\eta, \tag{5.5.1}$$

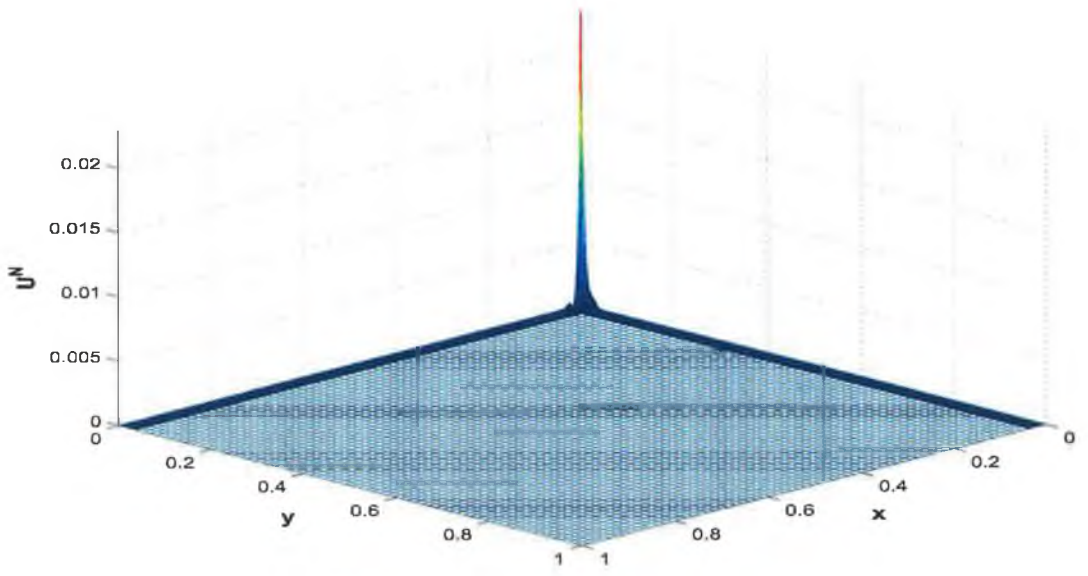

(a)

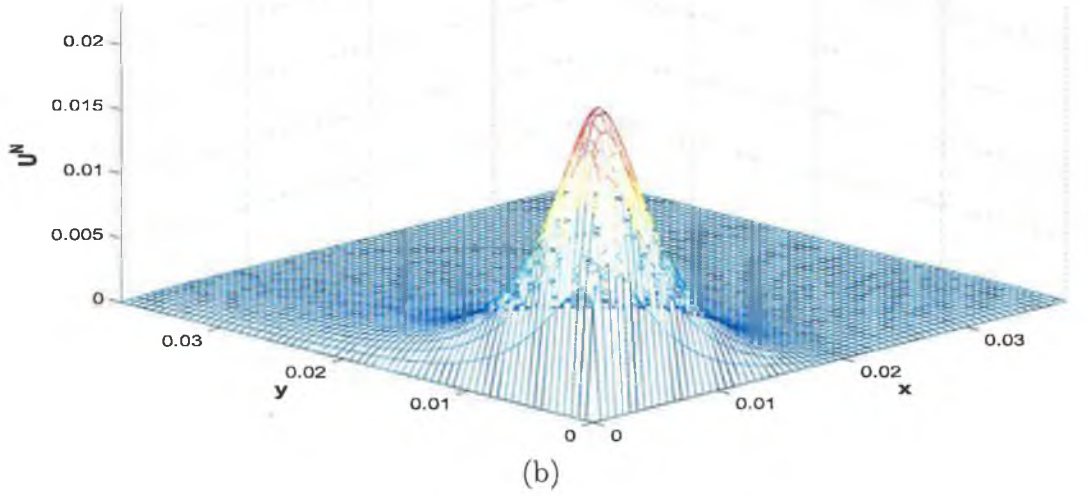

(b)

Figure 5.11: Absolute difference between the numerical solutions generated by Method 4.5.1 applied to problems 5.4.7 and 5.4.8 on (a) the whole mesh and (b) in the corner mesh region with $\varepsilon = 2^{-8}$ and $N = 128$.

ε	Number of Intervals N				
	32	64	128	256	512
2^{-9}	0.0198(3,3)	0.0215(4,4)	0.0229(7,6)	0.0239(10,9)	0.0244(17,15)
2^{-10}	0.0197(3,3)	0.0215(4,4)	0.0228(7,6)	0.0238(10,9)	0.0244(17,14)
2^{-11}	0.0196(3,3)	0.0214(4,4)	0.0228(7,6)	0.0238(10,9)	0.0244(17,14)
2^{-12}	0.0196(3,3)	0.0214(4,4)	0.0228(7,6)	0.0238(10,9)	0.0244(17,14)
2^{-13}	0.0196(3,3)	0.0214(4,4)	0.0228(7,6)	0.0238(10,9)	0.0244(17,14)
2^{-14}	0.0196(3,3)	0.0214(4,4)	0.0228(7,6)	0.0238(10,9)	0.0244(17,14)
2^{-15}	0.0196(3,3)	0.0214(4,4)	0.0228(7,6)	0.0238(10,9)	0.0244(17,14)
2^{-16}	0.0196(3,3)	0.0214(4,4)	0.0228(7,6)	0.0238(10,9)	0.0244(17,14)
2^{-17}	0.0196(3,3)	0.0214(4,4)	0.0228(7,6)	0.0238(10,9)	0.0244(17,14)
2^{-18}	0.0196(3,3)	0.0214(4,4)	0.0228(7,6)	0.0238(10,9)	0.0244(17,14)
2^{-19}	0.0196(3,3)	0.0214(4,4)	0.0228(7,6)	0.0238(10,9)	0.0244(17,14)
2^{-20}	0.0196(3,3)	0.0214(4,4)	0.0228(7,6)	0.0238(10,9)	0.0244(17,14)

Table 5.9: Maximum absolute differences between the numerical solutions generated by Method 4.5.1 applied to problems 5.4.7 and 5.4.8.

where m_1 and m_2 are constants. In this case the boundary of the domain $\hat{\Omega}_P$ is in general curved (see Figure 5.12). We will continue to assume that the coefficients of the convective terms in the original differential equation are constant. The corresponding transformed Problem Class is:

Problem Class 5.5.1.

$$\begin{aligned}(\varepsilon(au_{xx} + 2bu_{xy} + cu_{yy}) + a_1u_x + a_2u_y)(x,y) = f(x,y) \quad &in \ \ \Omega,\\ u(x,y) = 0 \quad &on \ \ \partial\Omega,\end{aligned}$$

where

$$a(x,y) = 1 + (2m_1y + m_2)^2, \quad b(x,y) = 2m_1y + m_2, \quad c(x,y) = 1,$$
$$a_1(x,y) = \alpha_1 + (2m_1y + m_2)\alpha_2 + 2\varepsilon m_1 > 0, \quad a_2(x,y) = \alpha_2 > 0.$$

We see in this case that some of the coefficients in the differential equation are now variable, in contrast to the situation for Problem Class 5.2.2, and that depending on the values of m_1 and m_2 the coefficient of the mixed derivative term may change

sign.

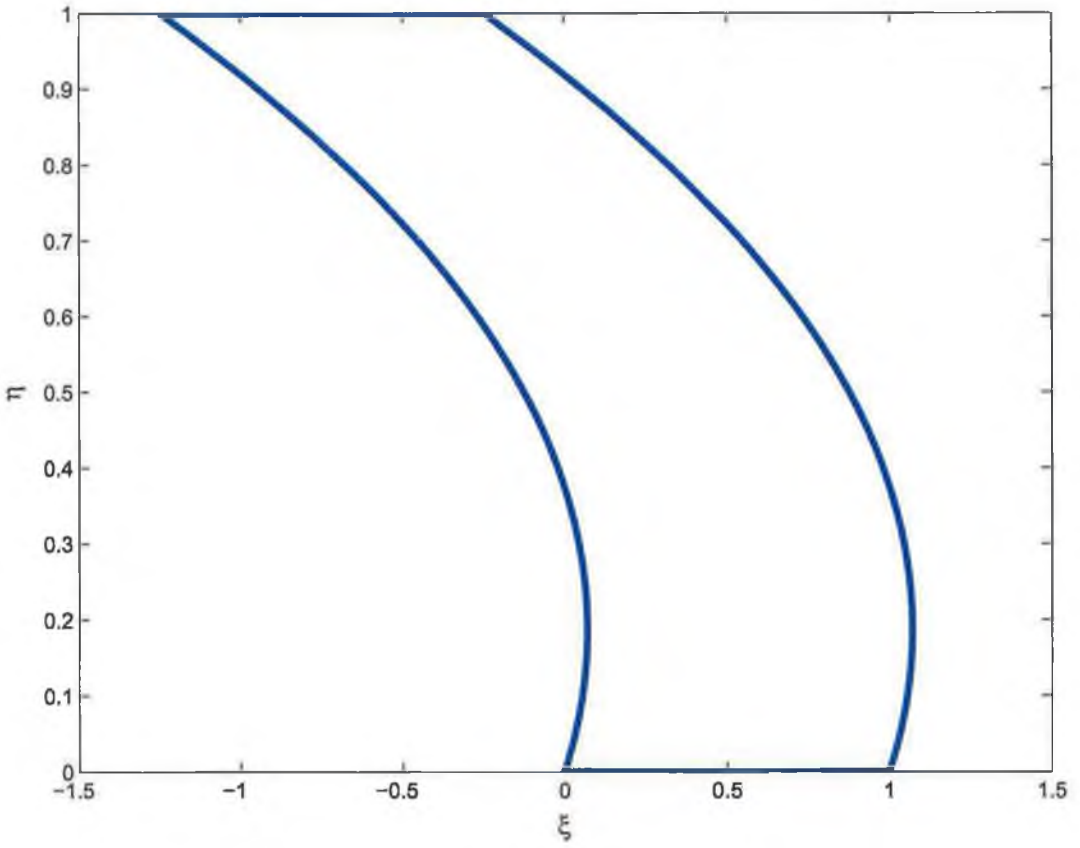

Figure 5.12: The domain $\hat{\Omega}_P$ with ϕ as defined in (5.5.1).

For our example we shall take the following values for the constants m_1, m_2, α_1 and α_2:

$$m_1 = 1, \quad m_2 = -0.5, \quad \alpha_1 = 2, \quad \alpha_2 = 1. \tag{5.5.2}$$

With these choices it can be verified that inequalities (4.5.8) are satisfied and so we may take $N_x = N_y = N$ in our calculations.

As in §5.3 we examine the performance of the method (in the perturbed case) by tabulating the computed orders of convergence, p_ε^N, and the computed ε-uniform orders of convergence, p^N, with these quantities defined as in that section. We see

ε	Number of Intervals N				
	8	16	32	64	128
2^{-9}	0.86	0.74	0.64	0.67	0.76
2^{-10}	0.86	0.75	0.65	0.67	0.76
2^{-11}	0.85	0.75	0.65	0.67	0.76
2^{-12}	0.85	0.75	0.65	0.67	0.76
2^{-13}	0.85	0.75	0.65	0.67	0.76
2^{-14}	0.85	0.75	0.65	0.67	0.76
2^{-15}	0.85	0.75	0.65	0.67	0.76
2^{-16}	0.85	0.75	0.65	0.67	0.76
2^{-17}	0.84	0.75	0.65	0.67	0.76
2^{-18}	0.84	0.75	0.65	0.67	0.76
2^{-19}	0.84	0.75	0.65	0.67	0.76
2^{-20}	0.84	0.75	0.65	0.67	0.76
p^N	0.84	0.75	0.65	0.67	0.76

Table 5.10: Computed orders of convergence, p_ε^N, and computed ε-uniform orders of convergence, p^N, for Method 4.5.1 applied to the problem from Problem Class 5.5.1 with m_1, m_2, α_1 and α_2 given by (5.5.2).

in Table 5.10 that the p_ε^N are essentially independent of ε and are approaching 1, as N is increased. This indicates that our method is ε-uniform for this problem for the range of ε considered. We also present a graph of a representative numerical solution plotted on the original domain for particular values of ε and N (Figure 5.13) and an illustration of how the piecewise-uniform fitted mesh would look on the original domain (Figure 5.14).

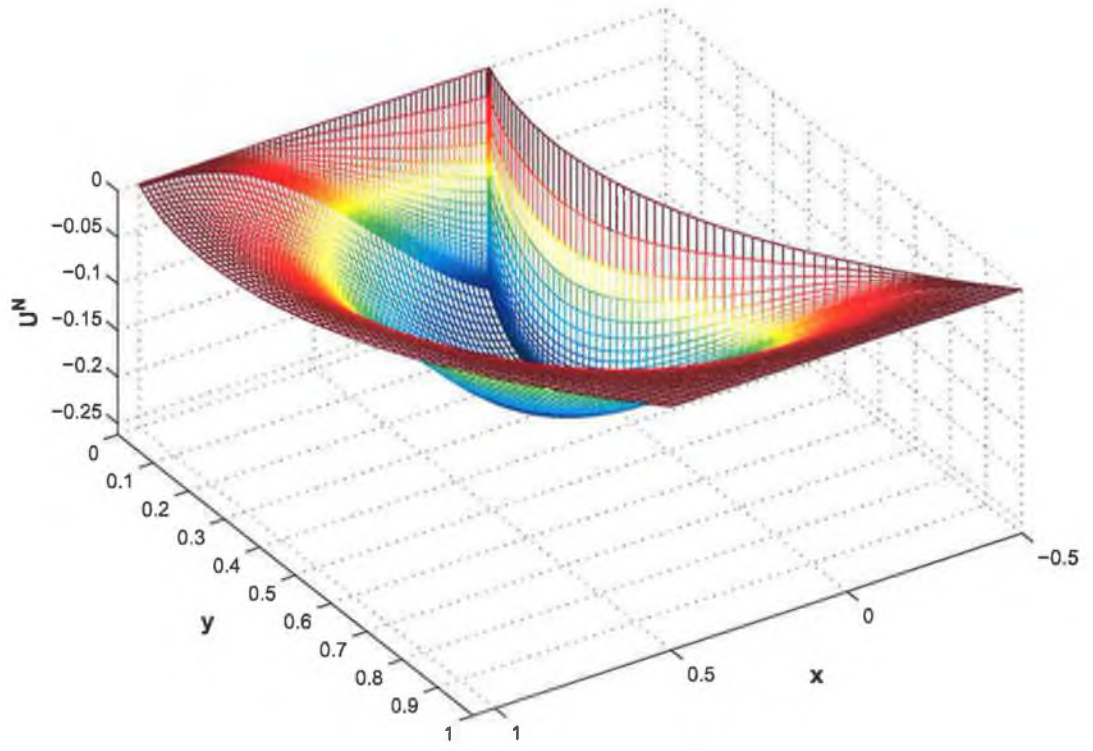

Figure 5.13: Plot of Numerical Solution generated by Method 4.5.1 applied to the problem from Problem Class 5.5.1 with m_1, m_2, α_1 and α_2 given by (5.5.2), $\varepsilon = 2^{-10}$ and $N = 128$ on original domain.

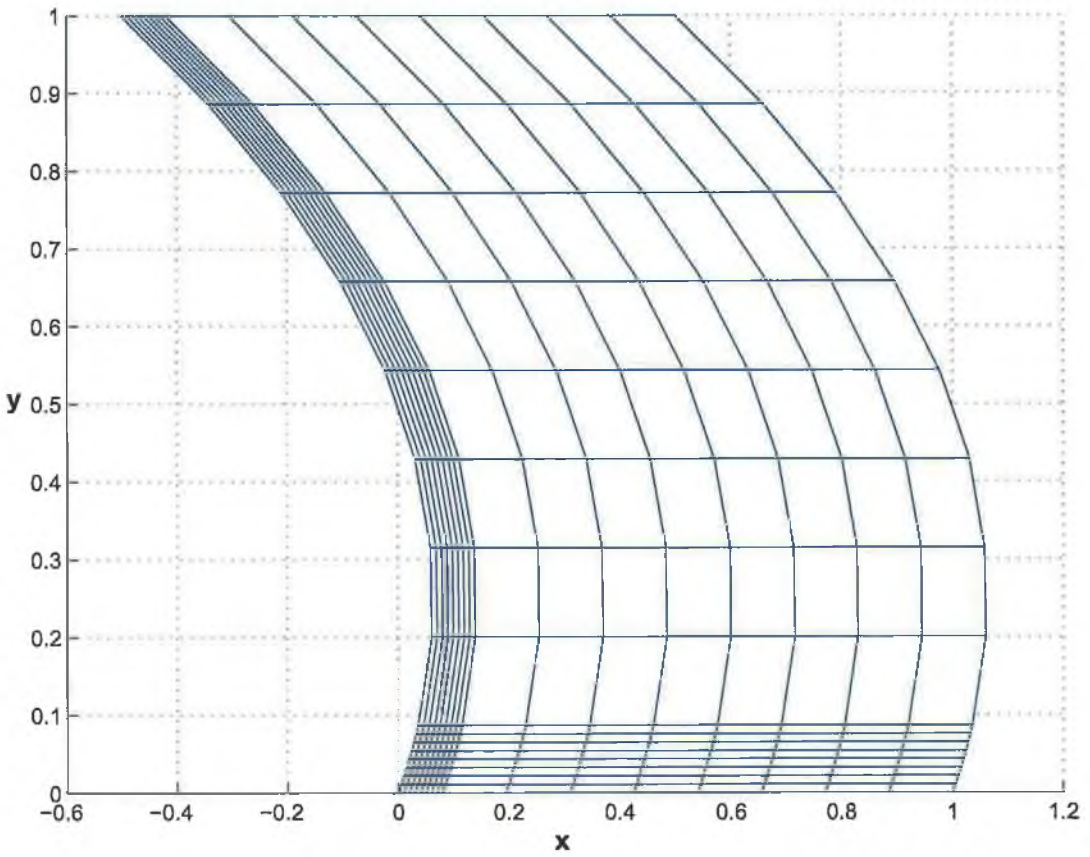

Figure 5.14: Piecewise-uniform fitted mesh for the problem from Problem Class 5.5.1 with m_1, m_2, α_1 and α_2 given by (5.5.2) on original domain.

Chapter 6

Conclusions

In summary, we present what we believe to be the main results and findings of this thesis.

- The nature and location of the boundary layers present in the solutions to problems posed on non-rectangular domains depends on the relationship between the geometry of the problem and certain coefficients in the differential equation.
- For a certain class of singularly perturbed parabolic problems posed on a non-rectangular domain it is possible to classify some of the problems into distinct subclasses and apply numerical methods based on piecewise-uniform fitted meshes to resolve the layers present.
- Singularly perturbed elliptic problems posed on non-rectangular domains present more difficulties than do corresponding parabolic problems, as a mixed derivative term is introduced into the differential equation under a transformation of the independent variables. In particular the construction of a monotone finite difference operator is a non-trivial task.
- It is possible to construct a monotone finite difference operator for a singularly perturbed elliptic equation with a mixed derivative if one considers schemes which are inconsistent.
- A numerical method based on a monotone, inconsistent difference scheme and

a piecewise-uniform fitted mesh generates numerical solutions which are ε-uniformly convergent in the perturbed case, i.e. when $\varepsilon \leq CN^{-1}$.

Bibliography

[1] V.B. Andreev. Anisotropic estimates of Green's function for a singularly perturbed two-dimensional monotone difference convection-diffusion operator and their application. *Comput. Math. Math. Phys.*, 43(4):521–528, 2003.

[2] V.B. Andreev and N.V. Kopteva. A study of difference schemes with the first derivative approximated by a central difference ratio. *Comput. Math. Math. Phys.*, 36(8):1065–1078, 1996.

[3] V.B. Andreev and I.A. Savin. The uniform convergence with respect to a small parameter of A.A. Samarskii's monotone scheme and its modification. *Comput. Math. Math. Phys.*, 35(5):581–591, 1995.

[4] N.S. Bakhvalov. Towards optimization of methods for solving boundary value problems in the presence of a boundary layer. *Zh. Vychisl. Mat. Mat. Fiz.*, 9(4):841–859, 1969. (In Russian).

[5] D.B. Creamer, J.J.H. Miller, and G.I. Shishkin. Discrete approximations of the Cauchy problem for a singularly perturbed Black-Scholes equation in a bounded subdomain. In *An International Conference on Boundary and Interior Layers*, Toulouse, 2004. ONERA.

[6] M. Dauge. *Elliptic Boundary Value Problems on Corner Domains.* Number 1341 in Lecture Notes in Mathematics. Springer Verlag, 1988.

[7] T.A. Davis. *UMFPACK Version 4.0 User Guide(`http://www.cise.ufl.edu/research/sparse/umfpack/v4.0/UserGuide.pdf`).* Dept. of Computer and Information Science and Engineering, Univ. of Florida, Gainesville, FL, 2002.

[8] D.N. de G. Allen and R.V. Southwell. Relaxation methods applied to determine the motion, in 2D, of a viscous fluid past a fixed cylinder. *Quart. J. Mech. Appl. Math.*, VIII(2):129–145, 1955.

[9] M. Dobrowolski and H.-G. Roos. A priori estimates for the solution of convection-diffusion problems and interpolation on Shishkin meshes. *J. Anal. Appl.*, 16(4):1001–1012, 1997.

[10] R.K. Dunne, E. O'Riordan, and G.I. Shishkin. Singularly perturbed parabolic problems on non-rectangular domains. In L. Vulkov, J. Waśniewski, and P. Yalamov, editors, *Numerical Analysis and Its Applications, Second International Conference, NAA 2000, Rousse, Bulgaria, June 2000*, pages 265–272. Springer-Verlag, 2001. Lecture Notes in Computer Science, 1988.

[11] R.K. Dunne, E. O'Riordan, and G.I. Shishkin. Boundary layers in singularly perturbed problems on non-rectangular domains. In S. Wang and N. Fowkes, editors, *Proceedings of BAIL2002*, pages 109–114, Perth, Western Australia, 2002. The University of Western Australia.

[12] R.K. Dunne, E. O'Riordan, and G.I. Shishkin. A fitted mesh method for a class of singularly perturbed parabolic problems with a boundary turning point. *Comput. Methods Appl. Math.*, 3(3):361–372, 2003.

[13] W. Eckhaus. *Asymptotic Analysis and Singular Perturbations.* North-Holland, Amsterdam, 1979.

[14] T.M. El-Mistikawy and M.J. Werle. Numerical method for boundary layers with blowing-the exponential box scheme. *AIAA J.*, 16:749–751, 1978.

[15] P. A. Farrell, A. F. Hegarty, J. J. H. Miller, E. O'Riordan, and G. I. Shishkin. *Robust Computational Techniques for Boundary Layers.* Chapman and Hall/CRC Press, Boca Raton, U.S.A., 2000.

[16] P. Grisvard. *Elliptic Problems in Nonsmooth Domains.* Pitman, 1985.

[17] P. Grisvard. *Singularities in Boundary Value Problems.* Masson, 1992.

[18] H. Han and R. B. Kellogg. Differentiability properties of solutions of the equation $-\varepsilon^2\Delta u + ru = f(x,y)$ in a square. *SIAM J. Math. Anal.*, 21:394–408, 1990.

[19] P.W. Hemker. *A Numerical Study of Stiff Two-Point Boundary Value Problems.* MCT 80, Mathematical Centre, Amsterdam, 1977.

[20] A.M. Il'in. Differencing scheme for a differential equation with a small parameter affecting the highest derivative. *Math Notes*, 6(2):596–602, 1969.

[21] A.M. Il'in. *Mathching of Asymptotic Expansions of Solutions to Boundary Value Problems.* American Math. Society Translations, Providence, 1992.

[22] R.B. Kellogg and A. Tsan. Analysis of some difference approximations for a singular perturbation problem without turning points. *Math. Comp.*, 32:1025–1039, 1978.

[23] N. V. Kopteva. Error expansion for an upwind scheme applied to a two-dimensional convection-diffusion problem. *SIAM J. Numer. Anal.*, 41(5):1851–1869, 2003.

[24] N.V. Kopteva. Uniform pointwise convergence of difference schemes for convection-diffusion problems on layer-adapted meshes. *Computing*, 66(2):179–197, 2001.

[25] O. A. Ladyzhenskaya, V. A. Solonnikov, and N. N. Ural'tseva. *Linear and Quasilinear Equations of Parabolic Type*, volume 23 of *Translations of Mathematical Monographs.* American Mathematical Society, USA, 1968.

[26] O. A. Ladyzhenskaya and N. N. Ural'tseva. *Linear and Quasilinear Elliptic Equations.* Academic Press, New York and London, 1968.

[27] T. Linß. Layer-adapted meshes for convection-diffusion problems. *Comput. Methods Appl. Mech. Engrg.*, 192(9-10):1061–1105, 2003.

[28] T. Linß and M. Stynes. Asymptotic analysis and Shishkin-type decomposition for an elliptic convection-diffusion problem. *Preprint 1998-4, Department of Mathematics, National University of Ireland, Cork*, 1998.

[29] T. Linß and M. Stynes. A hybrid difference scheme on a Shishkin mesh for linear convection-diffusion problems. *Appl. Numer. Math.*, 31(3):255–270, 1999.

[30] T. Linß and M. Stynes. Numerical methods on Shishkin meshes for linear convection-diffusion problems. *Comput. Methods Appl. Mech. Engrg.*, 190(28):3527–3542, 2001.

[31] T. Linß and R. Vulanović. Uniform methods for semilinear problems with an attractive boundary turning point. *Novi Sad Journal of Mathematics*, 31(2):99–114, 2001.

[32] V.D. Liseikin. On the numerical solution of singularly perturbed problems with turning points. *Comput. Math. Math. Phys.*, 41(1):55–83, 2001.

[33] P.P. Matus and I.V. Rybak. Difference schemes for elliptic equations with mixed derivatives. *Comput. Methods Appl. Math.*, 4(4):494–505, 2004.

[34] J.M. Melenk. *Hp-Finite Element Methods for Singular Perturbations.* Number 1796 in Lecture Notes in Mathematics. Springer, Berlin, New York, 2002.

[35] J. J. H. Miller, E. O'Riordan, and G. I. Shishkin. *Fitted Numerical Methods for Singular Perturbation Problems.* World Scientific Publishing Co., Singapore, 1996.

[36] J.J.H. Miller, E. O'Riordan, G.I. Shishkin, and L.P. Shishkina. Fitted mesh methods for problems with parabolic boundary layers. *Mathematical Proceedings of the Royal Irish Academy*, 98A(2):173–190, 1998.

[37] K.W. Morton. *Numerical Solution of Convection-Diffusion Problems*, volume 12 of *Applied Mathematics and Mathematical Computation.* Chapman and Hall, London, 1996.

[38] E. O'Riordan. Singular perturbation finite element methods. *Numer. Math.*, 44:425–434, 1984.

[39] H.-G. Roos. Layer-adapted grids for singular perturbation problems. *Z. Agnew. Math. Mech.*, 78(5):291–309, 1998.

[40] H. G. Roos, M. Stynes, and L. Tobiska. *Numerical Methods for Singularly Perturbed Differential Equations. Convection-Diffusion and Flow Problems.* Springer-Verlag, New York, 1996.

[41] A.A. Samarskii. *The Theory of Difference Schemes.* Marcel Dekker Inc., New York-Basel, 2001.

[42] A.A. Samarskii, P.P. Matus, V.I. Mazhukin, and I.E. Mozolevski. Monotone difference schemes for equations with mixed derivatives. *Comp. Math. Appl.*, 44(3-4):501–510, 2002.

[43] G.I. Shihskin. On finite difference fitted schemes for singularly perturbed boundary value problems with a parabolic boundary layer. *J. Math. Anal. Appl.*, 208(1):181–204, 1997.

[44] G. I. Shishkin. A difference scheme on a non-uniform mesh for a differential equation with a small parameter multiplying the highest derivative. *USSR Comput. Maths. Math. Phys.*, 23:59–66, 1983.

[45] G. I. Shishkin. A difference scheme for a singularly perturbed equation of parabolic type with a discontinuous initial condition. *Soviet Math. Dokl.*, 37(3):792–796, 1988.

[46] G. I. Shishkin. Approximation of solutions of singularly perturbed boundary value problems with a parabolic boundary layer. *Comput. Math. Math. Phys.*, 29(4):1–10, 1989.

[47] G. I. Shishkin. *Discrete Approximation of Singularly Perturbed Elliptic and Parabolic Equations.* Russian Academy of Sciences, Ural Section, Ekaterinburg, 1992.

[48] G. I. Shishkin. Grid approximation of singularly perturbed boundary value problems in a nonconvex domain with a piecewise smooth boundary. *Mat. Model.*, 11(11):75–90, 1999. (In Russian).

[49] G. I. Shishkin. Approximation of singularly perturbed convection-diffusion equations with low smoothness of the derivatives involved in the equation. In L.G.

Vulkov, J.J.H. Miller, and G.I. Shishkin, editors, *Analytical and Numerical Methods for Convection-Dominated and Singularly Perturbed Problems*, pages 111–121. Nova Science, N.Y., 2000. (Proceedings of the International Workshop, Lozenetz, Bulgaria, August 27-31, 1998).

[50] M. Stynes and E. O'Riordan. Uniformly convergent difference schemes for singularly perturbed parabolic diffusion-convection problems without turning points. *Numer. Math.*, 55:521–544, 1989.

[51] E.A. Volkov. Differentiability properties of solutions of boundary value problems for the Laplace and Poisson equations. *Proc. Steklov Inst. Math.*, 77:101–126, 1965.

[52] R. Vulanović and P.A. Farrell. Analysis of multiple turning point problems. *Rad. Mat.*, 8, 1992.

[53] R. Vulanović and P.A. Farrell. Continuous and numerical analysis of a multiple turning point problem. *SIAM J. Numer. Anal.*, 30(5):1400–1418, 1993.